Geotechnical Characterization of a Potential Shaft Backfill Material

NWMO TR-2013-03   **December 2013**

D.G. Priyanto, C-S. Kim and D.A. Dixon

Atomic Energy of Canada Limited

nwmo
NUCLEAR WASTE   SOCIÉTÉ DE GESTION
MANAGEMENT   DES DÉCHETS
ORGANIZATION   NUCLÉAIRES

Nuclear Waste Management Organization
22 St. Clair Avenue East, 6th Floor
Toronto, Ontario
M4T 2S3
Canada

Tel: 416-934-9814
Web: www.nwmo.ca

Geotechnical Characterization of a Potential Shaft Backfill Material

NWMO TR-2013-03

December 2013

D.G. Priyanto, C-S. Kim, and D.A. Dixon
Atomic Energy of Canada Limited

ABSTRACT

Abstract
This document presents the results of a shaft backfill properties evaluation undertaken for NWMO at AECL's Geotechnical Laboratory.

This work focused on determining the geotechnical properties evaluation of a mixture of 70% bentonite clay and 30% sand-sized aggregate by dry weight proportions. This blend of bentonite and aggregate was initially specified to be compacted to a dry density of 1.60 Mg/m^3 using conventional compaction techniques. Initial compaction testing established that a dry density of 1.80 Mg/m^3 was readily achievable using conventional dynamic compaction methodology, and so the reference dry density of this 70-30 bentonite-sand mixture (BSM) was defined as 1.80 Mg/m^3 for this testing program.

Before detailed geotechnical characterization was undertaken, the specific bentonite and sand components that were to be used were screened for suitability. This involved completion of basic physical, chemical and mineralogical characterization tests of the bentonite and sand. A series of geotechnical characterizations were done on the 70-30 BSM or bentonite on its own when groundwater conditions were distilled water or one of the three reference groundwater compositions associated with NWMO's groundwater formulations (i.e., CR10, SR160 and SR270 solutions). The geotechnical characterizations include: free swell tests, consistency (Atterberg) limits tests, modified compaction tests, swelling pressure and hydraulic conductivity tests, triaxial and 1D-consolidation tests to determine mechanical properties, gas permeability tests, and determination of soil-water characteristic curve (SWCC). The parameters measured from this testing program can be used as inputs to performance and safety assessments of shaft backfill in possible Deep Geological Repositories (DGRs) designed for the isolation of used nuclear fuel (UF) or low and intermediate level waste (LILW).

When the dry density of the compacted 70-30 BSM exceeded 1.80 Mg/m^3, the saturated hydraulic conductivity should be less than 3×10^{-12} m/s and swelling pressure higher than 900 kPa in all of the groundwater environments examined. This indicates that the 70-30 BSM is a potentially suitable material for use in shaft backfilling as it provides both a low hydraulic conductivity and will develop a substantial swelling pressure.

TABLE OF CONTENTS

LIST OF TABLES

Page

LIST OF FIGURES

1. INTRODUCTION AND PROJECT DESCRIPTION

This work was completed to provide Hydro-Mechanical (H-M) and mineralogical characterization information on a 70-30 Bentonite-Sand Mixture (BSM) considered as potential shaft backfill for a deep geological repository (DGR) constructed in either a sedimentary or crystalline geosphere. The parameters measured can be used as inputs to performance and safety assessments of shaft backfill in possible DGRs designed for the isolation of used nuclear fuel (UF) or low and intermediate level waste (LILW).

The specific analyses scheduled for completion in the course of this study are listed in Table 1. Four different test fluids were used in this project, which include: Distilled water (DW) and three reference salinities of groundwater (i.e., CR10, SR160, and SR270 solutions). The descriptions of the testing materials are discussed in Chapter 2. The results of the tests are described in Chapters 2 and 3. Chapter 4 summarizes the material properties of the 70-30 BSM obtained from this study. Appendix A provides references to the techniques used to analyse the materials examined in this study.

Table 1: Tests Completed as Part of Current Study

Tests and Parameter Determined	Solid Materials					
	Sand	Bentonite	70-30 Bentonite-Sand Mixture			
			Test Fluid			
			DW	DW	CR10	SR160	SR270
Compaction Properties[1]	-	√	√	√	√	√
Mineralogy (XRD)	√	√	-	-	-	-
Chemistry (XRF)	√	√	-	-	-	-
Consistency Limits[2]	-	√	√	√	√	√
Free Swell	-	√	√	√	√	√
Swelling Pressure, P_s[3]	-	-	√	√	√	√
Hydraulic Conductivity, K_{sat}[4]	-	-	√	√	√	√
Gas Conductivity, K_g	-	-	√	√	√	√
SWCC [5]	-	-	√	√	√	√
Triaxial cons. (K, κ, λ)[6]	-	-	√	√	√	√
1D-Consolidation Tests (M, C_c, C_s)	-	-	√	√	√	√
Triaxial CIŪ[7]	-	-	-	-	-	√

[1] Typical compaction curve requires more than 6 data points.

[2] Consistency limits are measures of the water contents at which the soil deformation is defined by plastic and liquid behaviour (also known as Atterberg Limits). This is an ASTM standard test for soils, providing indication of the mineralogical composition of the soil (high liquid limit is usually a sign of high swelling clay content).

[3] P_s = swelling pressure. At least 3 tests were done in each groundwater type for specimens at dry densities between 1.55 and 1.85 Mg/m^3.

[4] K_{sat} = saturated hydraulic conductivity. At least 3 tests were done in each groundwater type for specimens at dry densities between 1.55 and 1.85 Mg/m^3.

[5] SWCC = Soil Water Characteristic Curve. Multiple tests were required to develop the SWCC.

[6] Triaxial cons (K) = isotropic consolidation in a triaxial cell to determine bulk modulus K

[7] Triaxial CIŪ = undrained triaxial test. This test was done at the Royal Military College of Canada (RMC), AECL used the results to generate a material deformation description for the backfill.

2. MATERIAL EVALUATION

The shaft backfill materials (bentonite, sand and solutions) and their proportions (70-30) were defined by NWMO. NWMO specified four reference groundwater compositions (distilled water plus three saline solutions), to be used in conduct of material behaviour tests. It was therefore necessary to develop solution formulations that would meet the chemical specifications provided.

Before detailed characterization of the backfill's geotechnical properties was undertaken, the specific bentonite and sand components that were to be used were screened for suitability. This involved completion of basic physical, chemical and mineralogical characterization tests.

2.1   Pore Water Composition

NWMO provided the target composition for three reference groundwaters to be used in the course of this work (Table 2), in addition of the freshwater. The focus of this work was to determine the hydro-mechanical (H-M) behaviour of a potential shaft backfill. In order to closely simulate potential field conditions, solutions that contained essentially the same mono-divalent, divalent cation and anion distributions as have been observed in nature were used in this study. AECL developed formulations for these test solutions (Appendix B) and NWMO confirmed their suitability. In order to establish the as-prepared composition of the solutions used, samples of each solution were chemically analysed and where necessary adjusted to better match the target compositions. Detailed compositional information on the solutions prepared is presented in Section 2.3.1.

2.2   Chemical and Mineralogical Characterization of Backfill

2.2.1   Bentonite

Evaluation of literature associated with the mineralogical composition of various Wyoming bentonites led to the selection of a 200-mesh commercial bentonite product sourced from Wyoming USA (product trade name was NATIONAL BENTONITE Western Standard 200 mesh). This material was a typical high-quality bentonite product, similar in quality to the MX80 bentonite used in many European research programs, but that had been crushed to 200 mesh (fine powder) size. Mineralogical assessment of this bentonite was completed and compared to data from literature sources as well as the producer of the bentonite. X-ray diffraction analysis was the primary methodology used although some data related to the chemical composition was also obtained. The diffraction patterns are discussed in detail in Section 2.3.4. They confirmed the dominance of montmorillonite clay minerals in this product.

2.2.2   Sand

The sand-sized aggregate used was predefined to be a quartz-dominated material. A suitable, naturally deposited material (Quartz-rich with feldspar and minimal limestone component) was identified by AECL and accepted by NWMO for use in this project. It required water washing to remove the small fines (silt-clay) component as well as minor adjustment of the grain size distribution prior to its use. Preliminary mineralogical screening confirmed that it is quartz-feldspar rich and limestone-poor (see Section 2.3.4 for detailed description). The grain-size distribution of the sand material prepared for

use in this work is provided in Section 2.3.1. The prepared sand material was tested for grain size distribution and stored in labelled containers for use specifically in this project. This ensured that sufficient, qualified material was on hand to complete the work.

2.3   Material Preparation and Qualification

2.3.1   Preparation of Artificial Groundwater Solutions

In the description of the work provided by NWMO, distilled water and three reference salinities of groundwater were defined for inclusion in this project. For each of the saline solutions defined, a proposal for the chemical formulation that would closely match the target formulations was developed and sent to NWMO for approval. Based on the discussion of these formulations, slightly modified recipes were used to prepare the reference solutions. On completion of the mixing of the solutions, they were checked through conduct of three chemical analyses on each solution, two by an internal AECL analytical service and one by an outside commercial service. If necessary, the composition of the solutions could then have been modified through addition of salt materials, but this was not necessary.

Table 2 provides the results of the chemical analyses completed on the prepared solutions as well as the initial target compositions. The analytical values obtained by the analyses of identical samples of these solutions showed notable scatter which can be attributed to the very high ionic concentrations present in the saline solutions, which makes obtaining highly accurate results challenging. At high TDS (Total Dissolved Solid) levels the samples have to go through considerable dilution in order to make them suitable for analysis, which builds in a substantial range into the results. The results of the analyses of the saline solutions were actually quite consistent between the two analytical services and within 5-6% of the targeted concentrations. The nature of the testing being done in this study would not be able to discern the effects of such a small percentage deviation from the targeted values and the inherent limitations of the analytical results meant that attempting to further refine the solution formulations was not appropriate.

Table 2: Composition of Solutions Used in Testing

Solution, Analytical Service	pH	Ca	Mg	Na	K	Cl	SO$_4$*	TDS (g/L)
CR10								
AECL	6.56	2260	<0.5	1870, 1886	<0.5	6800*	1090*	12001
AECL		1630	<0.5	1440	14	6769*	1086*	12001
ALS	6.89	2370	1.4	2020	<0.3	7260	1230	12880
Average	**6.72**	**2087**	**<1**	**1804**	**<0.5**	**6943***	**1158**	**11992***
Target	**7**	**2241**	**-**	**1891**	**-**	**6140**	**1000**	**11272**
SR160								
AECL	6.14	12400	3000	32700, 40200	3	101400*	450*	157450-164950
AECL		16270	3860	41650	<0.5			163630
ALS	6.2	16300	3660	46000	<5	108000	490	174450
Average	**6.17**	**14990**	**3507**	**42617**	**<3**	**104700***	**470**	**165120***
Target	**6.5**	**14933**	**3899**	**39012**	**-**	**97684**	**420**	**155948**
SR270								
AECL	5.89	29600	7700	46100	11250	177462*	331*	272443
AECL		34100	8600	52400, 48200	12660	177000	330	280890-285190
ALS	5.98	33700	9140	52600	13800	199000	340	308580
Average	**5.93**	**32467**	**8480**	**49825**	**12570**	**184487***	**334**	**288163***
Target	**5.8**	**32000**	**8641**	**50101**	**12500**	**169976**	**432**	**273650**

* Analytical results were reported as being ± 10-12% for anions. For solutions of high ionic concentration, this uncertainty accounts for the variation between the target and the "measured" TDS (Total Dissolved Solid) contents.

2.3.2 Grain Size Distribution of Sand

The selection and characterization of the sand component was completed in July 2011 with identification of a quartz-dominated aggregate, sourced from a natural-occurring glacial-fluvial deposit in eastern Manitoba. It was necessary to adjust the grain-size distribution by sieving-out a portion of the material present in the naturally occurring sand and adding it to unaltered raw material, boosting the finer sand component present in the resultant mixture. This sand came from the same supplier as the sand component used in the Enhanced Sealing Project (ESP) (Martino et al. 2011), but it had a finer grain-size distribution. The particle size distribution of the sand component used for this study compared to the ESP project is illustrated in Figure 1. The sieving was done using a powered sieve machine (Figure 2a) and blending was done using a small concrete mixer (Figure 2b). The particle size distribution was determined according to ASTM C136-06. This sand was used in preparation of all the 70-30 BSM specimens in this study.
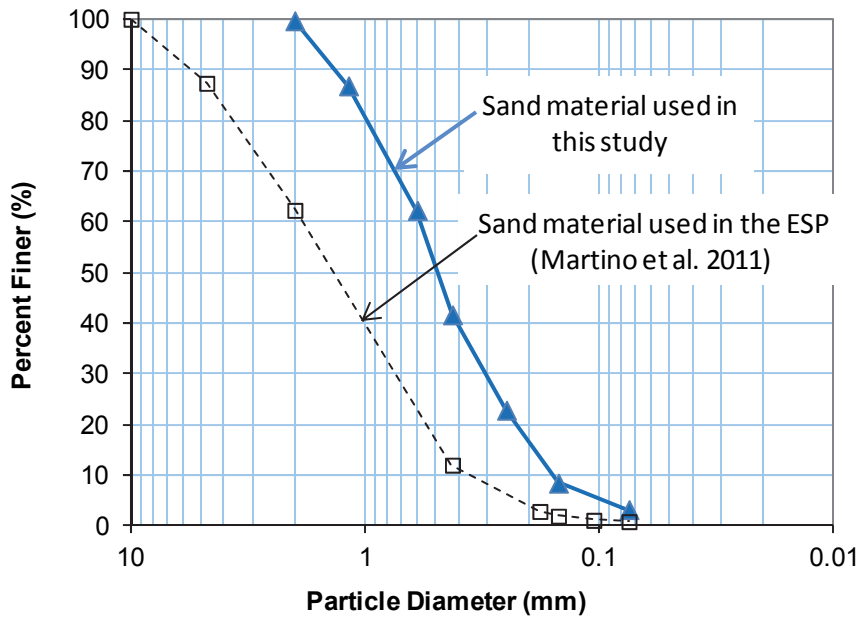
Figure 1: Particle-Size Distribution of Sand Used in This Study Compared to the Enhanced Sealing Project (ESP)'s Sand

**Figure 2: Equipment Used to Prepare Sand Component:
(a) Powered Sieve Machine; (b) Concrete Mixer**

2.3.3 Blending of Bentonite and Sand

Blending of the bentonite and sand materials was done by mixing and moisture conditioning small batches of oven dried raw materials on an as-required basis. This avoided material segregation that could occur when such dissimilar dry components were mixed and stored. Prior to initiation of this project, sufficient bulk supplies of bentonite and sand were stored separately to ensure uniformity of source materials for

the duration of this project. The stored materials were oven-dried (at temperature 110 ± 5°C for at least 24 hours according to ASTM D2216-10) prior to their use and then carefully weighed and mixed with pre-defined quantities of the solutions prepared for use.

2.3.4   Mineralogical and Chemical Evaluations of Bentonite and Sand

2.3.4.1 Mineralogy

To confirm the compositional suitability of the bentonite (very high swelling clay content), X-ray diffraction (XRD) analyses were completed on the National Standard bentonite material. Additionally, to confirm that the sand material used did not contain undesirable components (e.g., high calcite content, pyrite), XRD tests were also completed on the sand material.

Figures 3 and 4 show the XRD test completed on the National Standard bentonite material by the University of Manitoba, as well as traces collected from literature sources and supplied by Halliburton Industrial Products, the producer of National Standard Bentonite. These bentonite analyses show the consistency in the composition of Wyoming bentonites of the general type used in this study over more than a 20 year span. Minor variations in the peak magnitudes and minor components composition occur but these are not an issue with respect to material quality and in all cases the swelling clay content can be confidently reported as being >75% and likely closer to 80-90% of the solid phase of the bentonite (this report assumes a smectite content of 80% in the conduct of later analyses). These values are consistent with those reported for MX-80 used by SKB in their research program (Karnland 2010). This conclusion is also supported by the results of other material characterizations (e.g., high free-swell capacity (Section 3.1)) and the high liquid limit (Section 3.2) observed for the clay under distilled water (DW) conditions.

Figure 5 presents the results of the XRD tests completed on the sand used in this study and the mineralogical composition is summarised in Table 3. The composition of the sand was clearly a quartz and feldspar-dominated system with only minor content of calcite. These traces both clearly show a quartz-feldspar material and only a minor carbonate component. The semi-quantitative analysis completed by SGS on the sand sample showed 59% quartz, 38% various feldspars, and 3% calcite. It should be noted in Figure 5, that like the traces obtained for the bentonite materials, the wavelength of the X-rays used in the two analyses are different (Cu and Co), resulting in different angles where X-ray diffraction is observed.

(From University of Manitoba, September 2011)

(From Haliburton Industrial Products (HIP*, September 2012)
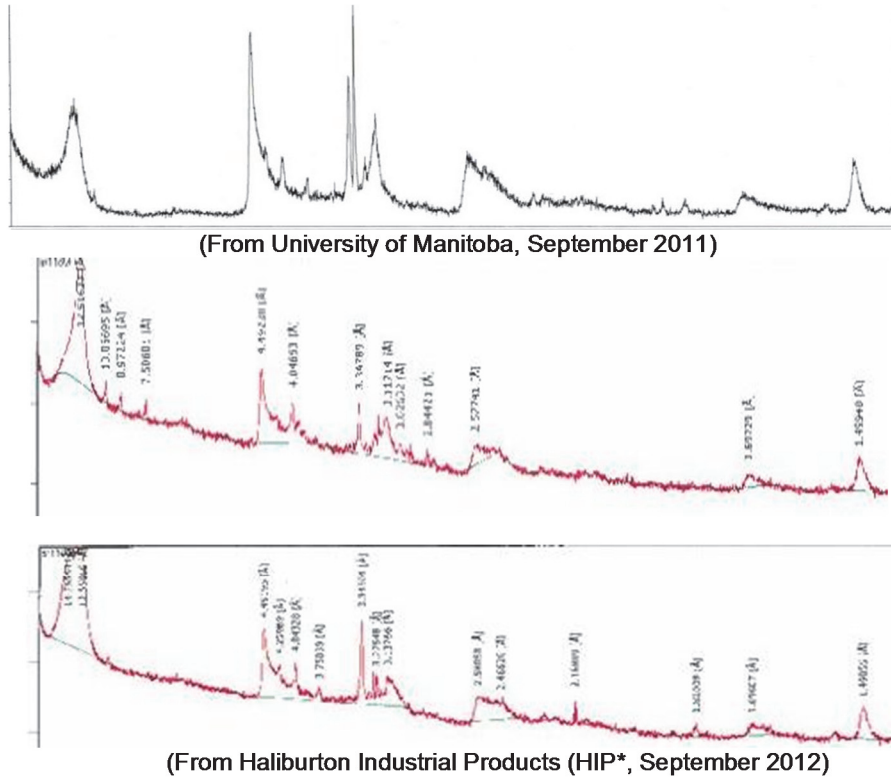
Note: Horizontal axis = Two-Theta (deg);
        Vertical axis = Intensity (%)

Figure 3: X-Ray Diffraction Traces for National Standard Bentonite

Diffraction patterns for Wy-2 Wyoming montmorillonite (Gautier et al. (2010))

Diffraction pattern for MX-80 Wyoming bentonite (Dixon and Miller (1995))
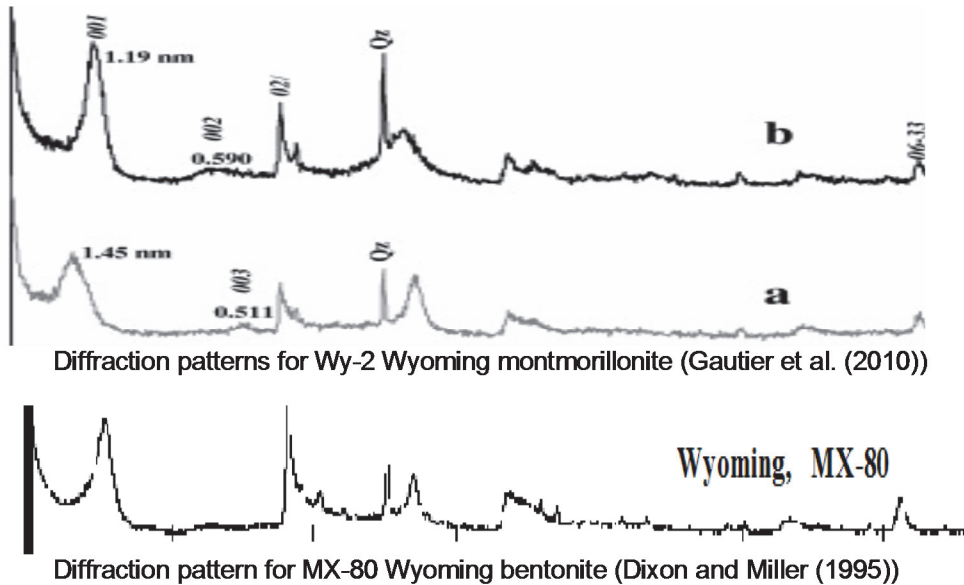
Note: Horizontal axis = Two-Theta (deg);
        Vertical axis = Intensity (%)

Figure 4: Typical X-Ray Diffraction Traces Obtained for Bentonites of the Type Used in the Current Study (Using Cu-Kα Wavelength)

01-079-1910 (C) - Quartz - SiO2
01-076-1819 (C) - Albite low - Na(AlSi3O8)
01-081-2027 (C) - Calcite, syn - Ca(CO3)
01-084-0709 (C) - Microcline - KAlSi3O8
01-075-0861 (C) - Tremolite - Na.38K.12Ca1.8Mg5Fe.01Al.24Si7.84O24
01-076-0948 (C) - Anorthite - Ca(Al2Si2O8)
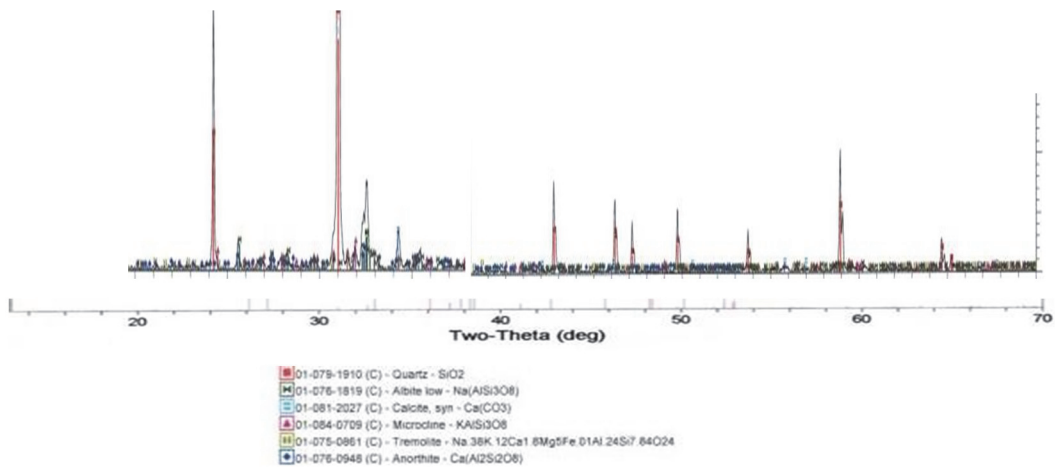
Diffraction Pattern for Sand Obtained Using Co-Kα Radiation (SGS)
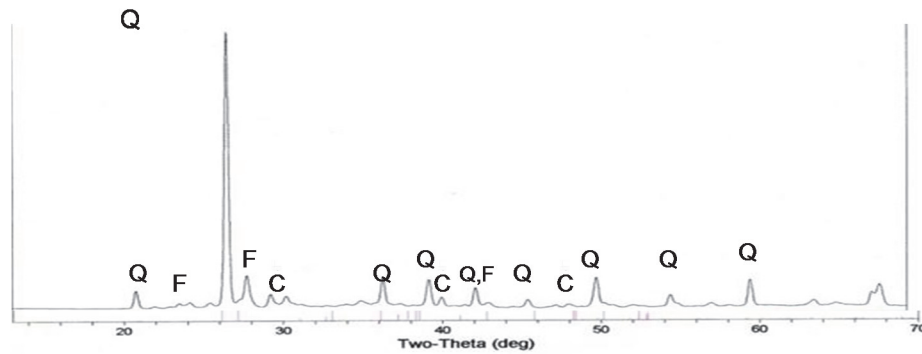
Diffraction Pattern for Sand Obtained Using Cu-Kα Radiation (University of Manitoba)

Note: Horizontal axis = Two-Theta (deg);
        Vertical axis = Intensity (%)

Figure 5: X-Ray Diffraction Traces for Sand

2.3.4.2 Chemical Composition

In addition to the mineralogical assessment completed on the bentonite and sand materials, a chemical assay was also done. These data, produced through X-ray florescence provide a measure of the elements present in these materials. The elemental composition is presented in Table 4, and show both samples are essentially identical. They vary only slightly in their chemical composition, which indicates that they are also similar mineralogically.

Table 3: Mineralogical Composition of Bentonite and Sand

Wt %	Bentonite Producer's Colony	Analyses Lovell	Sand SGS
Quartz	5	2	59.4
Feldspar (Orthoclase) ,	trace	---	---
Feldspar (Albite)	---	---	14.5
Feldspar (Anorthite)	---	---	8.3
Feldspar (Microcline)	---	---	11.8
Plagioclase feldspar (incl. Andesine)	trace	4	---
Calcite	---	trace	3
Opal	2	5	---
Clinoptilolite	---	trace	---
Dioctahedral smectite	91	85	---
Illite	2	4	---
Goethite	---	---	---
Pyrite	---	---	---
Tremolite	---	---	2.9
Goethite	---	---	---

Table 4: Chemical Composition of Bentonite and Sand

Wt %[+]	Bentonite						Sand
	HIP Colony*	HIP Lovell*	Literature (Dixon 1994)	Literature (Gautier et al 2010)	Literature (Gautier et al 2010)	SGS	Sand (SGS)
Si as SiO_2	66.32/**69.23**	64.06/**68.51**	63.6/**67.44**	67.65	68.06	58.8/**66.59**	79.6
Al as Al_2O_3	21.16/**22.09**	20.56/**21.99**	21.4/**22.69**	22.06	20.53	19/**21.5**	7.23
Ca as CaO	0.80/**0.84**	1.08/**1.16**	0.66/**0.7**	1.06	2.02	1.07/**1.21**	3.92
Na as Na_2O	2.09/**2.18**	2.52/**2.70**	2.7/**2.86**	1.5	1.34	2.23/**2.53**	2.04
Mg as MgO	2.59/**2.70**	2.27/**2.43**	2.03/**2.15**	2.8	2.94	2.24/**2.54**	0.76
Fe as Fe_2O_3	1.73/**1.81**	1.87/**2.00**	3.78/**4.00**	4.61	4.15	3.66/**4.15**	1.54
K as K_2O	0.29/**0.30**	0.30/**0.32**	0.31/**0.33**	0.2	0.69	0.53/**0.60**	1.31
Cr as Cr_2O_3	0.01	0.03	---	---	---	---	0.02
Mn as MnO	0.08	0.04	---	0.01	0.13	0.02	0.03
Ti as TiO_2	0.12	0.18/**0.19**	---	0.11	0.15	0.14/**0.16**	0.13
V as V_2O_5	0.05	0.02	---	---	---	---	---
LOI	<4.2**/0	<6.5**/0	5.7/0	0	0	11.7/0	2.89
Sum	99.5 est	99.5 est		100	100	99.5	99.5
S	0.3 est	0.3 est	Nr	Nr	Nr	0.27	---
C(t)	0.3 est	0.3 est	Nr	Nr	Nr	0.3	0.63

[+] Loss on Ignition (LOI) varies, resulting in variation in results. To normalise the analysis to solids-only components the values reported in literature have been corrected to eliminate the water component (revised data presented in bold-red in this table)
*Samples from two separate bentonite deposits used to produce commercial bentonite products.
** Values include structural water components.
Note: "est" is estimated quantity in bentonite assuming S and C values for SGS are the same as in the manufacturer's specimens.
HIP = Halliburton Industrial Products, producers of National Standard Bentonite.
Nr = not reported in analysis

3. GEOTECHNICAL CHARACTERIZATION

A series of basic physical and mechanical tests have been completed on the 70-30 bentonite-sand mixture, as well as for the bentonite on its own for the free-swell and consistency limits tests, in order to determine the geotechnical properties of the shaft backfill with the effect of groundwater salinity. These geotechnical characterizations include:

- free swell tests,
- consistency (Atterberg) limits tests,
- modified compaction tests,
- swelling pressure and hydraulic conductivity tests,
- triaxial and 1D-consolidation tests to determine mechanical properties,
- gas permeability tests, and
- determination of soil-water characteristic curve (SWCC).

3.1   Free Swell Tests

Free Swell Index (FSI) is a measure of the ability of a material to swell under conditions of no confinement and unlimited supply of water. In total there were two material formulations (100% bentonite and 70-30 bentonite-sand mixture (BSM)) and four liquid compositions tested (i.e., DW, CR10, SR160, and SR270). Each free swell test was replicated three times in order to increase confidence in the results obtained. FSI is normally expressed as millilitres in a water-filled volumetric cylinder occupied by 2 grams of loose, oven-dried clay (it is sometimes also expressed in terms of mL/g) (e.g., ASTM D5890-11, Lee and Shackelford 2005). Table 5 provides a summary of the results obtained, showing the substantial detrimental effect of salinity on clay swelling.

Table 5: Free Swell Index (FSI) of 100% Bentonite and 70-30 BSM (mL/2g)

Material	Liquid	TDS (g/L)	Dry weight (g)	Final Volume (mL)			Free Swell Index (mL/2g)			
				Trial 1	Trial 2	Trial 3	Trial 1	Trial 2	Trial 3	Average
100% Bentonite	DW	0	5	32	34	-	12.8	13.6	-	13.2
100% Bentonite	CR10	10	5	26	26	27	10.4	10.4	10.8	10.5
100% Bentonite	SR160	160	5	16	17	16	6.4	6.8	6.4	6.5
100% Bentonite	SR270	270	5	10	10	10	4.0	4.0	4.0	4.0
70-30 BSM	DW	0	5	20	-	25	8.0	-	10.0	9.0
70-30 BSM	CR10	10	5	19	18	18	7.6	7.2	7.2	7.3
70-30 BSM	SR160	160	5	11	10	11	4.4	4.0	4.4	4.3
70-30 BSM	SR270	270	5	8.5	9	8.5	3.4	3.6	3.4	3.5

Figure 6 shows that the Free Swell Index (FSI) (mL/2g) versus the solution concentration (Total Dissolved Solid (TDS) (g/L)) for 100% bentonite and 70-30 BSM. Figure 7 shows the photographs of selected free swell tests at the end of the tests. As expected, for the same material, an increase of TDS results in a decrease of FSI. For solutions with

similar TDS concentration, the FSI of 100% bentonite is greater than the 70-30 BSM, by approximately 30% (the difference in the amount of smectite present). The 100% bentonite and 70-30 BSM materials appear to maintain at least a small free swell capacity in solutions having up to 160 g/L TDS, but once TDS reached 270 g/L, essentially no swelling capacity remained in the loose material and the FSI represents a volume close to what would be occupied by a non-swelling material of similar granularity (e.g., crushed illitic shale has a FSI ~2 (Quigley 1984; Dixon 1995)).
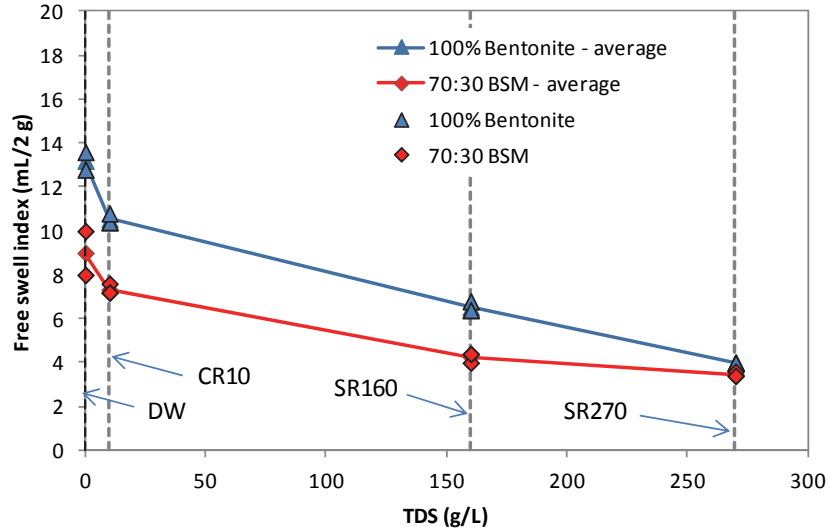
Figure 6: Results of Free-Swell Tests

(a) Free Swell Tests of 100% Bentonite with Different Solutions

(b) Free Swell Tests of 70-30 Bentonite-Sand Mixture with Different Solutions
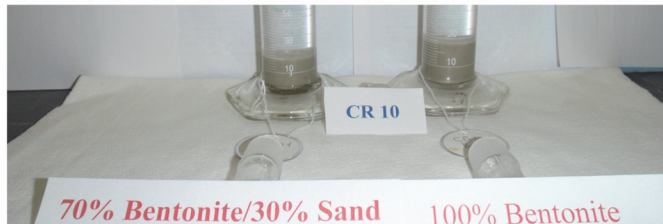
(c) Free Swell Tests in CR10-solution: 70-30 Bentonite compared to 100% Bentonite

Figure 7: Photographs of Selected Free-Swell Tests

3.2   Consistency (Atterberg) Limits

Consistency (Atterberg) Limits provide a measure of the gravimetric water content at which a soil changes its deformation behaviour from plastic to semi-solid states (plastic limit, PL) and from plastic to semi-liquid states (liquid limit, LL). Both the 100% bentonite and the 70-30 BSM were tested in each of the four groundwater compositions in order to provide a measure of the effect of salinity on the deformation characteristics of these materials. The LL of the clay under distilled water conditions also provides a means of estimating the relative abundance of smectite in the raw clay. A very high LL (>250%) in distilled water is indicative of a high smectite content. High quality bentonites (>75% montmorillonite) from Wyoming are typically quoted as having LL of 450-550 % (by dry weight). The difference between LL and PL is the Plasticity Index (PI) which is the range of water content over which a soil behaves plastically. These tests are conducted according to the ASTM D4318-10 and the results are provided in Table 6.

Table 6 shows that the bentonite used in this study has a LL of >500% in distilled water, which is consistent with a material of very high montmorillonite content. Based on these results a conservative estimate of 80% smectite content in the bentonite was used in the evaluation of the behaviour of the shaft backfill. As expected, the addition of a non-swelling component reduces the LL of the clay or bentonite-sand mixture under each liquid composition evaluated. For a given material (100% bentonite or 70-30 BSM), an increase of the TDS concentration in the liquid used to prepare the specimens, also reduced their LL's (Figure 8). As with the free swell tests above, these LL tests indicate that under very high salinities, the 100% bentonite or 70-30 BSM materials behave much as a non-swelling material would.

Table 6: Consistency Limits Test Results

Solid	Pore fluid	Liquid Limit, LL (%)	Plastic Limit, PL (%)	Plasticity Index, PI (%)
70-30 BSM	DW	341*	31	309
70-30 BSM	CR10	124	30	94
70-30 BSM	SR160	51	26	24
70-30 BSM	SR270	30	22	8
100% Bentonite	DW	514*	67	447
100% Bentonite	CR10	155	28	127
100% Bentonite	SR160	66	23	43
100% Bentonite	SR270	41	31	10

* Such high Liquid Limit values in an untreated bentonite indicate a sodium-dominated material with a very high (>75%) swelling clay (montmorillonite) content.
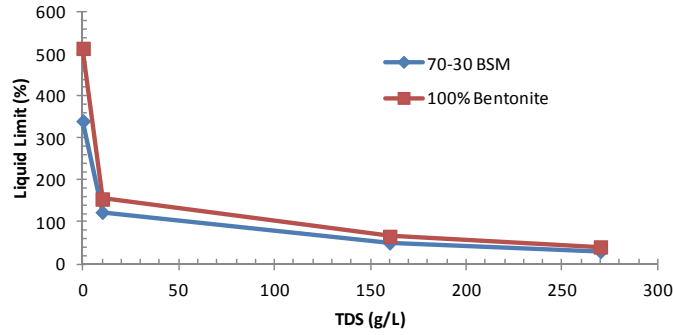
(a)
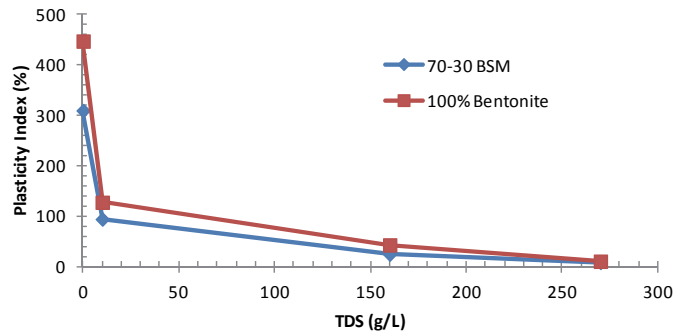
(b)

Figure 8: Liquid Limit (LL) and Plasticity Index (PI) of 100% Bentonite and 70-30 BSM for Different Pore fluids

3.3   Modified Compaction Tests

The effects of water content and composition on achieving a high degree of material densification using a fixed dynamic compaction effort is important with regards to determining how sensitive the material will be to the effects of any incoming water during the backfill placement process.

A series of compaction tests were completed for each of the four groundwater compositions considered in this project. Testing was done on both the 70-30 BSM (with four groundwater composition) and 100% bentonite material (with distilled water only) in order to evaluate the effect of aggregate on the densification behaviour of backfill. Compaction was done using a fixed-compaction effort approach (degree of compactive effort equivalent to the Modified (aka Heavy) Compaction as defined by ASTM D1557-78). The tests were done using a calibrated compaction device referred to as the "Miniature Compaction" mould (Figure 9), used for the tests (Dixon et al. 1985). This technique provides a means of completing a large range of compaction tests in a timely manner and using only a small quantity of material for each test sample. It should be noted that this device can only be used in materials having fine-grained aggregate component(s) as coarser materials will result in wall effects becoming evident. The particle size of the materials examined in this study were small enough that the effects of compaction mould size are not discernible (as per Dixon et al. 1985) and so there was

no need to adjust sand quantity of gradation in the conduct of the compaction tests and no sand particles were removed from the mixture to facilitate the test.

Figure 9: Miniature Compaction Mould (Inside Diameter = 32 mm)

The compaction tests included those done using distilled water as well as saline solutions as the mixing fluid (i.e., CR10, SR160 and SR270 solutions). Compaction tests done using distilled water as the mixing fluid do not require any special handling of the results during analysis, but those done using a saline solution need to be evaluated with the effects of salt addition considered. This is due to the fact that during oven-drying process to measure the water content of the compacted specimens, water will be removed, but the salt present in the pore fluid will remain with the soil. This salt adds dry weight of the specimen and affects the calculation of the zero air voids (ZAV). These corrections are done according to the ASTM D4542-07 procedure. The water content ($\bar{w}$) and dry density ($\overline{\rho_{dry}}$) corrected for the soluble salt content can be calculated using the following equations.

$$\bar{w} = \frac{w}{1-r-rw} \tag{1}$$

$$\overline{\rho_{dry}} = \frac{\rho}{1+\bar{w}} \tag{2}$$

where:
    ρ is the measured bulk density, which is the ratio of total mass to the total volume (m^3).
    r is the salinity of the solution, which is the ratio of mass of soluble salt in a unit mass of salt solution (unitless = kg/kg).
    w is the measured gravimetric water content during oven-drying process according ASTM D2216-10, which is the ratio of mass of water (M_w) to the mass of dry material remaining after oven-drying process (e.g., soil + salt) (unitless = kg/kg) and calculated as follows.

$$w = \frac{M_{wet}-M_{dry}}{M_{dry}} = \frac{M_w}{M_{soil}+M_{salt}} \tag{3}$$

where:
    M_{wet} is mass of specimen prior to oven-drying process (kg).

M_{dry} is mass of specimen after oven-drying process (kg).
M_w is mass of water (kg).
M_{soil} is dry mass of soil solid (kg).
M_{salt} is mass of salt remaining after oven-drying process (kg).

The results obtained from the modified compaction tests are presented in Table 7 and the water content versus dry density before and after the correction for the soluble salt component are shown in Figure 10a and 10b, respectively.

Without the correction due to salt content, the plots also show sensitivity of the compaction characteristics to the groundwater composition (Figure 10a). The higher is the salinity of the solution, the greater is the dry density that can be achieved for a given compaction effort. Table 7 summarized the results of the maximum dry density and optimum moisture content (w) (OMC). The maximum dry density increased consistently from 1.82 to 1.93 Mg/m^3 as salinity went from zero to 270 g/L. Similarly, the gravimetric water content needed for achieving maximum compaction density decreased from ~16% to ~12% as salinity increased.

Figure 10b shows the analyses of dry densities ($\overline{\rho_{dry}}$) and water content ($\overline{w}$) corrected due to salt solution according to Equations (1) and (2) for the 70-30 BSM material. After correction due to salt solution, the maximum dry densities and optimum corrected water contents show apparently low sensitivity to salt content. The maximum dry density for different pore fluid is between 1.82 to 1.86 Mg/m^3 and the optimum moisture content is between 15 to 16%. The compacted density test results proved to be much higher than initially anticipated (dry density of >1.80 Mg/m^3 as opposed to the originally anticipated 1.60 Mg/m^3), based on data previously reported. Because the fluids have different densities, the ZAV for each fluid are also different and they are shown in Figure 10b. All the data points are always located under the ZAV lines.
Figures 10a and 10b also show the compaction data obtained for 100% bentonite using deionised water. The maximum dry density of the 100% bentonite is substantially less than the 70-30 BSM (i.e., 1.63 Mg/m^3 versus 1.82 to 1.93 Mg/m^3). If these values are compared based on the Effective Montmorillonite Dry Density (EMDD) parameter, the 100% and the 70-30 BSM have values of 1.42 and 1.45 Mg/m^3 respectively for a freshwater-compacted material. This indicates that in a freshwater environment the materials should exhibit very similar swelling pressure and hydraulic conductivity behaviour. Calculation of the EMDD are discussed in Section 3.4.1

As the values obtained in the compaction trials were higher than initially anticipated for maximum dry density of a 70-30 BSM, the reference density for testing was increased from 1.60 to 1.80 Mg/m^3 and deformation, gas permeability, hydraulic conductivity and swelling pressure testing was done at this new, higher density. This density increase adversely affected the ability to complete the initially planned triaxial consolidation testing under low salinity conditions and made conduct of other tests problematic. As a result, some changes in initially planned test methodologies were required (see Sections 3.4 and 3.5).

Table 7: Modified Compaction Test Results

Material	Liquid	Without Salt Correction		With Salt Correction	
		Max Dry Density (Mg/m^3)	OMC* (%)	Max Dry Density' (Mg/m^3)	OMC'* (%)
70-30 BSM	Distlled Water (DW)	1.84	16	1.83	16
70-30 BSM	CR10 Solution	1.84	15	1.83	16
70-30 BSM	SR160 Solution	1.90	13	1.86	16
70-30 BSM	SR270 Solution	1.93	12	1.86	16
100% Bentonite	Distilled Water (DW)	1.61	23	1.61	23

* OMC= Optimum Moisture Content, water content at which maximum densification) is achieved.

* OMC'= Optimum Moisture Content, water content after correction due to salt content $(\overline{w})$ at which maximum densification is achieved.
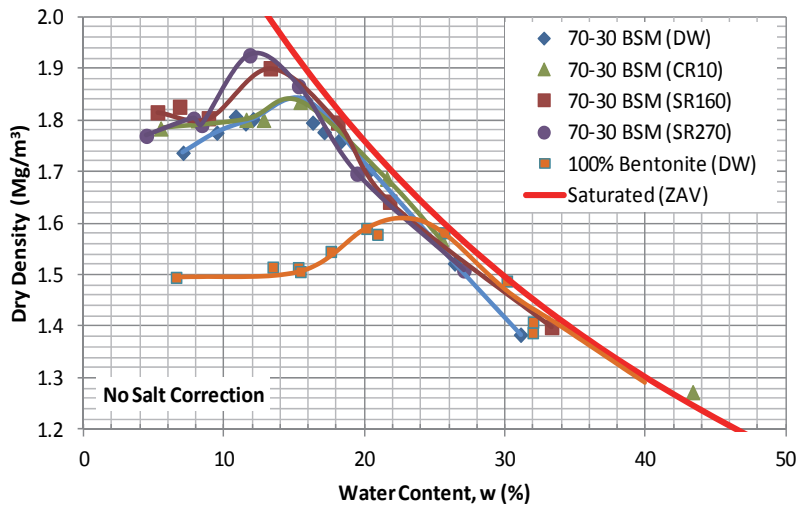
(a) Before Correction for salt content
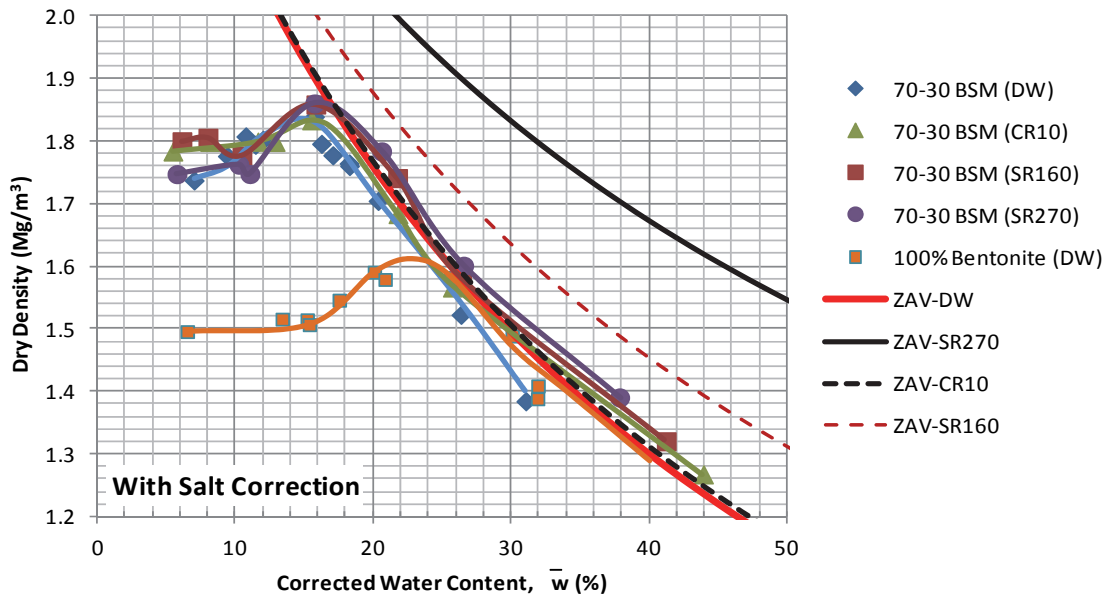
(b) After Correction for Salt Content

Figure 10: Dry Density-Water Content Relationships for 70-30 BSM Prepared Using Reference Solutions

3.4 Swelling Pressure (P_s) and Hydraulic Conductivity (K_w) Tests

The 70-30 BSM proposed for use in shaft backfilling needs to have its swelling pressure and hydraulic conductivity characteristics established through laboratory measurement. The testing methods used to obtain these values are described by Dixon (1995). The original testing plan was to prepare all the specimens using distilled water and then use four different fluids to percolate the specimens. This would simulate a DGR where the backfill would likely be prepared using deionised water and the local saline groundwater would subsequently saturate the backfill. In order to be consistent with other testing and characterization programs, NWMO requested that similar fluids be used to prepare and percolate the specimens. Specimens CR10-1600-1, CR10-1700-1, and CR10-1800-1 were prepared prior establishing this protocol and so they were made with distilled water and percolated with the CR10 solution. As the CR10 solution has relatively low salinity (~10 g/L TDS), no substantially different behaviour was anticipated for specimens prepared with distilled water and CR10 solution. The remaining of the tests used similar fluids to prepare and percolate the specimens. Having similar fluid for mixing and percolating the specimens makes interpretation of the results simpler as there is no uncertainty regarding the chemical composition of the pore fluid.

Additionally, the target dry densities of the first three specimens percolated with distilled water were 1.55, 1.60, and 1.65 Mg/m^3 (i.e., DW1550-1, DW1600-1, and DW1650-1). Like the first tests done with CR10 solution, these three tests were started prior to the increase of the target dry density of the backfill from 1.65 to 1.80 Mg/m^3. As a result several additional tests were done at a target density of 1.80 Mg/m^3.

The method of preparing the specimens for use in determining the swelling pressure (P_s) and hydraulic conductivity (K_w) means that their as-built state will likely vary somewhat from the target. This is usually associated with specimen rebound following installation in the test cell or installation of the pressure transducers after initial thickness measurement. Consequently, the mass and volume measurements made immediately before and after test completion were used to initially define the specimen's density. End-of-test densities were determined from the measured masses (wet and dry), an assumption that the specimens were solution-saturated and that the porefluid had the same composition and density as the solution percolated through it. The range of densities examined allowed for confirmation that these materials followed the pre-established EMDD-P_s and EMDD-K_w relationships for smectite-rich materials. Once the EMDD relationship was confirmed, the density needed to achieve target swelling pressure (P_s) or hydraulic conductivity (K_w) were defined using the existing formula.

3.4.1 Calculation of Effective Montmorillonite Dry Density (EMDD)

The calculation of the EMDD in this document was done using the following method. The smectite minerals dominate the behaviour of the clay fraction in the bentonites and the smectite content in bentonite varies from different global sources. The term 'effective montmorillonite dry density' (EMDD) was derived (Baumgartner and Snider 2002) to single out the role of montmorillonite in soil behaviour and is expressed as follows:

$$\text{EMDD} = \frac{M_m}{(V_m + V_v)} = \frac{f_m \cdot f_c \cdot \rho_d}{\left[1 - \left(\frac{(1-f_c) \cdot \rho_d}{G_a \cdot \rho_w}\right) - \left(\frac{(1-f_m) \cdot f_c \cdot \rho_d}{G_n \cdot \rho_w}\right)\right]} \tag{4}$$

where: ρ_d = dry density of soil (kg/m^3);

$\quad\quad \rho_w$ = density of water (kg/m^3);

$\quad\quad f_c$ = mass fraction of clay in dry solids;

$\quad\quad f_m$ = mass fraction of montmorillonite in clay fraction f_c;

$\quad\quad G_a$ = specific gravity of aggregate solid;

$\quad\quad G_n$ = specific gravity of non-montmorillonite component in clay;

$\quad\quad G_s$ = specific gravity of all soil solids;

$\quad\quad M_m$ = mass of montmorillonite component (kg);

$\quad\quad V_m$ = volume occupied by montmorillonite component (m^3); and

$\quad\quad V_v$ = volume of void (m^3).

The following coefficients were used to calculate EMDD for the 70-30 BSM for this study: G_s = 2.72, f_m = 0.8, f_c = 0.7, G_a = 2.65, and G_n=2.645.

3.4.2 Test Results

As previously described, testing was originally planned such that three dry densities that span the target as-placed dry density (1.60 Mg/m^3) would be tested for each of the four groundwater compositions considered. These data would be compared to the results produced through use of the EMDD parameter developed to allow for material behaviour prediction and the existing literature database. As the results of the compaction testing resulted in an increase in the target density of the backfill to 1.80 Mg/m^3 and this new, higher density was used as the target maximum dry density for the sets of three tests. At a dry density of 1.80 Mg/m^3 (EMDD=1.44 Mg/m^3) the 70-30 BSM is anticipated to exhibit much more substantial P_s and lower K_w values than initially planned for. This resulted in an increase in the testing time required since lower K_w and higher P_s properties values were present.

An increase of reference dry density also complicated the conduct of triaxial and 1D-consolidation testing to determine mechanical properties at the reference dry density. As the reference dry density increases, higher pressure was required to be applied in the triaxial and 1D-consolidation tests. The required pressure for triaxial testing corresponding to the reference dry density was greater than the maximum capacity of the triaxial apparatuses, especially for testing with distilled water. Consequently, 1D-consolidation tests were added to increase the maximum pressure that can be used in the tests. A new 1D-consolidation test apparatus set-up was developed in order to test the 70-30 BSM at reference dry density. This new 1D-consolidation cell had larger cross section area to accommodate sand component in the 70-30 BSM, and larger area means greater load. Further discussions of the triaxial and 1D-consolidation tests are described in Sections 3.5 and 3.6.

Figure 11 shows the hydraulic conductivity and swelling pressure test set-up. In total 12 testing systems were used with 4 sets of 3 cells used (each set containing one of the four different percolating liquids (i.e., distilled water, CR10, SR160, and SR270 solutions)). A load cell was used to measure the swelling pressure in each of the testing cells so each cell measured swelling pressure and hydraulic conductivity on the same

specimen. Pressure transducers were used to monitor the hydraulic pressure applied to the liquid reservoir.

Figures 12, 13, 14, and 15 show the swelling pressure versus time for each of the tests percolating with different liquids. Swelling pressure was defined based on the effective stress concept (i.e., swelling pressure = total pressure – average hydraulic pressure acting across the specimen). The vertical shifts present in these plots were typically followed by return of the swelling pressure to its previous values and was the result of changing the hydraulic head on the specimens, or closing of the outflow valve, both of which change the hydraulic head in the test cells and required some time to equilibrate. The time needed to complete each of the swelling pressure tests ranged from 25 to 225 days, depending on the target dry densities and types of liquids.

Table 8 summarizes the results of the swelling pressure and hydraulic conductivity tests. The properties in Table 8 were measured at the end of the test, when the specimen reached swelling pressure equilibrium. The gravimetric water content (w) was the water content measurement from oven-dry process according to ASTM Standard 2216-10. The corrected water content due to salt content ($\overline{w}$) and dry density were calculated according Equations (1) and (2) based on ASTM D4542-07. Equation (4) was used to calculate the EMDD from dry density.

Six (6) Apparatus for Testing Using DW and CR10 Solutions

Six (6) permeability board ready for tests using SR160 and SR270 solutions

Figure 11: Swelling Pressure and Hydraulic Conductivity Tests Set-up
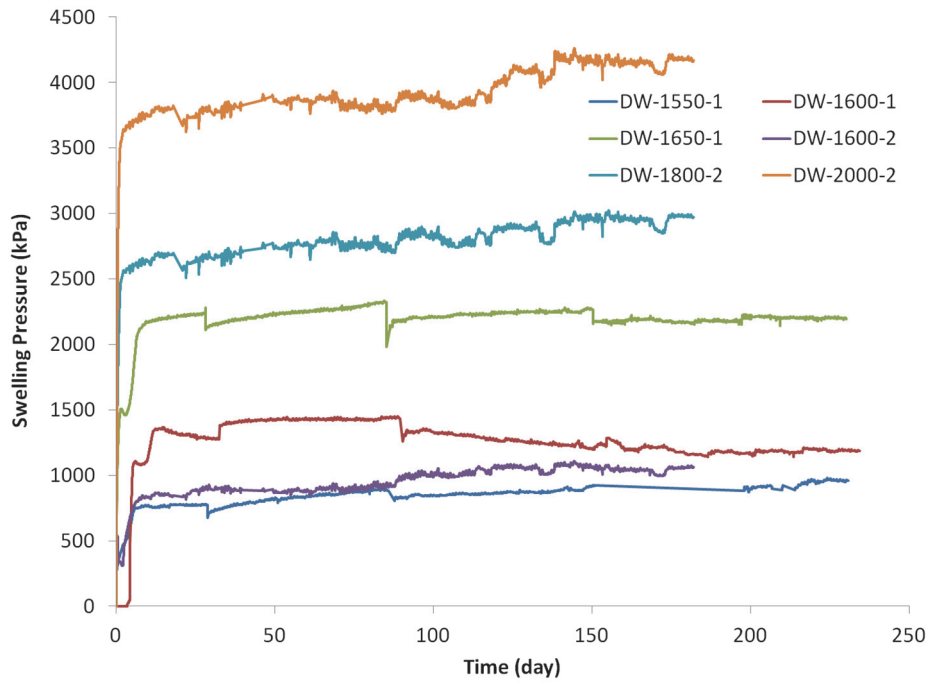
Figure 12: Swelling Pressure versus Time for Specimens Percolated with Distilled Water
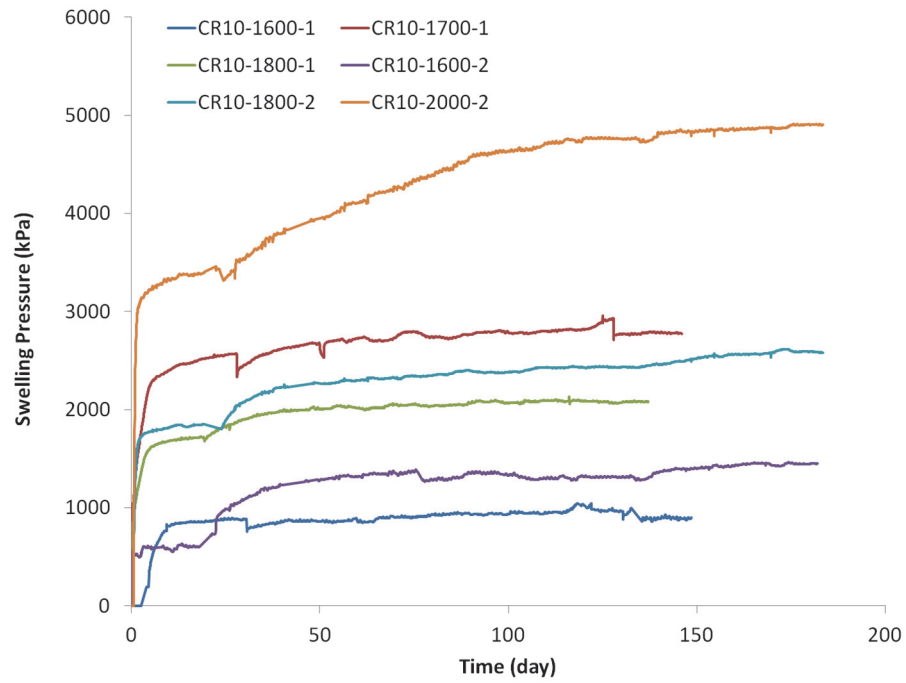
Figure 13: Swelling Pressure versus Time for Specimens Percolated with CR10 Solution
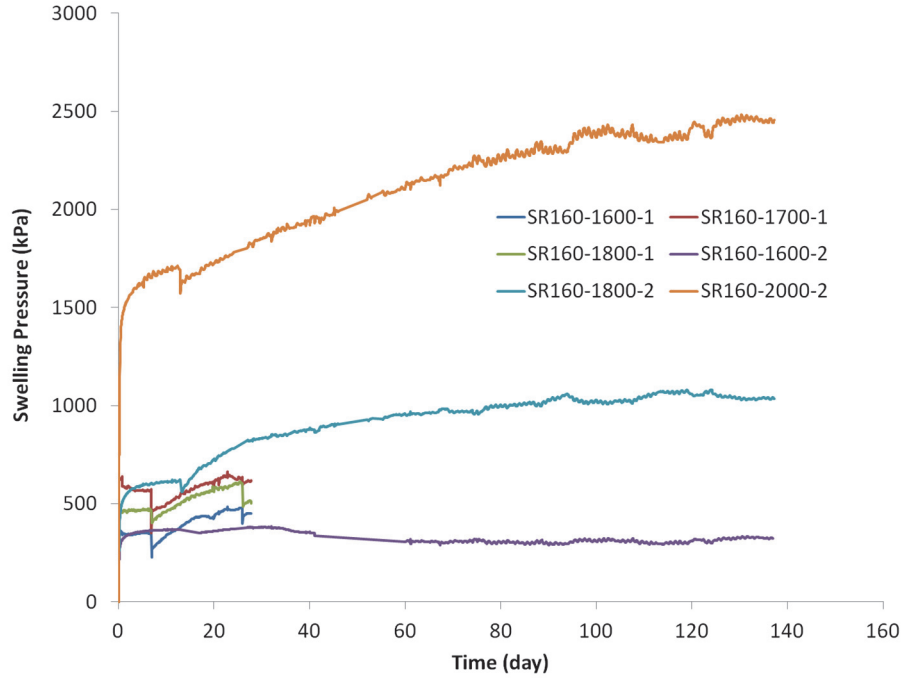
Figure 14: Swelling Pressure versus Time for Specimens Percolated with SR160 Solution
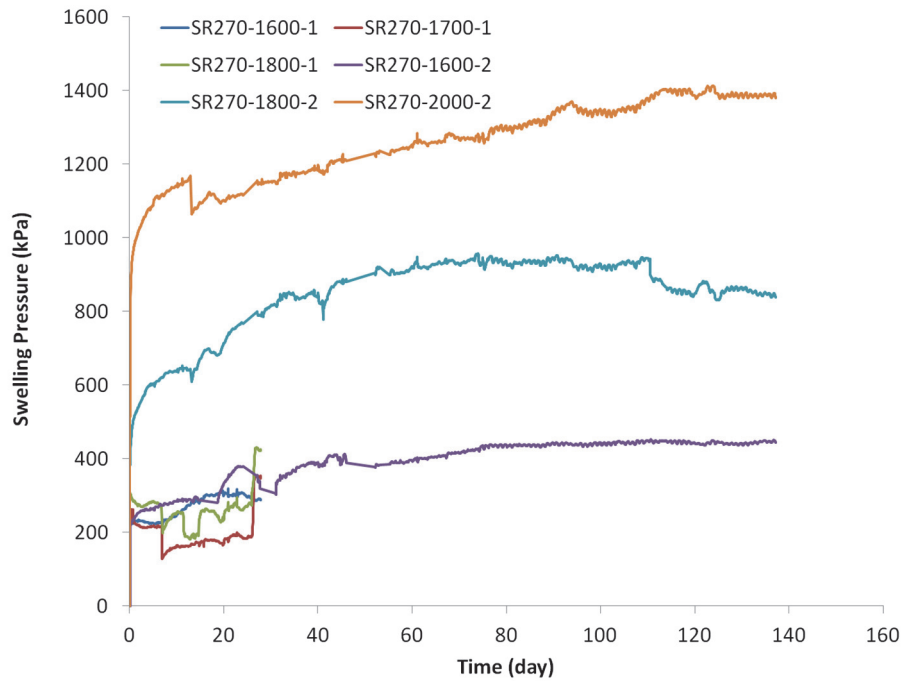
Figure 15: Swelling Pressure versus Time for Specimens Percolated with SR270 Solution

Table 8: Summary of Swelling Pressure and Hydraulic Conductivity Results

Specimen	Mixing liquid	Percolating liquid	Gravimetric water content, W (%)	Corrected water content, w̄ (%)	Dry density Mg/m³	EMDD Mg/m³	Swelling Pressure, P_s (kPa)	Hydraulic Conductivity K_w (m/s)
DW1550-1	DW	DW	34.71	34.71	1.40	1.02	960	4.27E-13
DW1600-1	DW	DW	31.52	31.52	1.46	1.08	1190	2.59E-13
DW1650-1	DW	DW	26.57	26.57	1.58	1.20	2200	1.57E-13
DW1600-2	DW	DW	32.26	32.26	1.45	1.07	1060	6.52E-13
DW1800-2	DW	DW	24.94	24.94	1.62	1.24	3000	1.48E-13
DW2000-2	DW	DW	20.88	20.88	1.73	1.36	4200	1.91E-13
CR10-1600-1	DW	CR10	30.80	31.21	1.47	1.09	900	6.83E-13
CR10-1700-1	DW	CR10	24.27	24.58	1.63	1.25	2780	2.33E-13
CR10-1800-1	DW	CR10	26.51	26.84	1.57	1.19	2080	3.13E-13
CR10-1600-2	CR10	CR10	28.88	29.25	1.52	1.14	1450	5.28E-13
CR10-1800-2	CR10	CR10	24.73	25.04	1.62	1.24	2580	2.24E-13
CR10-2000-2	CR10	CR10	20.88	21.13	1.74	1.37	4900	1.25E-13
SR160-1600-1	SR160	SR160	21.77	26.43	1.65	1.27	450	2.75E-12
SR160-1700-1	SR160	SR160	22.15	26.91	1.64	1.26	615	1.70E-12
SR160-1800-1	SR160	SR160	21.65	26.27	1.65	1.28	515	1.31E-12
SR160-1600-2	SR160	SR160	25.00	30.52	1.55	1.17	320	1.55E-11
SR160-1800-2	SR160	SR160	20.65	25.02	1.68	1.31	1035	1.65E-12
SR160-2000-2	SR160	SR160	15.33	18.40	1.87	1.52	2450	2.28E-13
SR270-1600-1	SR270	SR270	21.40	29.61	1.62	1.24	290	3.83E-11
SR270-1700-1	SR270	SR270	20.92	28.90	1.63	1.26	350	1.55E-11
SR270-1800-1	SR270	SR270	19.61	26.98	1.68	1.30	420	7.25E-12
SR270-1600-2	SR270	SR270	23.28	32.39	1.56	1.18	445	4.31E-11
SR270-1800-2	SR270	SR270	18.98	26.06	1.70	1.33	840	2.19E-11
SR270-2000-2	SR270	SR270	14.37	19.45	1.88	1.53	1380	7.00E-13

Figures 16 and 17 shows hydraulic conductivity (K_w) and swelling pressure (P_s) versus EMDD, respectively, from the shaft backfill examined in this project. Trend lines for each of the percolation liquids are shown in these figures. As expected, these trend lines indicate that an increase of EMDD results in an increase of swelling pressure and a decrease of hydraulic conductivity. An increase of the permeant liquid salinity also tends to increase hydraulic conductivity and decrease the swelling pressure. It can be seen in Figures 16 and 17 that there is little discernible difference in the results for systems tested with fresh (deionized) water and those for the low-salinity (CR10 solution). This is consistent with previously reported results and indicates that at the target, as-placed density, the system is not especially sensitive to small variations in the composition of the percolating fluid. Based on these data points, the K_w and P_s corresponding to the dry density of 1.80 Mg/m³ and EMDD of 1.44 Mg/m³ were calculated for each of the water types examined and are provided in Table 9.

Table 9: Swelling Pressures and Hydraulic Conductivities Corresponding to Dry Density of 1.80 Mg/m³ (EMDD=1.44 Mg/m³ (smectite = 80%)) for 70-30 BSM

Percolating Liquid	Hydraulic Conductivity* (m/s)	Swelling Pressure* (kPa)
Distilled water	8×10^{-14}	6500
CR10	7×10^{-14}	8000
SR160	4×10^{-13}	1500
SR270	3×10^{-12}	900

* calculated from equations shown in Figures 16-17
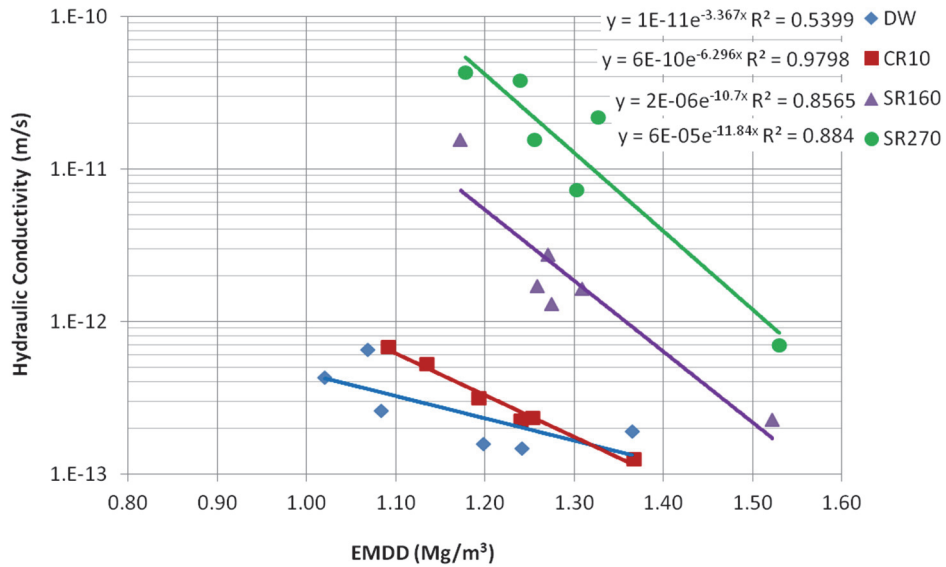
Figure 16: Hydraulic Conductivity versus EMDD for 70-30 BSM
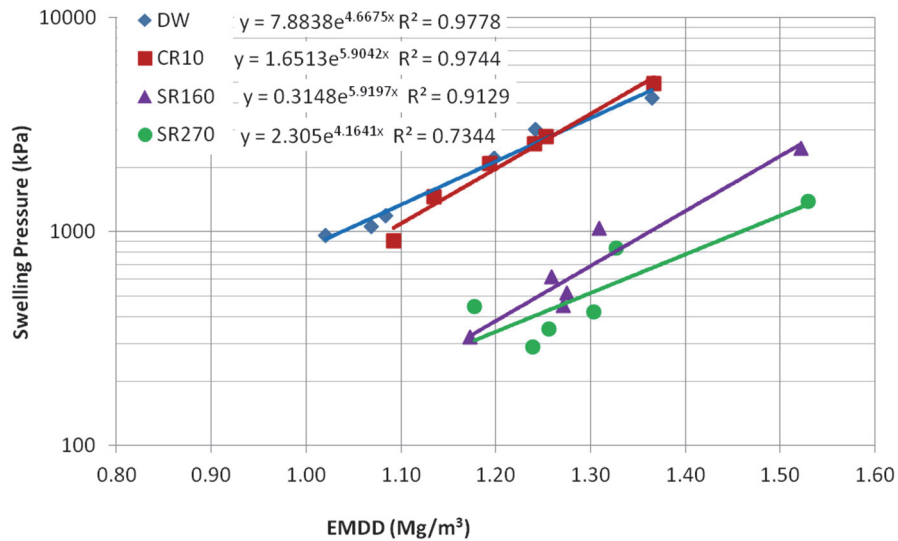
Figure 17: Swelling Pressure versus EMDD for 70-30 BSM

In Figures 18 and 19, the data from this study (Table 9, Figures 16 and 17) are compared to the trendlines generated from a large database (i.e., several hundred data values) of swelling pressure and hydraulic conductivity measurements for bentonites of various smectite contents and under similar pore fluid compositions found in literature.

As expected these new data show that for similar EMDDs, an increase of the percolating pore liquid salinity tends to increase hydraulic conductivity and decrease the swelling pressure of the specimens. The swelling pressure and hydraulic conductivity measurements made on the materials examined in this study are consistent with the database trend lines generated from a large literature-derived database of measurements, confirming the applicability of the EMDD concept to this proposed shaft backfill. This means that it should be possible to predict with confidence what the swelling pressure or hydraulic conductivity will be under a wide range of density and pore liquid compositions.
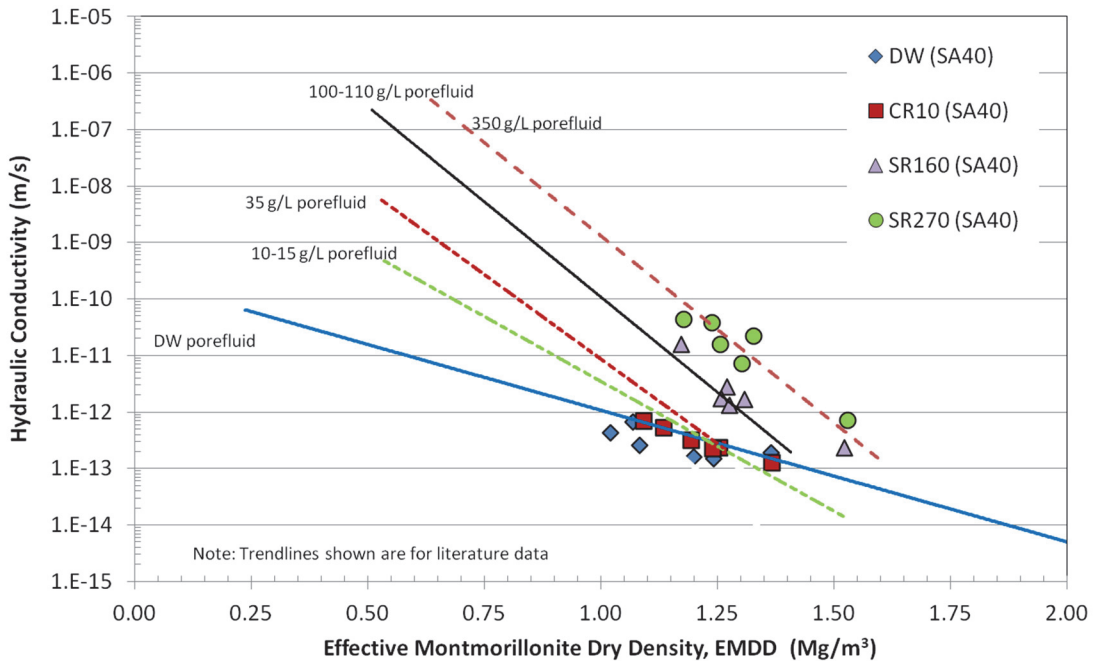
Figure 18: Hydraulic Conductivity versus EMDD from this Study Compared to Trend Lines Generated from Literature Data
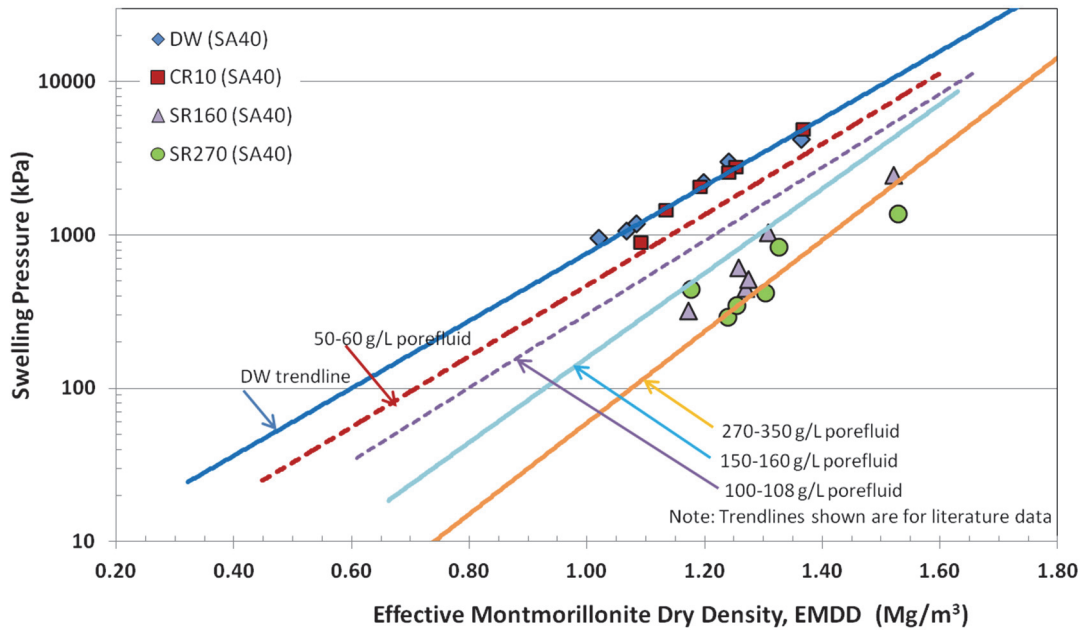
Figure 19: Swelling Pressure versus EMDD from this Study Compared to Trend Lines Generated from Literature Data

3.5 Triaxial Isotropic Consolidation and 1D-Consolidation Tests to Determine Mechanical Properties

3.5.1 Test Methods

The conduct of a series of isotropic (triaxial) consolidation tests was included as part of the original work scope for this project. Four (4) triaxial consolidation cells and frames at AECL's Geotechnical Laboratory were refurbished and commissioned for conduct of this activity (see Figure 20). Each cell was dedicated only for one type of solution to avoid any chance of mixing of the percolating liquid.

Several system trials using 70-30 BSM were undertaken in mid-October 2011 to determine the optimal manner of testing and confirm the ability of the triaxial system to determine the Bulk Modulus (K). Initial evaluation for a reference dry density of 1.60 Mg/m^3 indicated that the AECL triaxial system would be able to work over the entire range necessary to obtain bulk modulus measurements for the materials specified. Subsequently the reference backfill dry density was changed from 1.60 to 1.80 Mg/m^3 (EMDD increase from 1.22 to 1.44 Mg/m^3). This dry density increase resulted in a very substantial increase in the swelling pressure that must be counteracted in order to accomplish consolidation under reference dry density, where swelling pressure increased from approximately 2 MPa to greater than 4 MPa for specimen with distilled water or the low salinity CR10 solution. The four triaxial equipments have maximum cell pressure of 1.70 MPa and maximum back pressure of 0.20 MPa, corresponding to maximum effective stress of 1.50 MPa. Note that under saturated condition, the effective stress is the difference between cell and back pressures. This would be insufficient for the conduct of tests using low TDS solutions (DW and CR-10). Subsequent trials using the SR-160 and SR-270 solutions indicated that the triaxial

system might be usable for these materials, but this was not considered to be a certainty.
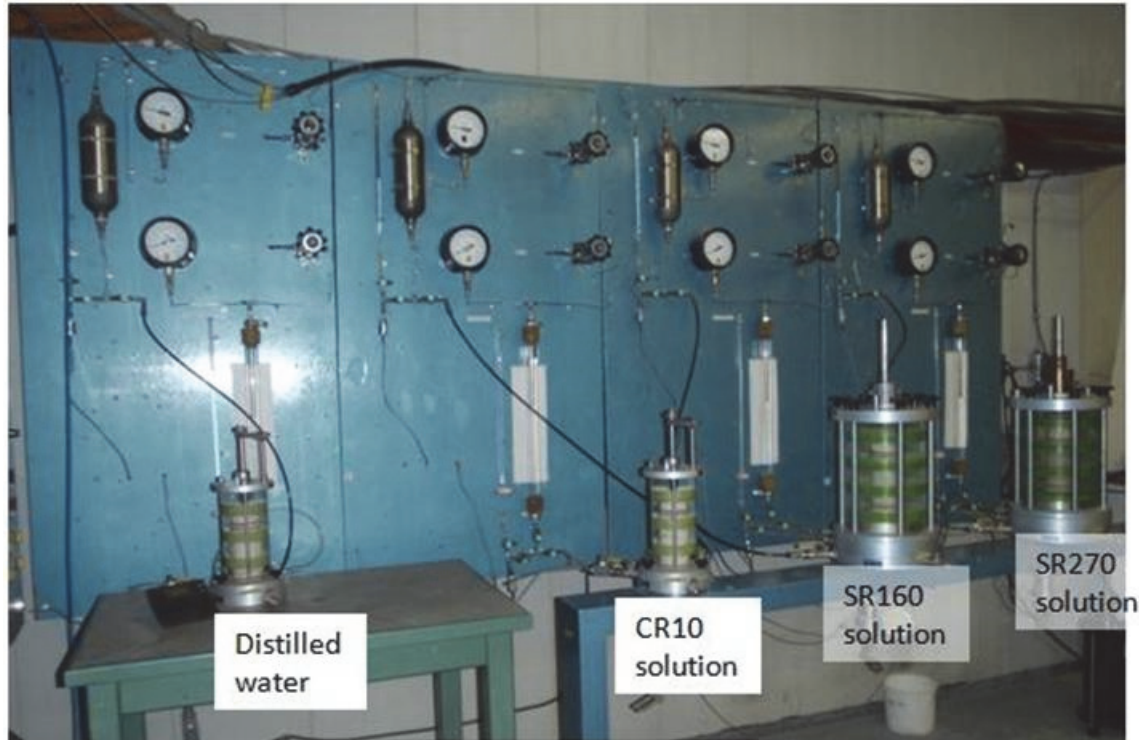
Figure 20: Four Triaxial Cells Used for Testing

In order to ensure successful completion of the mechanical properties tests needed in this study, 1D-consolidation rather than triaxial consolidation was selected for use in the distilled water and CR-10 specimens as well as for the saline specimens. The 1D-consolidation cells have a greater maximum pressure (>16 MPa) compared to the triaxial cell (1.70 MPa total stress), so they were used to complete the majority of the testing. The results of the triaxial and 1D-consolidation tests are presented in the following.

3.5.2 Isotropic Consolidation in Triaxial Tests

3.5.2.1 Preparation of Specimens and Preliminary Tests

The triaxial specimens were prepared to a target dry density of 1.80 Mg/m^3, and water content of 18%, which corresponds to the degree of saturation > 90%. At the beginning of the project, all the specimens were prepared using distilled water (DW) as the mixing liquid since it is anticipated that DW would be used to prepare the backfilling material in the DGR. It was subsequently decided that the mixing and percolating liquids should be similar. This approach was consistent with work being done elsewhere and it ensured that the salinity of the pore liquid would be consistent throughout the tests.

Table 10 summarizes initial properties of triaxial tests done as part of this study. The triaxial specimens were 50 mm in diameter and 90 mm in height. The specimens were precompacted in 5 lifts, this compaction method was consistent with previous tests done on the 50-50 BSM (e.g., Blatz 2000, Anderson 2002). Each specimen was compacted to pre-determined height and the compaction pressures for each lift were measured

using a pressure transducer. Some of the results of the compaction pressure measurements are shown in Figure 21. The peak load during compaction was in the range of 5 to 10 MPa. These values may correspond to preconsolidation pressure of the specimens, and were significantly greater than the maximum confining pressures that can be applied in the triaxial tests (~1.70 MPa cell pressure), so the preconsolidation pressure could not likely be observed using triaxial tests. This further demonstrated the reason why most of the testing was done using 1D-consolidation cells where loads up to 16 MPa were applied. Note that this was not the maximum capacity of the 1D-consolidation cell or loading frame.

Table 10: Initial Properties of the Triaxial Specimens

Specimen Name	TX-DW	TX-CR10	TX-SR160	TX-SR270*
Mixing Liquid	DW	CR10	SR160	SR270
Percolating Liquid	DW	CR10	SR160	SR270
Diameter (mm)	50.523	50.07	50.19	50.15
Height (mm)	91.18	91.95	92.26	92.26
Weight (g)	374.09	381.4	385.97	388.23
Water content (%)	18.40	19.81	17.69	16.39
Water content, corrected*(%):	18.40	20.05	21.32	22.32
Bulk density (Mg/m^3):	2.046	2.107	2.115	2.130
Dry density (Mg/m^3):	1.728	1.755	1.743	1.742
EMDD (Mg/m^3):	1.361	1.389	1.377	1.376

Note:
*Corrected water content was calculated using Equation (1). Correction was due to salt residue in specimens after oven-drying process.
**This specimen was terminated due to leakage.

Figure 22 shows the results of an initial swelling under constant confining pressure of the dry density the DW specimen. The specimen experienced significant swelling, even when cell pressure applied was 1.1 MPa. Because the cell's pressure limit was 1.7 MPa, the range of the load increment was very limited and the preconsolidation pressure of the specimen was not observed. It should be noted that due to large swelling in this triaxial specimen during initial saturation stage, the density of the specimen was significantly lower (1.2 Mg/m^3) than the reference dry density of 1.80 Mg/m^3. This specimen therefore did not provide the values needed at the reference dry density and so were retested using the 1D-consolidation methods. Details of the 1D-consolidation tests are provided in Section 3.5.3.
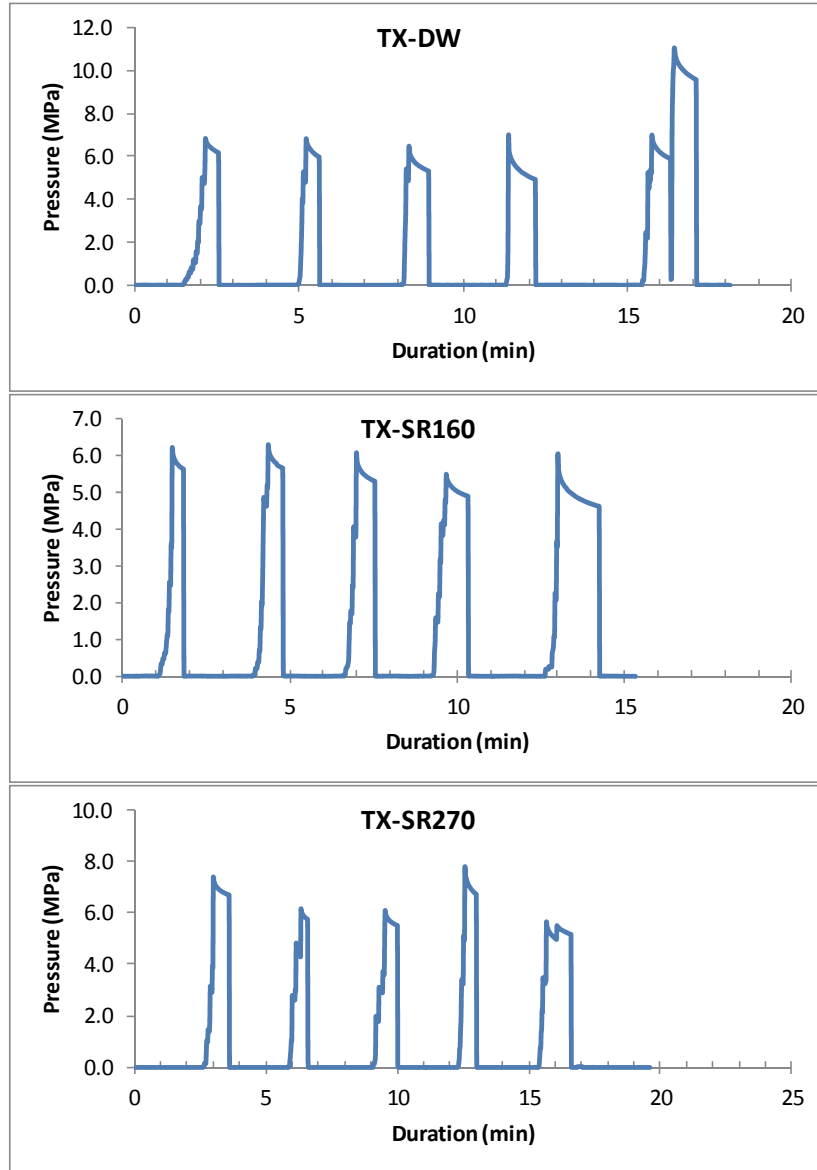
Note: The graphs for specimen TX-CR10 was not shown. The peak loads for specimen TX-CR10 were 5.5, 5.5, 8.0, 9.0, and 7.5 MPa for the 1st , 2nd, 3rd, 4th and 5th lifts, respectively.

Figure 21: Compaction Pressures Applied During Triaxial Specimen Preparation
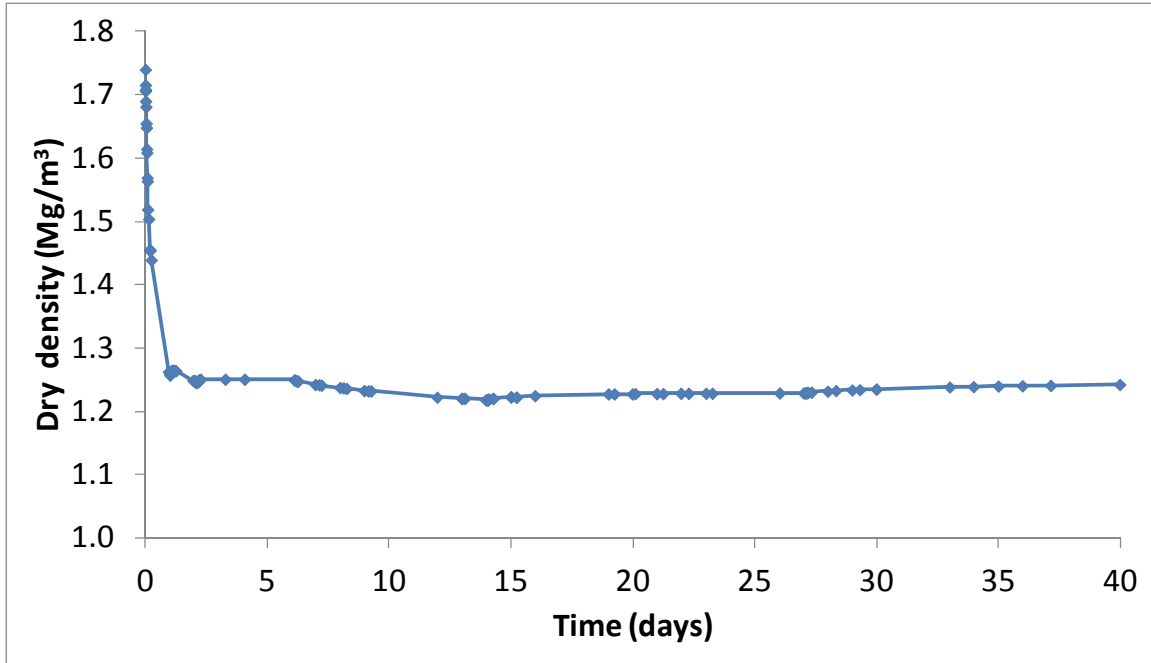
Figure 22: Initial Dry Density Change at the Beginning of Triaxial Test of Specimen Prepared with Distilled Water (Specimen TX-DW)

3.5.2.2 Results of Isotropic Consolidation in Triaxial Tests-Drained

Drained isotropic consolidation testing involved applying a constant confining pressure to the specimen while allowing (and measuring) water to leave (or enter) the specimen via the top and bottom drains associated with the specimen. The volume of water added to or expelled from the specimens was monitored using a burette. Cell and back pressures were monitored using pressure transducers. The effective stress was the difference between the cell pressure and the back pressure in a saturated specimen. Throughout the test, the back pressure was set to approximately ~200 kPa, except at the beginning of the test where the higher back pressure (~up to 400 kPa) was applied to reduce the saturation time. The measurements of the volume of water added to, or expelled from the specimens and the effective stress of each specimen are shown in Figures 23 to 26.

There was a problem associated with the triaxial test done using SR270 solution (specimen TX-SR270), where water continues to be lost from the closed system due to a slight leak in the back and cell pressure lines, as salt deposit could be observed at those locations. Consequently, the volume measurements for the SR270 specimen therefore would not be representative of what actually existed in the specimen. The results of this triaxial test cannot be used for further analyses. In this study, the results of the 1D-consolidation tests were more reliable, as the measurements of volume change was not affected by either the pore liquid composition or any pressurization system.

The relationship between mean effective stress (p′) and specific volume (V) for the four triaxial tests with different liquids (DW, CR10, SR160 and SR270 solutions) are shown in Figures 26(a) and 26(b). The specific volume corresponding to the reference dry density of 1.8 Mg/m^3 is also shown. The specimens with distilled water and CR10 solution (TX-DW and TX-CR10) experienced significant swelling prior to the start of loading, which

resulted in end-of-test dry densities that were lower than the reference dry density. Prior to the start of loading, specimens TX-DW and TX-CR10 had dry densities of approximately 1.2 Mg/m³ (V=2.2) and 1.5 Mg/m³ (V=1.8), respectively (Figure 26).

Almost no swelling was observed in Specimen TX-SR160, even when very low effective stress (~200 kPa) was applied to the specimens (see Figures 25). This shows how the high salinity liquid used to prepare the specimens may significantly affect the mechanical response of the specimens.
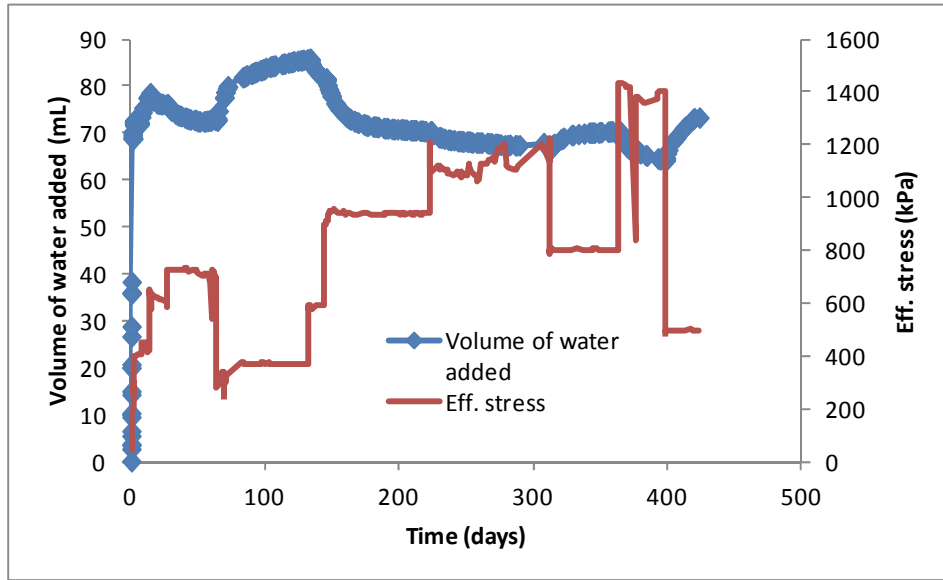
Figure 23: Volume of Water Added to Specimen and Effective Stress Measurements from Specimen TX-DW
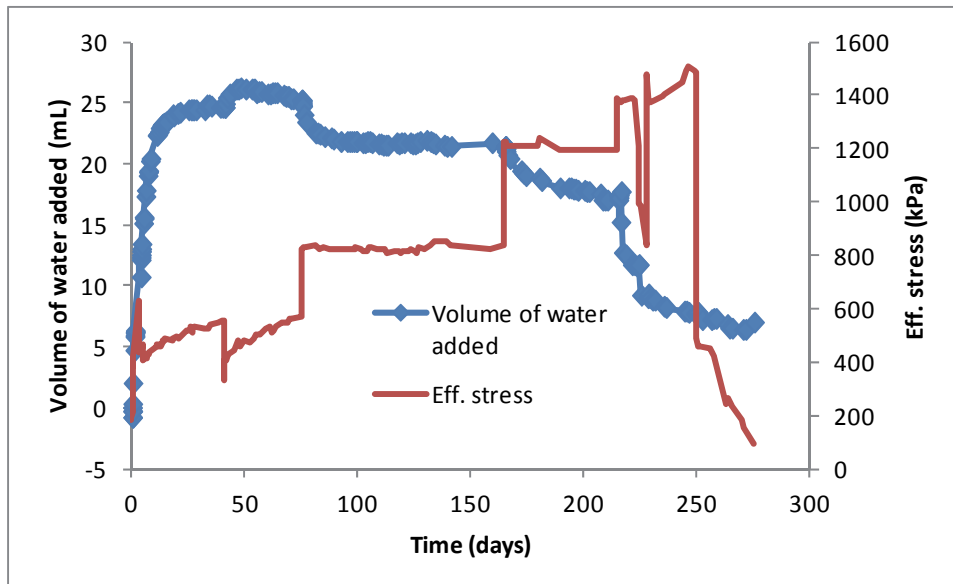
Figure 24: Volume of Water Added to Specimen and Effective Stress Measurements from Specimen TX-CR10
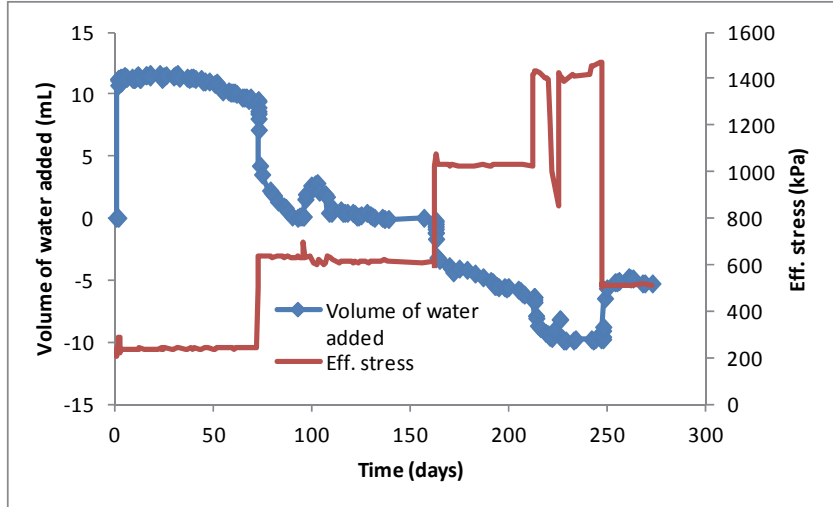
Figure 25: Volume of Water Added to Specimen and Effective Stress Measurements from Specimen TX-SR160
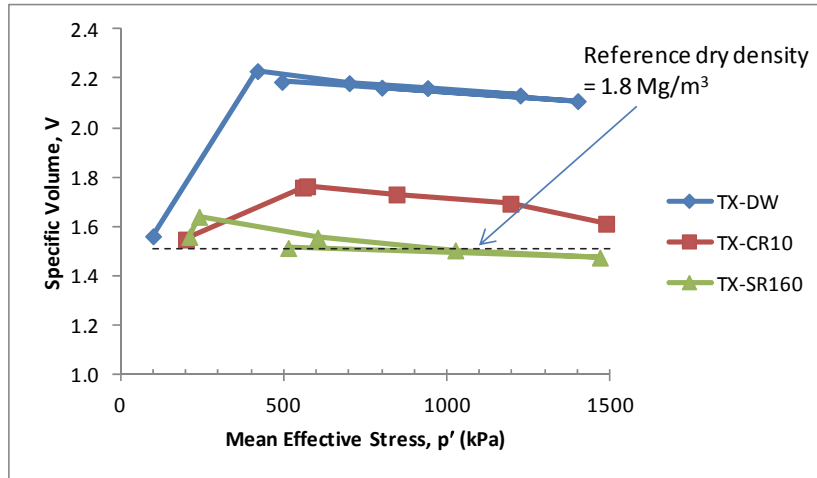
(a)   p in linear axis
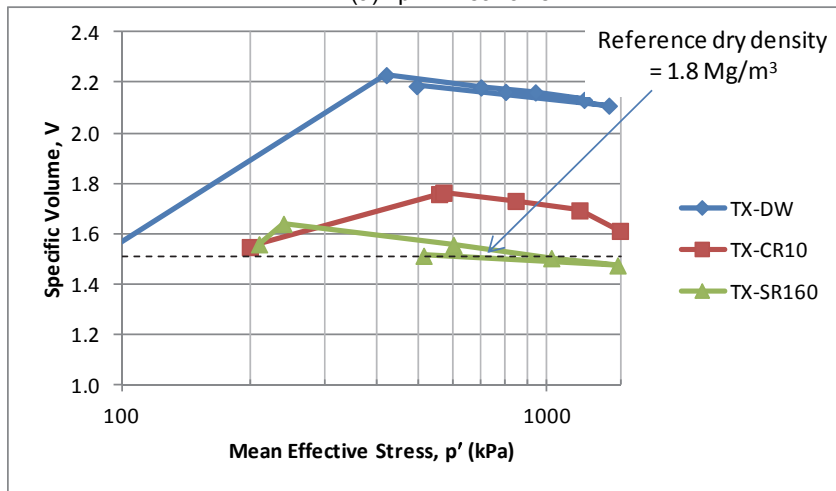
(b)   p in linear axis

Figure 26: Results of Triaxial Tests for This Study

3.5.3   1D-Consolidation Tests

3.5.3.1 Background

The triaxial testing apparatus presented in Section 3.5.2 was only capable of observing specimen behaviour under low confining pressures. The maximum cell pressure that can be applied in the triaxial tests discussed previously was 1.70 MPa, if the back pressure of 0.2 MPa was applied, the maximum effective isotropic stress was equal to 1.50 MPa. This maximum effective stress limit in the triaxial cell was lower than swelling pressure of the material at reference dry density of 1.80 Mg/m^3 under DW and CR10 salinity conditions. This resulted in large volumetric swelling of the triaxial specimens during saturation stage, even when the cell pressure applied close to the maximum pressure, resulting in dry density that was significantly lower than 1.80 Mg/m^3. This means that the mechanical parameters obtained from these tests may not be representative of what would exist at-or-near the target densities for the backfill. As the initial dry density was significantly lower than the target dry densities for the backfill, the mechanical parameters (e.g., bulk modulus (K) or swelling pressure (P_s)) at reference dry density would actually be higher than what would be observed in the triaxial tests. Through use of the EMDD parameter it is possible to confirm that these materials conform to the established swelling pressure- EMDD relationships for BSM and can be used to estimate the swelling pressure that will develop at the target density for the backfill. The measurements of the swelling pressure at the reference dry density of 1.8 Mg/m^3 from the 1D-consolidation test agrees with the swelling pressure test in this study (~6.5 MPa for distilled water specimens) (see Specimen DW-1800-2 (Figure 12) and Specimen 1DC-DW-2 (Figure 30)).

As a result of the triaxial equipment limitations, 1D-consolidation (1DC) tests were used in order to evaluate the behaviour of the materials at reference dry density (1.80 Mg/m^3). The 1DC test was able to apply higher pressure. Maximum pressure up to 16 MPa was used and this pressure did not represent the maximum capacity of the machine. Testing of the material using the 1DC test allowed evaluation of the material at densities above and below the reference dry density. This wider range of consolidation pressure (0 to 16 MPa) also allows for better evaluation of any non-linearity of the mechanical properties of the materials.

3.5.3.2 1D-Consolidation Test Apparatus

The conduct of these tests requires the use of a high-capacity loading frame, a very stiff and robust test cell and the ability to accurately monitor the deformation of the specimen. To accomplish monitoring, the 1D-consolidation tests used a Material Testing System (MTS) deformation testing machine to provide load and deformation monitoring (Figure 27). A load cell and an LVDT connected to the Data Logger System were used to measure the pressure and displacement of the specimen.

This MTS frame (Figure 27) was the same machine that was previously used to test Highly Compacted Bentonite (HCB) materials (Baumgartner et al. 2008, Priyanto et al. 2008a, 2008b). However, due to the presence of sand material, a larger size of specimen was required, so the cell used to test the HCB (28.1 mm diameter) could not be used and greater load cell capacity was also required. A larger cell was developed to be able to test the reference backfill material over the load range desired and to meet the ASTM requirements (D2435-11) for specimen size for a given maximum grain size of material. The backfill specimens tested in this work had a diameter of 50 mm and

thickness of 20 mm, compacted in single lift to a dry density of 1.80 Mg/m^3 and an initial gravimetric water content of 18%, which corresponds to >85% degree of saturation.
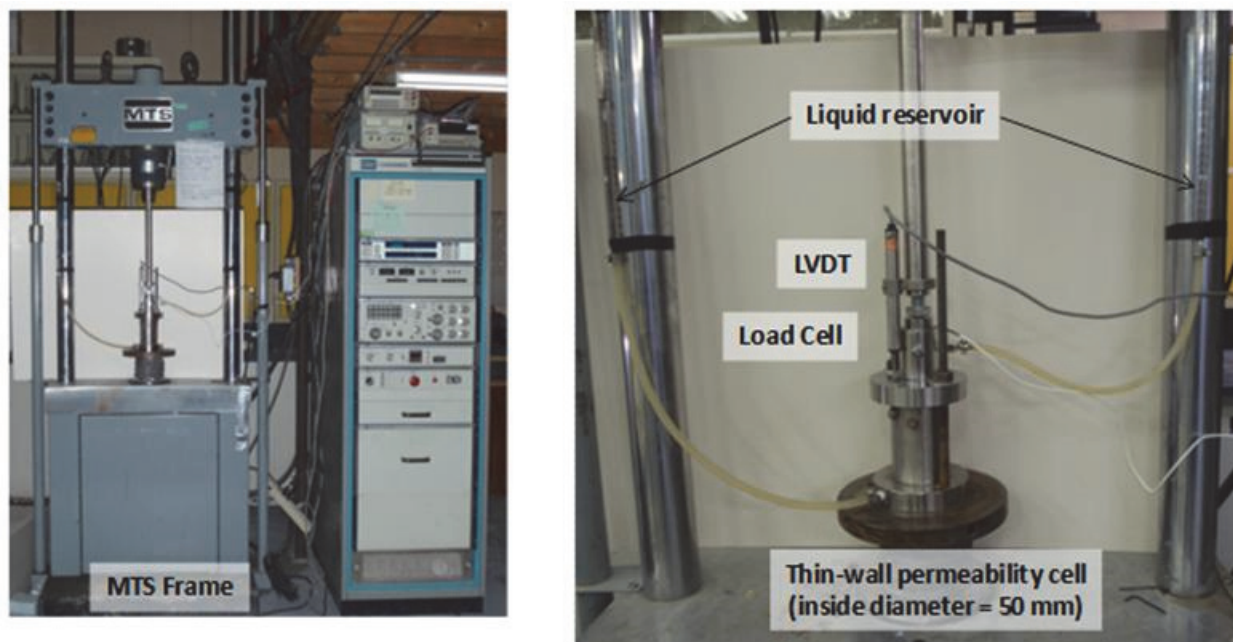
Figure 27: Test Setup of 1D-Consolidation Tests

3.5.3.3 Consolidation Testing Matrix

Table 11 summarizes the initial as-built properties of the specimens used in 1D-consolidation testing. A total of 4 tests were completed.

Table 11: Initial Properties of the Specimens for 1D-Consolidation Tests

Specimen Name	1DC-DW-1*	1DC-DW-2	1DC-CR10	1DC-SR160-1*	1DC-SR160-2	1DC-SR270
Mixing Liquid	DW	DW	CR10	SR160	SR160	SR270
Percolating Liquid	DW	DW	CR10	SR160	SR160	SR270
Diameter (mm)	50.70	49.96	49.62	49.93	49.79	49.62
Height (mm)	20.70	20.70	20.35	20.71	19.96	21.30
Weight (g)	85.51	83.30	82.09	84.14	83.95	87.24
Water content (%)	17.40	17.75	15.31	15.31	16.08	16.39
Water content, corrected$^+$ (%):	17.40	17.75	15.49	18.38	19.33	22.32
Bulk density (Mg/m^3):	2.05	2.05	2.09	2.07	2.16	2.12
Dry density (Mg/m^3):	1.74	1.74	1.81	1.75	1.81	1.73
Duration (days):	7	84	68	54	82	36

* These tests failed and were repeated
$^+$ Corrected due to salt and calculated using Equation 1.

3.5.3.4 Specimen Preparation

The specimens were prepared as follows:
- The bentonite and sand materials were dried in the oven at temperature of 110±5°C for at least 24 hours.
- The pre-determined amount of bentonite, sand and liquid were mixed to achieve 70-30 BSM with target water content. This mixture was then stored in a refrigerator inside a sealed container for at least 24 hours prior to specimen compaction to ensure the consistency of the moisture content of the mixture.
- The filter disks used for tests were saturated and de-aired prior to installation of the specimen.
- When installed, the prepared mixture was placed in the cell and compacted as a single lift to predetermined thickness, corresponding to the target dry density of 1.80 Mg/m^3 using a hydraulic press. The pressure during compaction was measured, as it may represent the pre-consolidation pressure of specimens (see Figure 28). Target dry density was achieved based on the pre-determined thickness not pressures; consequently the pressure applied for the specimen compactions varies from 5 to 11 MPa. Note that the measurements of the compaction pressures were beyond the requirements of this study.
- After compaction, the cell was placed in the MTS machine and connected to the liquid reservoir. The load cell and LVDT were then attached to measure stress and displacement during the test. The diagram of the test set-up is shown in Figure 29.
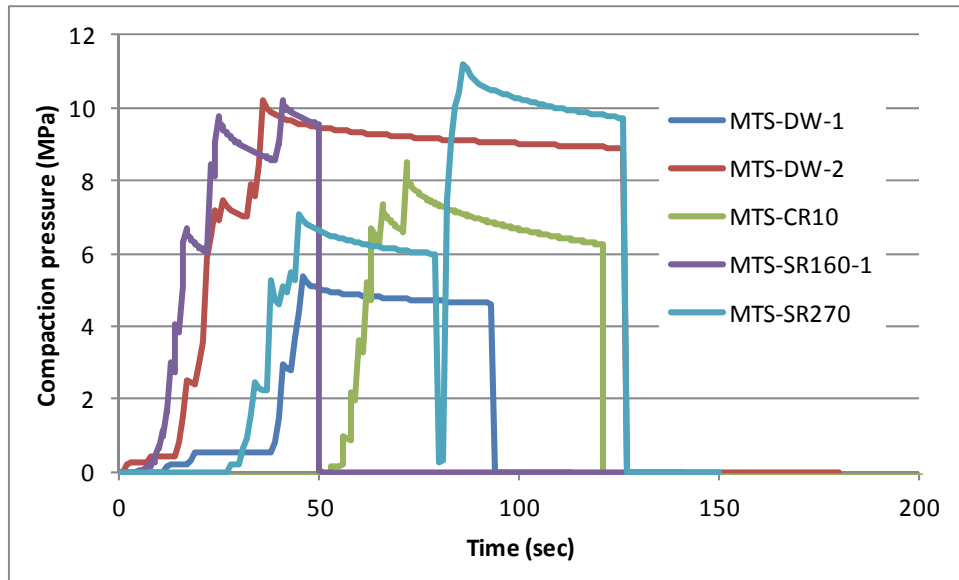
Figure 28: Pressure Applied During Specimen Compaction
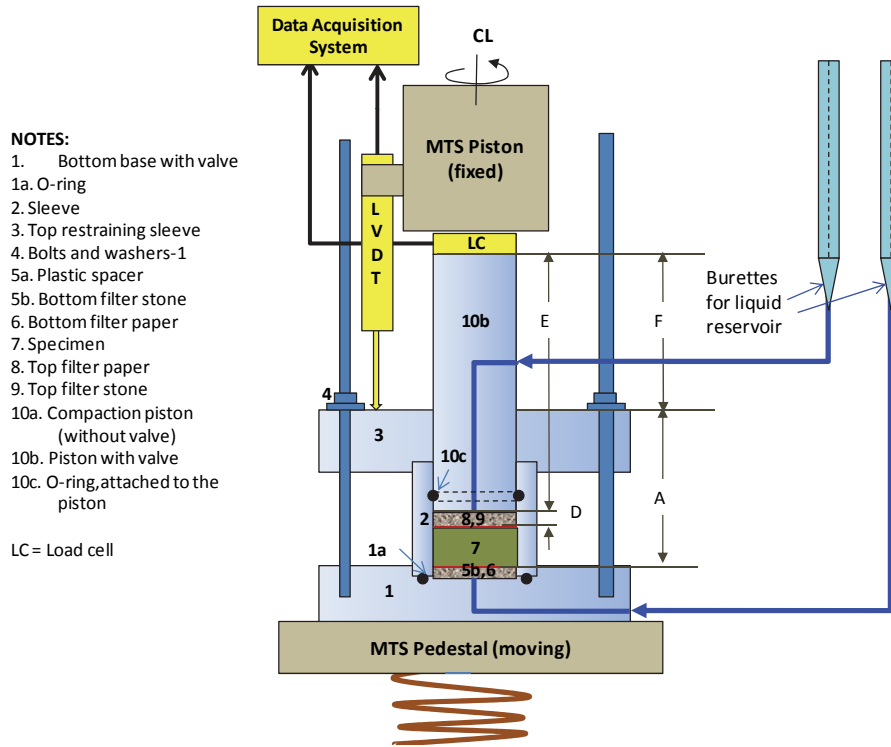
Figure 29: Diagram of the 1D-Consolidation Test using MTS Machine for Backfill Material

3.5.3.5 Results

Initially, the MTS machine was set to maintain a constant specimen volume during saturation, which was similar to the geometry of the swelling pressure tests presented in Section 3.4. During this stage specimen strain was minimal and the pressure acting against the restraint piston increased up to the swelling pressure of the specimen. These data were included in Figure 30 and shows that the swelling pressure of the material was within the range of the swelling pressure measured using the smaller cell. Following the constant volume stage, the load on the piston was increased and the displacement was measured.

Typical results of 1D-consolidation tests are shown in Figures 31 through 33 and complete results of the 1D-Consolidation Tests are provided in Appendix D, which include:
- pressure and displacement measurements (Figure 31);
- displacement versus time for each load increment (Figure 32); and
- log vertical stress versus void ratio (Figure 33).
- Coefficient of consolidation (c_v) and estimated hydraulic conductivity for each load increment.
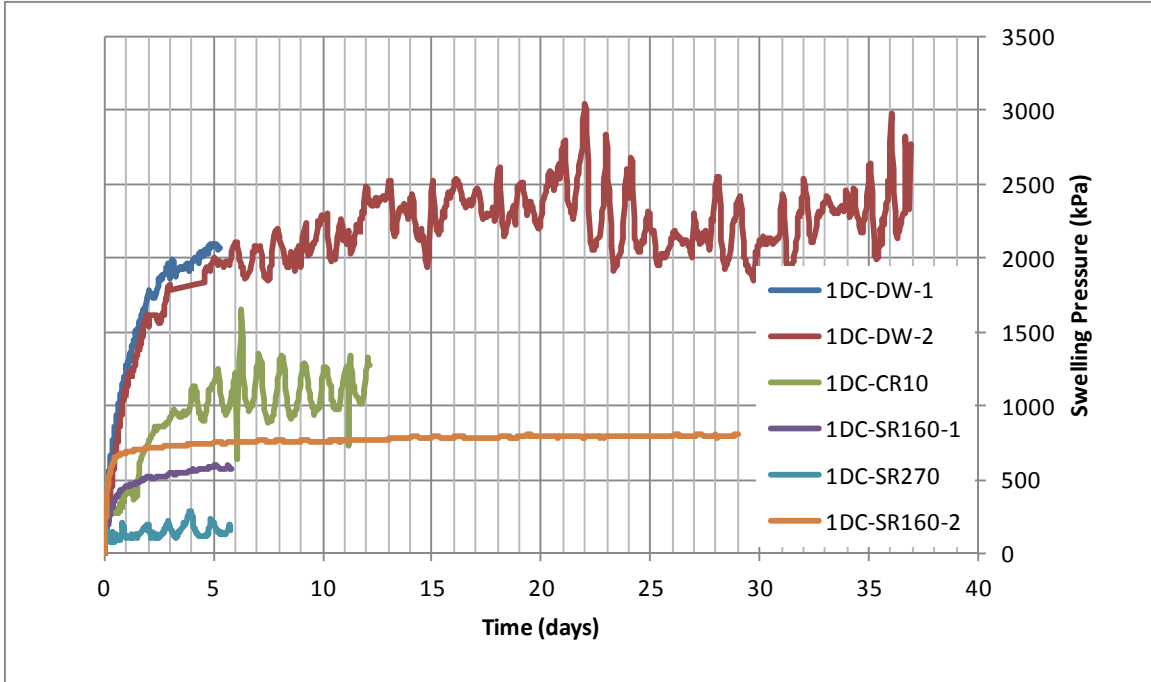
Figure 30: Swelling Pressure Measured during 1D-Consolidation Tests
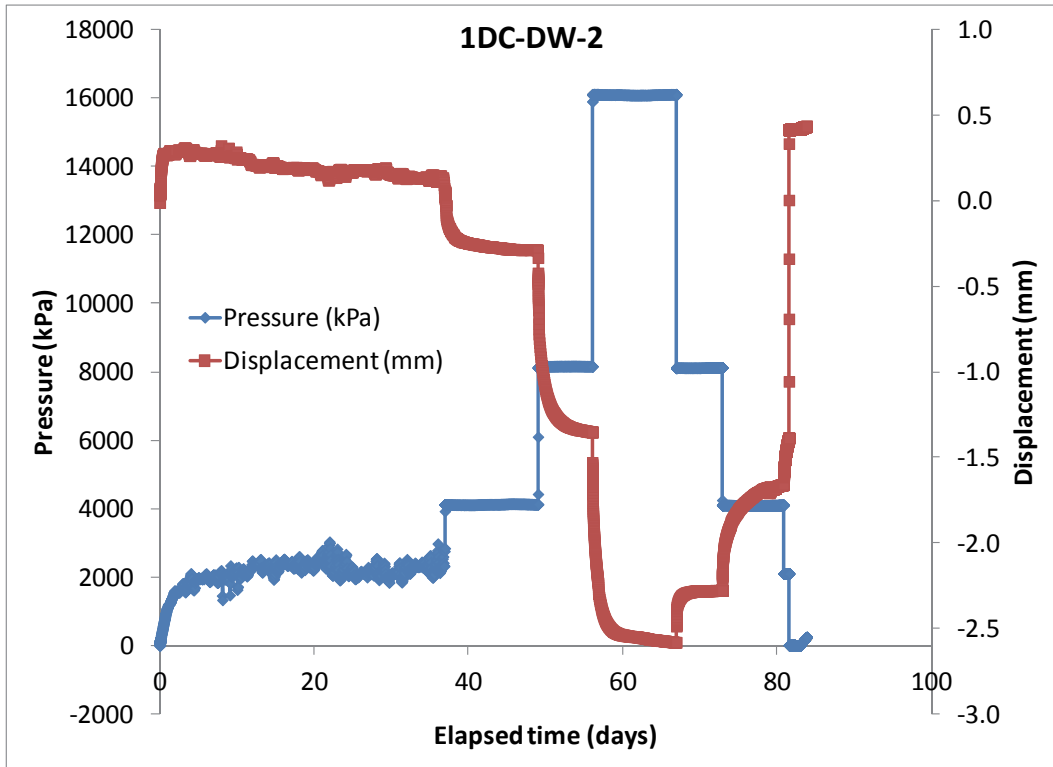
Figure 31: Pressure and Displacement Measured During 1D-Consolidation Tests of Specimen 1DC-DW-2
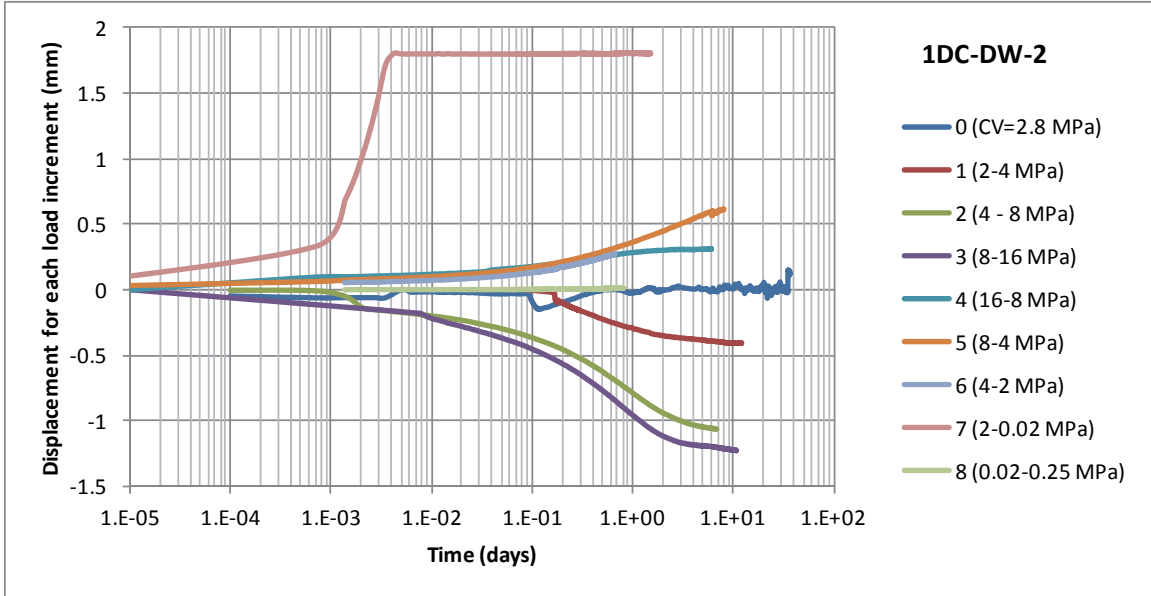
Figure 32: Void Ratio versus Time for Each Load Increment
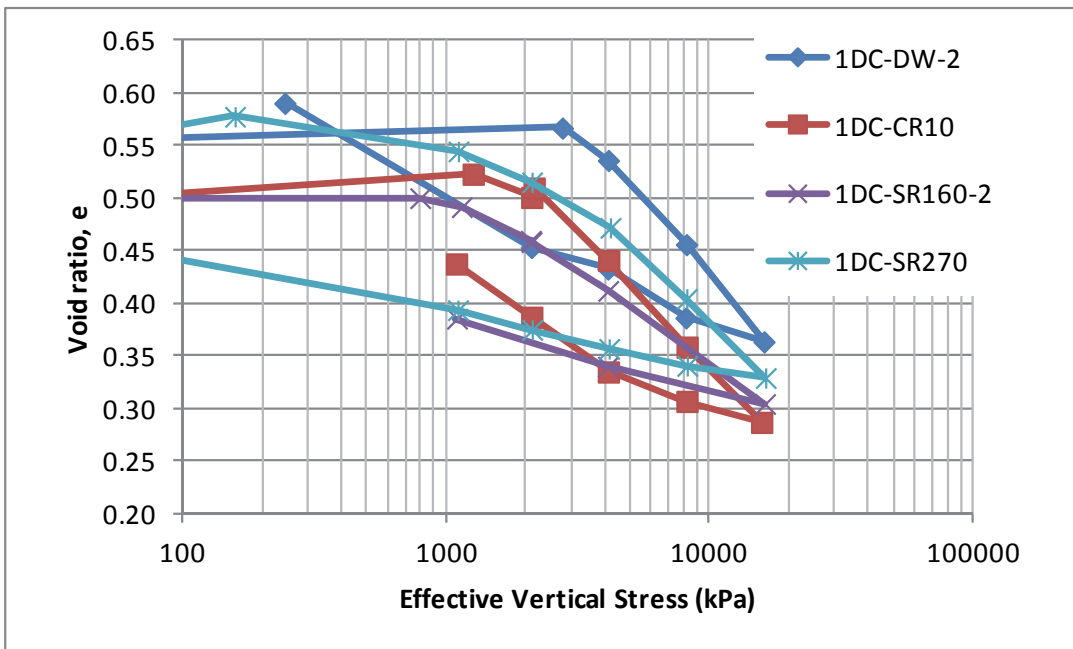
Figure 33: Void Ratio versus Vertical Effective Stress

3.5.4 Determination of Mechanical Properties from the Results of Triaxial Tests and 1D-ConsolidationTests

The main objective of the triaxial and 1D-consolidation tests is to evaluate the mechanical behaviour of the backfilling material, particularly the determination of bulk modulus (K). As expected for soil material, the results show that the material is not linear elastic, so that determination of a single value of K does not necessarily represent this parameter's magnitude over the entire range of stress state that might be encountered. An elasto-plastic model would be more suitable to describe the mechanical behaviour of the backfill material.

3.5.4.1 Determination of Elasto-plastic Model Parameters (C_c, C_s, κ, and λ)

The following elasto-plastic parameters can be determined from the results of the triaxial and 1D-consolidation tests:
-     Swelling Index (C_s) and Compression Index (C_c); and
-     Kappa (κ) and Lambda (λ).

The definitions of these parameters and how they were determined are illustrated in Figure 34. Void ratio (e) and specific volume (V = 1+e) increase with an increase of stress at different slopes (κ or λ), depending on the stress history of the specimen. Parameters C_c and C_s are the slopes of log (vertical effective stress) (σ_v) versus void ratio (e) during loading and unloading stages, respectively (Figure 34a). Parameters λ and κ are the slopes of natural log of mean effective stress (i.e., ln (p') versus specific volume (V)) during loading and unloading stages (Figure 34b).
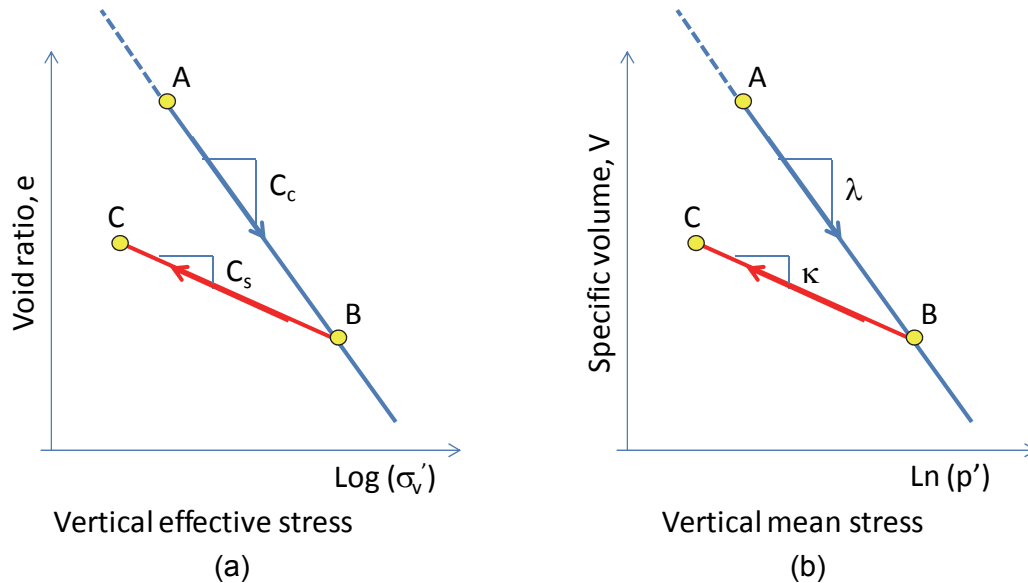
Figure 34: Definitions of Parameters C_c, C_s, λ, and κ

3.5.4.1.1   Parameters Cc and Cs from 1D-Consolidation Tests

The typical results of the 1D-consolidation tests are shown in Figure 34 as a relationship between vertical effective stress and void ratio. The parameters C_c and C_s can be

determined from the results 1D-consolidation tests. Point B in Figure 34 is the maximum stress and the void ratio corresponding to the maximum stress. The values of C_c and C_s, initial void ratio and the location of maximum stress as reference points are shown in Table 12. Parameters C_c and C_s tend to decrease with increasing salinity. This behaviour is similar to that observed in 1D-consolidation tests of highly compacted bentonite (HCB), dense backfill (DBF), and light backfill (LBF) materials (Priyanto et al. 2008a, 2008b).

Table 12: Compression Index (C_c) and Swelling Index (C_s)

Specimen	C_c	C_s	Initial void ratio, e	Point B in Figure 34a Maximum stress (kPa)	Point B in Figure 34a Void ratio corresponding to maximum stress
MTS-DW-2	0.292	0.102	0.558	16065	0.364
MTS-CR10	0.258	0.082	0.503	15744	0.287
MTS-SR160-2	0.173	0.069	0.500	16222	0.305
MTS-SR270	0.210	0.055	0.569	16312	0.329

The results of the triaxial tests are shown as the relationship of the mean effective stress (p′) and specific volume (V) (Figure 36), so that parameters κ and λ can be directly calculated from the results.

In this study, parameters κ and λ were also determined from the results of 1D-consolidation tests. In this analysis, for simplicity the mean effective stress (p′) was assumed equal to the vertical effective stress (σ_v′). Figures 35 to 39 show the p′-V relationships of 1D-consolidation tests compared to the triaxial tests for specimens with distilled water (DW), CR10, SR160, and SR270 solutions, respectively. For specimens prepared with DW, CR10, and SR160, the results of 1DC were comparable with the TX tests (Figures 37, 38 and 39, respectively). Mechanical properties of the specimen prepared with SR270 were determined from the results of 1D-consolidation test, as the triaxial test results for specimen TX-SR270 was not available due to cell leakage. Volume measurement in the 1D-consolidation test was not affected by the leakage, so it was more reliable to test the material under high salinity condition.

The data shown in Figures 35 through 39 present a consistent description of the backfill behaviour using either 1DC or TX test technique when plotted in p′-V space. For this reason, it is possible to determine parameters κ and λ from the results of the 1DC tests. Table 13 shows the parameters κ and λ from TX tests and 1DC tests.
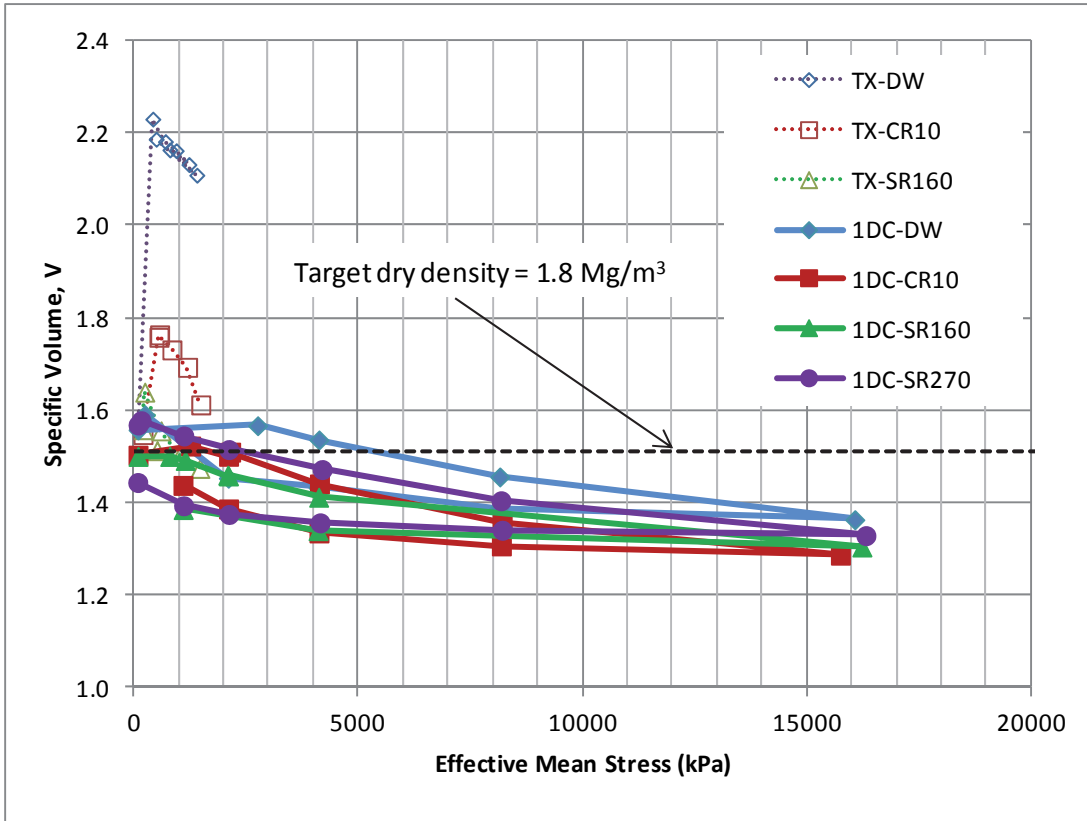
Figure 35: Specific Volume versus Effective Mean Stress from 1DC and TX Tests
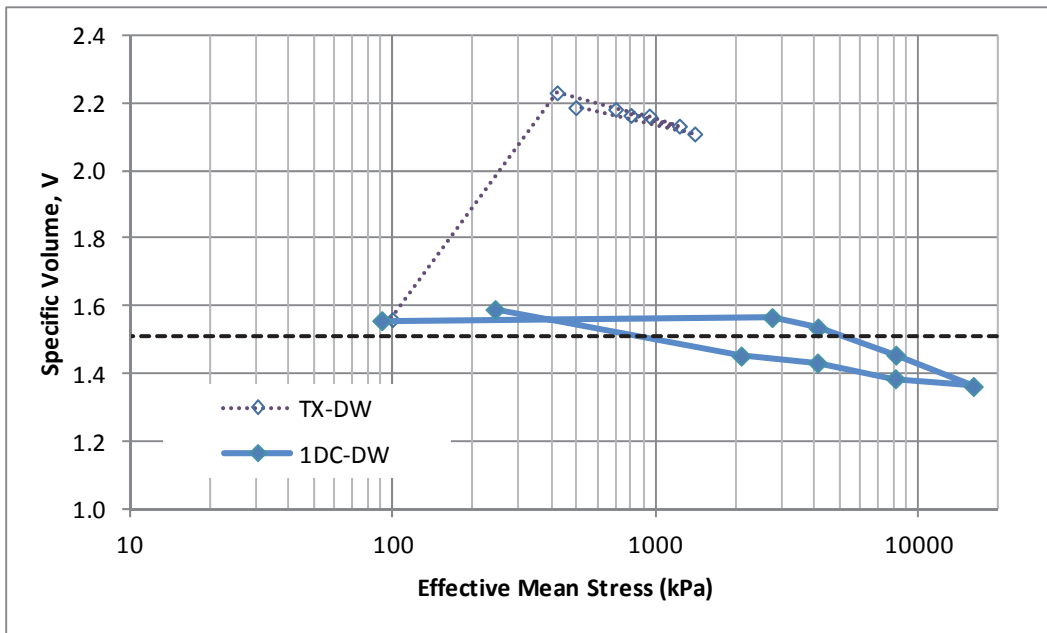
Figure 36: Effective Mean Stress versus Specific Volume for 1DC Tests Compared to TX Tests for Specimens with Distilled Water
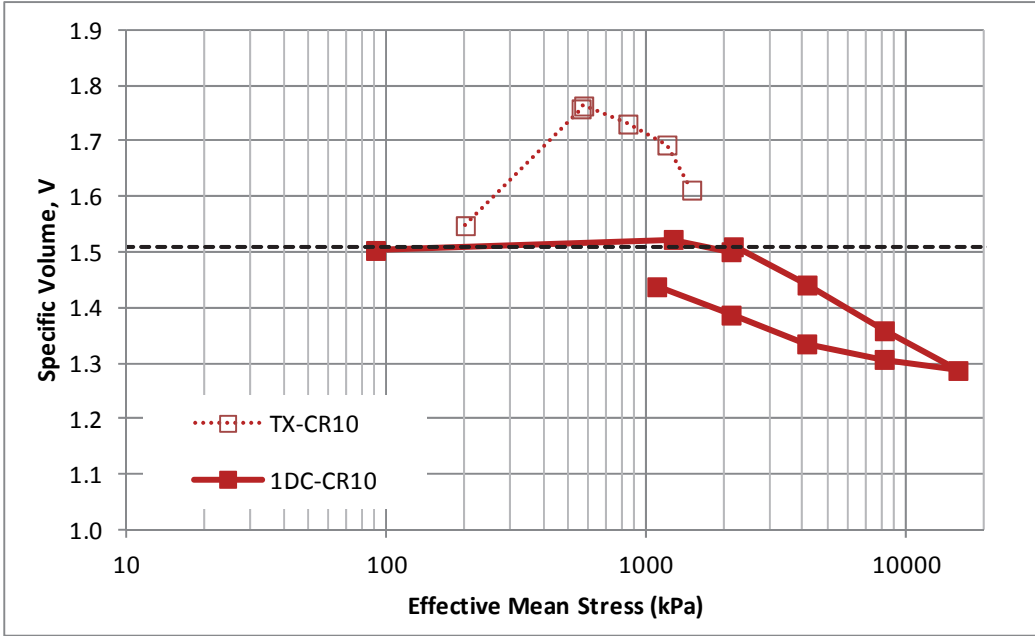
Figure 37: Effective Mean Stress versus Specific Volume for 1DC Tests Compared to TX Tests for Specimens with CR10 Solution
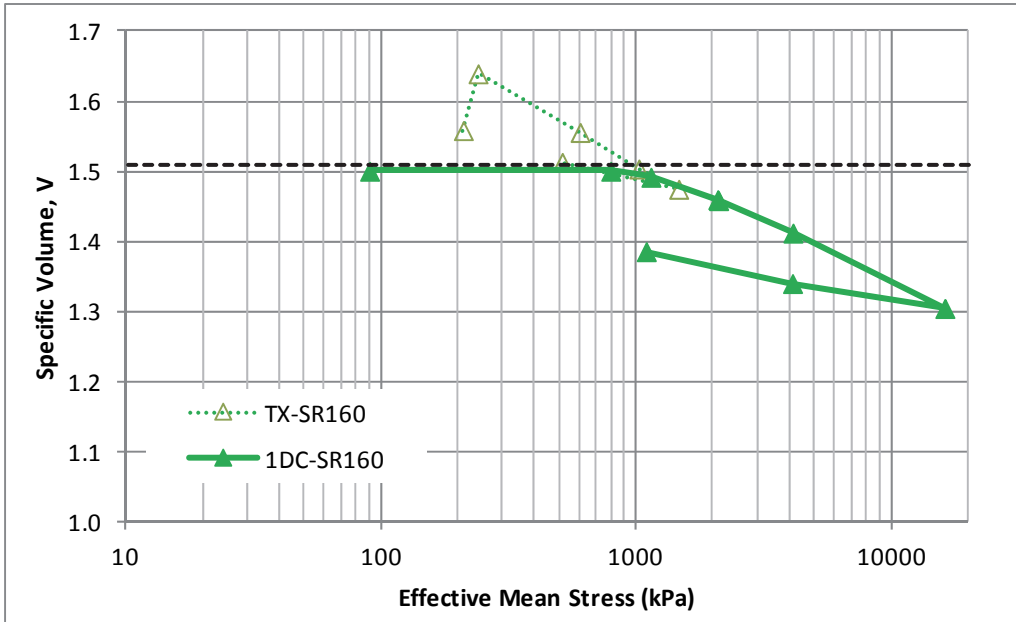
Figure 38: Effective Mean Stress versus Specific Volume for 1DC Tests Compared to TX Tests for Specimens with SR160 Solution
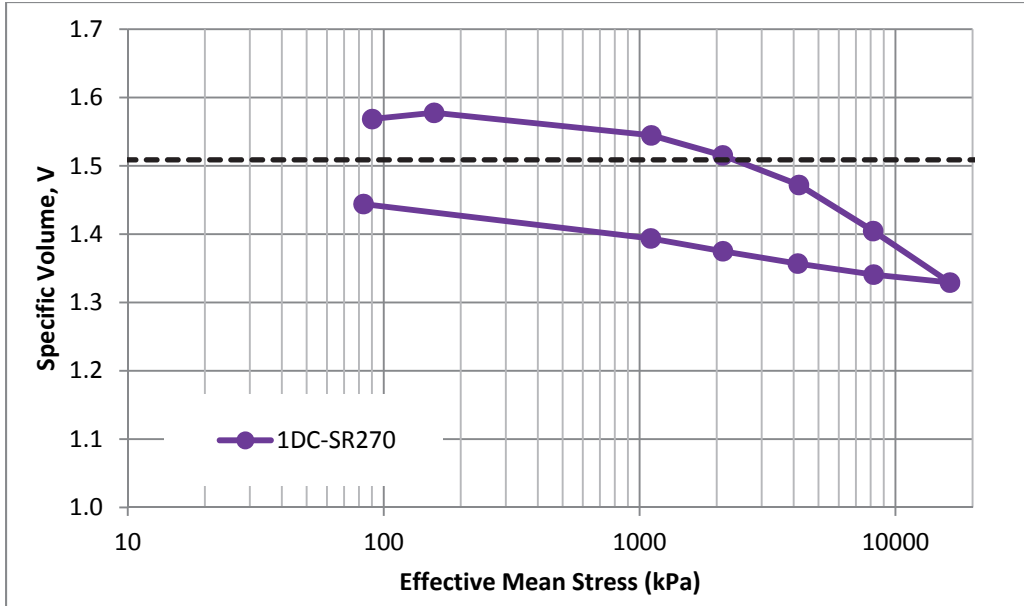
Figure 39: Effective Mean Stress versus Specific Volume for 1DC Tests for Specimens with SR270 Solution

Table 13: Parameters κ and λ Determined from the TX and 1DC Tests

Specimen	TDS of pore liquid (g/L)	κ	λ
TX-DW	0	0.074	0.095
TX-CR10	10	NA	0.095
TX-SR160	160	0.037	0.091
TX-SR270	NA	NA	NA
1DC-DW	0	0.054	0.127
1DC-CR10	10	0.056	0.093
1DC-SR160	160	0.030	0.075
1DC-SR270	270	0.020	0.105

Figure 40 shows the relationships of parameters κ and λ with the pore liquid salinity in term of Total Dissolved Solid (TDS, g/L). Parameters κ and λ determined using 1DC tend to be slightly lower than the TX tests, except for the specimen prepared with distilled water. There was a large difference between the results of TX and 1DC tests for specimen prepared with DW, which likely due to the large swelling that occurs at the beginning of the TX tests, which made the dry density of the TX test specimen prior to the pressure increment significantly lower than the reference dry density. Parameter κ tends to decrease with an increase of pore liquid salinity. Parameter λ tends to decrease when the pore liquid salinity increases from 0 to 160 g/L, then it increased afterward. The change of this trend may be due to data inaccuracy that may need to be confirmed in the future research. In general, parameter λ for specimen with saline pore liquid was always less than the distilled water.
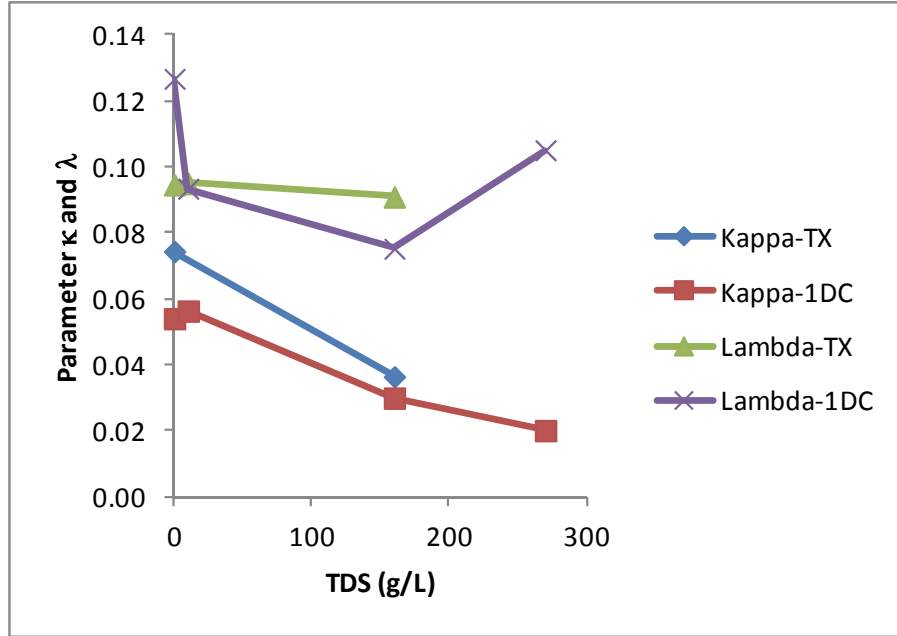
Figure 40: Parameters κ and λ as a Function of Total Dissolve Solid (g/L) of Pore Liquid

3.5.4.2 Determination of Elastic Parameter

Although determination of a single linear-elastic parameter for this backfilling material will not represent the behaviour of the material over a range of density and salinity conditions, it is possible to evaluate each increment of the linear elastic properties from the results of 1DC and TX tests. Numerical modelling using a linear elastic model is easier to execute than using more complex elasto-plastic models, and it can be use for preliminary scoping analyses. Consequently, determination of the elastic parameter range at the reference dry density is beneficial to provide input to preliminary numerical models.

3.5.4.2.1   Bulk Modulus (K) from the 1DC Tests Results

The determination of bulk modulus from the results of 1D-consolidation tests was done according the following method. The 1D-modulus (*M*) can be calculated from two incremental stress state points of void ratio (*e*) and vertical stress (σ_v) relationship. The 1D-Modulus (M) can be calculated as:

$$M = \frac{\sigma_{v1} - \sigma_{v2}}{(e_1 - e_2)/(1 + e_1)}$$

(5)

where: σ_{v1} and σ_{v2} are vertical stresses at points 1 and 2 respectively; e_1 and e_2 are void ratio at points 1 and 2, respectively (see Figure 41).
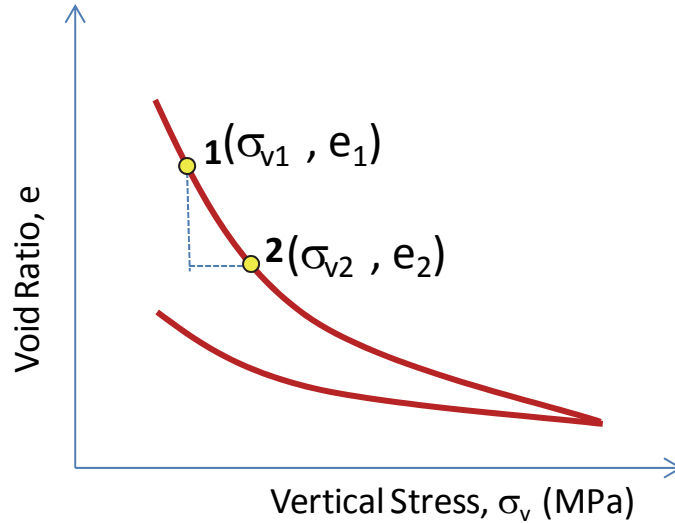
Figure 41: Definition of 1D-Modulus (M)

Young's modulus (E) and Bulk Modulus (K) can be determined from the following equation, if the Poisson's ratio (v) is known.

$$E = \frac{M(1+v)(1-2v)}{1-v}$$

(6)

$$K = \frac{E}{3(1-2v)}$$

(7)

Figure 42 shows the 1D-Modulus (M) determined from the results of 1DC tests. As expected, the 1D-modulus tends to increase with increasing dry density. For a given dry density, M for a specimen with distilled water tends to be greater than a specimen with saline solution. There is no clear trend of how an increase in the pore liquid salinity affects M. The value of 1D-modulus (M) at the reference dry density is between 7 to 70 MPa.

Figure 43 shows the bulk modulus (K) calculated from the results of 1DC tests using Equations (6) and (7). The bulk modulus corresponding to the reference dry density is between 5 to 50 MPa. In this study, the value of v is assumed equal to 0.32, which is typical value for backfilling material. Young's modulus (E) and bulk modulus (K) calculated from Equation (6) can be sensitive on the value of v (e.g., Davis and Selvadurai 1996). The scope of this project did not allow for directly measurement of the value v. It is recommended that the Young's modulus (E) and bulk modulus (K) should be recalculated using Equation (6) and (7), if a new value v is determined.

Since stress-strain relationship of the material is dependent on the loading-unloading stages and preconsolidation pressure, the values of 1D-modulus (M) and bulk modulus (K) are different whether the load increases or decreases and under normally or overly consolidated stages. The value of M and K during unloading state (following C_s and κ lines in Figure 34) should be greater than loading state (following C_c and λ lines in Figure 34).
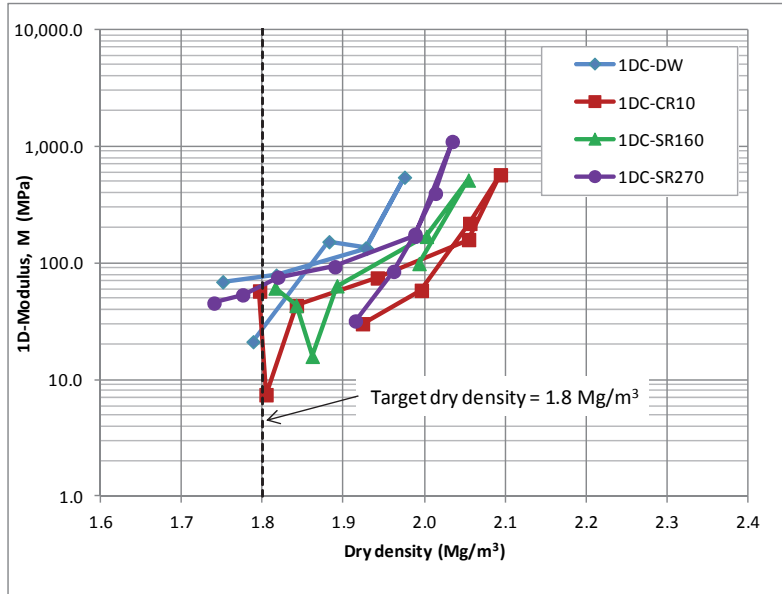
Figure 42: 1D-Modulus (M) Determined from the Results of 1D-Consolidation Tests
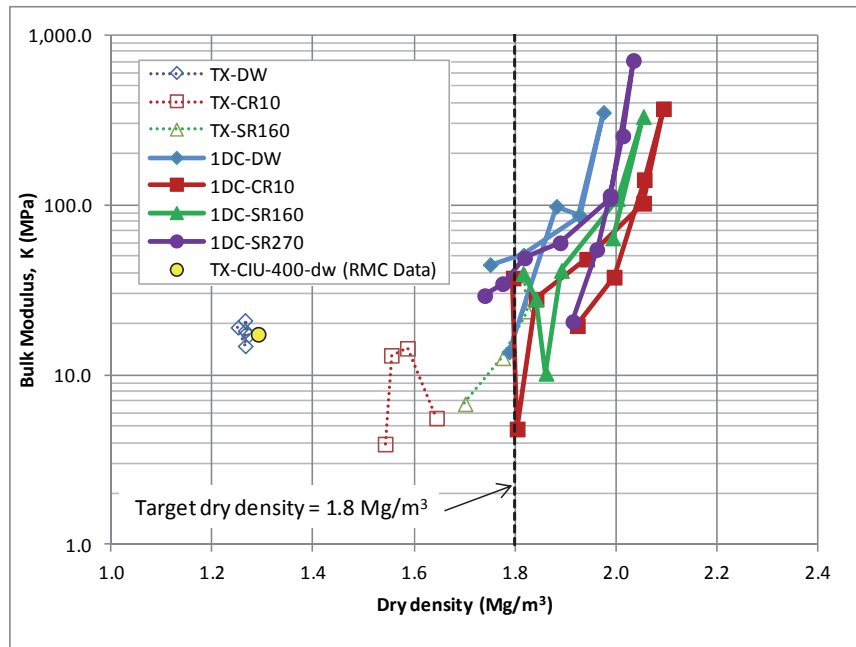
Figure 43: 1D-Modulus (M) Determined from the Results of 1D-Consolidation Tests

3.5.4.2.2 Determination Bulk Modulus (K) from the TX Tests Results

The bulk modulus (K) of the backfill material is determined from the results of TX isotropic consolidation and one of the TX consolidated undrained tests done at the Royal Military College of Canada (RMC) for comparison purposes.

The bulk modulus (K) can be determined from the results of TX isotropic consolidation tests as follows:

$$K = \Delta p' / \Delta(\varepsilon_v) \tag{8}$$

where:

$\Delta p'$ is the incremental of mean effective stress (i.e., $p' = (\sigma_1+\sigma_2+\sigma_3)/3 - u_w$), and

σ_1, σ_2 and σ_3 are the 1st, 2nd, and 3rd principal stresses, respectively. In the case of isotropic consolidation test, $\sigma_1 = \sigma_2 = \sigma_3$ and u_w is the pore water pressure.

$\Delta(\varepsilon_v)$ is the incremental volume strain. Volume strain (ε_v) can be calculated from the specific volume (V) using the following equation.

$$\varepsilon_v = (V - V_{initial})/V_{initial} \tag{9}$$

where V and $V_{initial}$ are the current and initial specific volumes, respectively.

Figure 44 shows how K was determined from TX test results. The bulk modulus (K) derived from TX tests are comparable with those calculated of K from 1DC tests, especially when the initial dry density is close to the reference dry density (e.g., Specimen TX-SR160). K for specimens prepared with distilled water tends to be greater than for specimens with saline solution. Bulk modulus tends to increase with an increase of dry density.
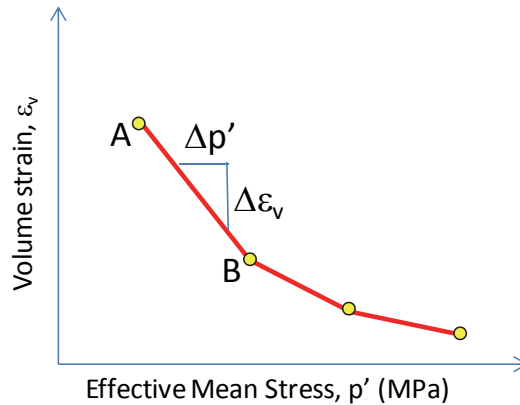
Figure 44: Definition of Bulk Modulus (K)

Young's modulus (E) can be determined from the data of Consolidated Isotropic Undrained (CIU) tests, provided by the RMC (Royal Millitary College of Canada). The specimen was prepared at lower dry density (~1.60 Mg/m^3). After saturation state, the specimen also experienced large swelling and the dry density after saturation was approximately ~1.20 Mg/m^3. Shearing was done after saturation. The deviatoric stress (q) versus axial strain (ε_1) during shearing is shown in Figure 45.

Young's modulus (E) was determined as follows. The peak deviatoric stress (q) was equal to ~325 kPa. One-third of peak stress was ~108 kPa, which corresponds to axial strain of 0.577%. E was equal to the slope of red linear line in Figure 45, and it was equal to 18.8 MPa. Bulk modulus (K) was calculated using Equation (7) and equal to

17.4 MPa. The plot of K calculated using the TX-CIU-400-dw (RMC) was comparable to the results of the TX test.

In conclusion, considering all the data shown in Figure 43, at reference dry density of 1.80 Mg/m³ the bulk modulus (K) was in the range between 4 to 50 MPa. This value range was provided as a guideline for preliminary analyses. Using a single value of linear elastic parameters is not recommended, since the material is not linear elastic. The use of more complex models (e.g., elastic-plastic model) is more suitable to describe the mechanical behaviour of the 70-30 BSM material.
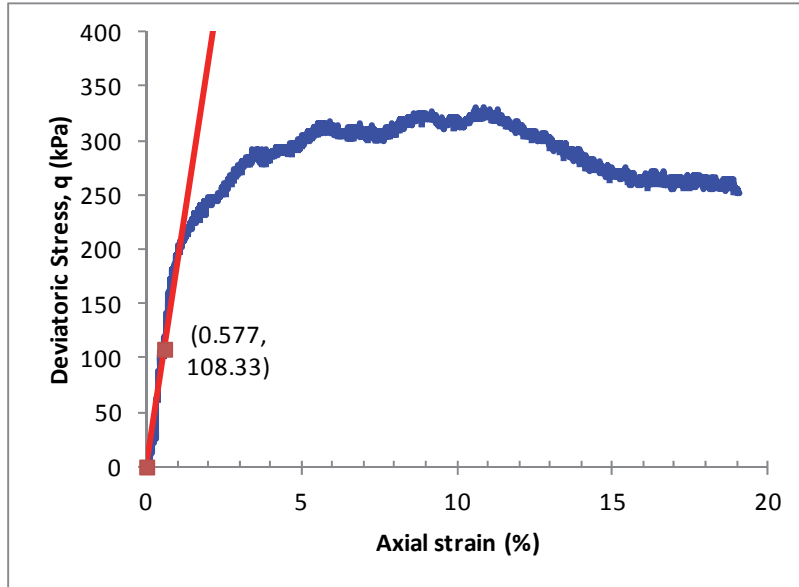
(This figure is a courtesy of Dr. G. Siemens and B. Lim (RMC))

Figure 45: Deviatoric Stress (q) versus Axial Strain from Specimen CIU400_DW

3.6   Determining the Relationship between Gas Permeability and Suction

As a DGR for low and intermediate level radioactive waste materials will contain materials that generate gas during their decay it is important to understand how such gas will move within the repository as well as through engineered barriers materials such as the shaft backfill. In order to determine the relationship between gas permeability and suction, gas permeability was measured on materials prepared with a range of degree of saturation (Sw) conditions. In conjunction with these permeability tests, the soil-water characteristic curve (SWCC) defining the relationship between soil suction and degree of saturation were also measured.

3.6.1   Gas Permeability Tests

3.6.1.1 Laboratory Test Method

A number of potential methods exist that can be used to measure gas movement into and through water saturated and unsaturated materials. Examination of the possible means led to the selection of a technique that involves exposing one end of a confined specimen to a known volume of gas having a known pressure and then monitoring the

decay of the gas pressure as the gas forces its way into the specimen. This technique was described in detail by Villar (2002).

The basic testing process involved in measuring gas permeability consisted of a triaxial chamber, a gas tank, a water tank, a constant pressure supply system, and a data acquisition system (Figure 46). A cylindrical specimen of compacted 70-30 bentonite-sand mixture (BSM) (diameter of 50 mm and height of 100 mm) was inserted into a triaxial chamber with porous stones placed at the top and bottom of the specimen and then this assembly was sealed using two latex membranes. Vacuum grease was applied on the top cap and bottom pedestal to prevent any loss of gas. Nitrogen gas was injected into the gas tank of a known volume at a pressure of 100 kPa. A cell pressure of 300 kPa was constantly applied to the water tank pressurizing water into the triaxial chamber. Both the gas and water tanks were instrumented with pressure sensors and connected to a data acquisition system that records the pressure of gas and water into the triaxial chamber. Since the gas tank and these pressure sensors were sensitive to changes in temperature, special care was taken to keep a constant temperature during testing by submerging the Nitrogen gas tank in an electric constant-temperature water bath. The exposed pressure sensors were covered by a Plexiglas cylinder to prevent any air flow (Figure 46). The inlet at the upper part of the specimen was left open to the atmosphere during the test. This test allowed the air in the tank to exit to the atmosphere through the specimen, while the decrease in pressure in the gas tank was measured with time.

Preliminary tests were done to examine the reliability of the equipment and ensure that the information desired could be collected using the selected test technique. A series of trials were completed on the same specimen to ensure that the testing set-up was reliable. A constant temperature of 20°C was achieved in this testing set-up and the cell water pressure remained constant at 300 kPa.

This trial was successful in obtaining a gas permeability measure and so further testing was carried out using this method with the exception of using a lower gas pressure (100 kPa), since this was beneficial in avoiding gas breakthrough mechanisms (Graham et al. 2002). Subsequent testing was done using triaxial specimens with diameter of 50 mm and height of approximately 100 mm with target dry density of 1.80 Mg/m^3 and various degrees of water saturation (Sw) (30 to 90 %).

The results of the gas permeability test are presented in term of gas conductivity (K_g) having a unit of m/s. The conductivity to gas (K_g) was calculated in accordance with the following equation (Yoshimi & Osterberg 1963):

$$K_g = 2.3 \times \frac{V \times l \times \rho_g \times g}{A \times \left(P_{atm} \times {P_0}/{4}\right)} \times \frac{-Log_{10}\left({P(t)}/{P_0}\right)}{t - t_0}$$

(10)

Where
- K_g is the conductivity to gas (m/s),
- V   is the volume of the tank (m^3),
- l   is the length of the sample (m),
- A   is the surface area of the sample (m^2),

ρ_g is the density of gas (kg/m^3),

P_{atm} is atmospheric pressure (N/m^2),

P_0 is the excess pressure over atmospheric pressure in time t_0 (s) (N/m^2)

$P(t)$ is the excess pressure over atmospheric pressure in time t (s) (N/m^2)

g   is the gravitational acceleration (= 9.81 m/s)
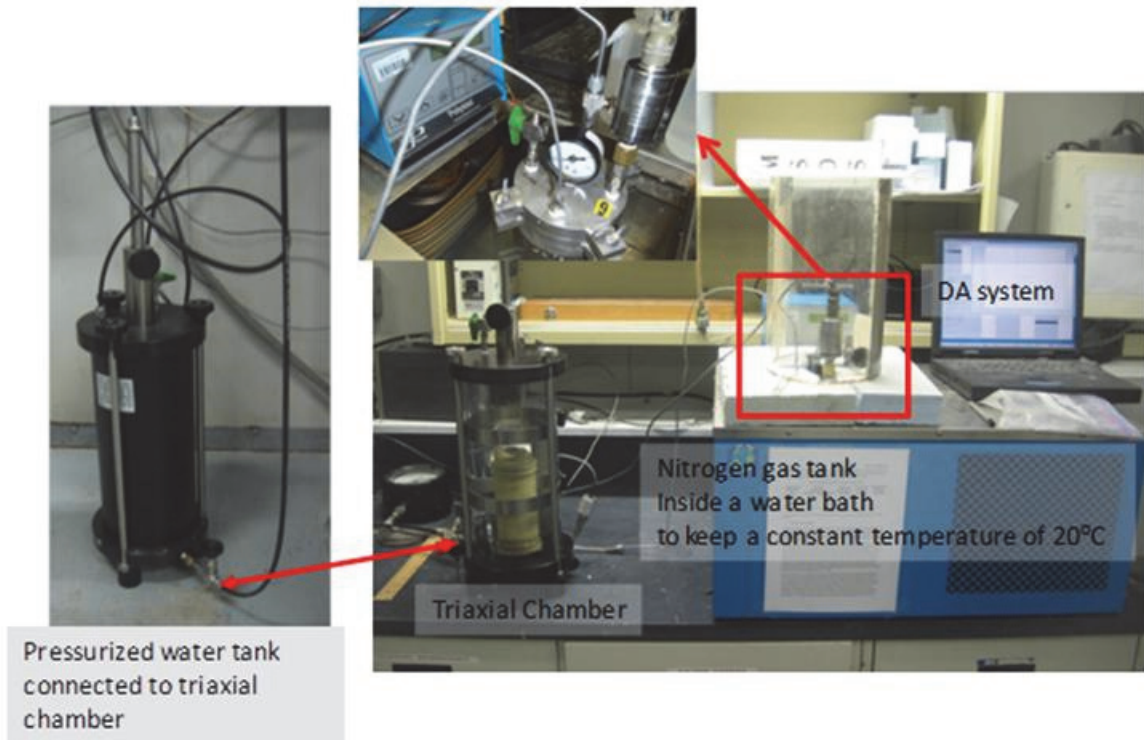
Figure 46: Gas Permeability Tests Set-up

3.6.1.2 Test Matrix

A total of 24 tests were completed with specimens prepared to three different target dry densities (1.60, 1.70, and 1.80 Mg/m^3) using different pore water solutions (i.e., distilled water and CR10, SR160 and SR270 saline solutions). Table 14 lists the test matrix for the gas permeability tests and the test results. Figures 47 through 50 show the evolution of gas pressure plotted based on the degree of saturation for specimens prepared with distilled water. These figures show that how the pressure decay in the gas supply chamber of the testing system decreases slowly and for a given degree of saturation, an increase of dry density results in a slower decrease of gas pressure.

Table 14: Testing Matrix of Gas Permeability Tests and Results

No	Specimen	Target Dry Density (Mg/m³)	Mixing liquid	Target Sw (%)	Water Content (%)	Gas Conductivity, K_g (m/sec)
1	DW-1.8-10	1.80	Distilled water	10	1.9	2.37E-09
2	DW-1.8-30			30	5.8	5.90E-10
3	DW-1.8-50			50	9.4	1.95E-10
4	DW-1.8-70			70	12.8	5.27E-11
5	DW-1.8-90			90	16.9	5.76E-14
6	DW1.7-10	1.70	Distilled water	10	2.2	5.58E-09
7	DW1.7-30			30	6.6	2.12E-09
8	DW1.7-50			50	11	4.59E-10
9	DW1.7-70			70	15.4	3.82E-11
10	DW1.7-90			90	19.9	7.43E-14
11	DW1.6-10	1.60	Distilled water	10	2.63	1.64E-08
12	DW1.6-30			30	7.79	6.04E-09
13	DW1.6-50			50	12.9	1.25E-09
14	DW1.6-70			70	18	4.10E-11
15	DW1.6-90			90	23.2	4.94E-14
16	CR10-10	1.80	CR10-Solution	10	1.6	3.30E-09
17	CR10-50			50	9.9	2.08E-10
18	CR10-90			90	16.4	2.00E-12
19	SR160-10	1.80	SR160 solution	10	1.9	2.29E-09
20	SR160-50			50	9.4	2.33E-10
21	SR160-90			90	18.2	7.73E-13
22	SR270-10	1.80	SR270 solution	10	2.9	2.29E-09
23	SR270-50			50	11.7	2.33E-10
24	SR270-90			90	19.4	7.73E-13

3.6.1.3 Distilled water tests

The results obtained from the gas permeability tests completed on specimens prepared with distilled water were evaluated and plotted based on the relationship between gas conductivity versus (1) dry density, (2) degree of saturation, and (3) water content.

Figure 52 shows gas conductivity (K_g) plotted against the degree of saturation for specimens using distilled water for given dry densities. As expected, the gas conductivity values decrease with increasing the degrees of saturation. The gas conductivity seems to be dependent on dry density at lower degree of saturation; however this trend shows up only where the degree of saturation is less than approximately 50%. At the degrees of saturation higher than 50%, there is little effect of changing dry densities on gas conductivity. This indicates that gas conductivity is dominated by the dry density of the specimen only at the degree of saturation less than ~ 50% and at higher degrees of saturation gas movement is controlled by the degree of saturation of the specimen.

Gas conductivity for those specimens prepared using distilled water was plotted against water content for given dry densities are presented in Figure 53. As water content

increases, gas conductivity becomes lower in the specimens. It clearly shows that lower dry density results in higher gas conductivity at a given water content.

Figure 54 shows gas conductivity versus dry density based on various degrees of saturation. At degrees of saturation less than 50%, gas conductivity decreases with increasing dry density. However where the degree of saturation is >50%, gas conductivity values become relatively constant as dry densities increase, indicating there is little effect of increasing dry densities on gas conductivity at higher degree of saturation over 50%.
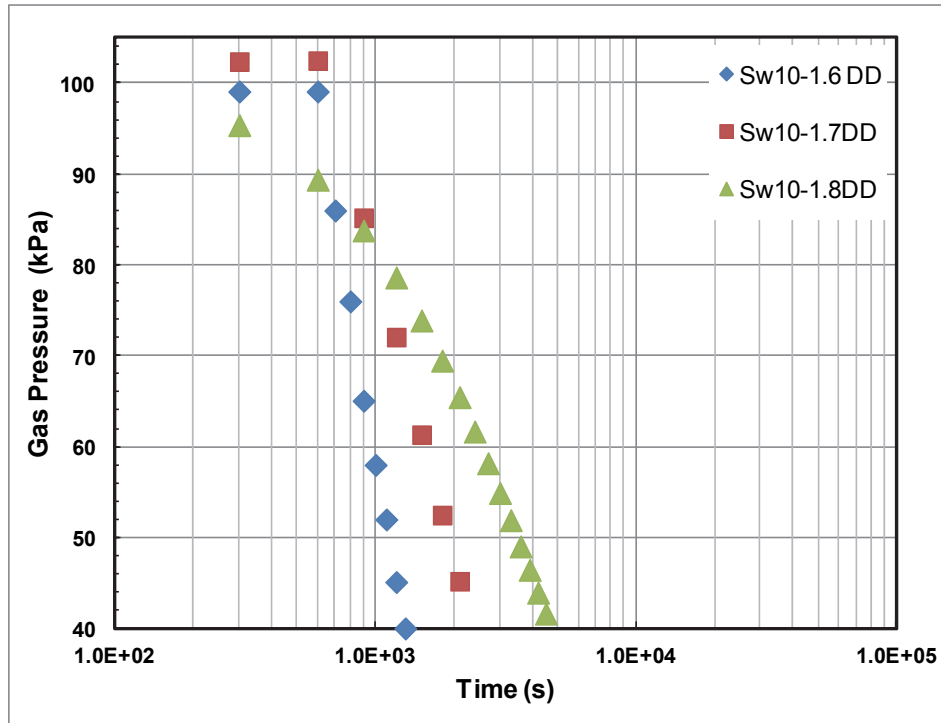
Figure 47: Gas Pressure vs. Time for Specimens Using Distilled Water at Dry Densities (DD) of 1.6, 1.7 and 1.8 Mg/m^3 and Degree of Saturation (Sw) of 10%
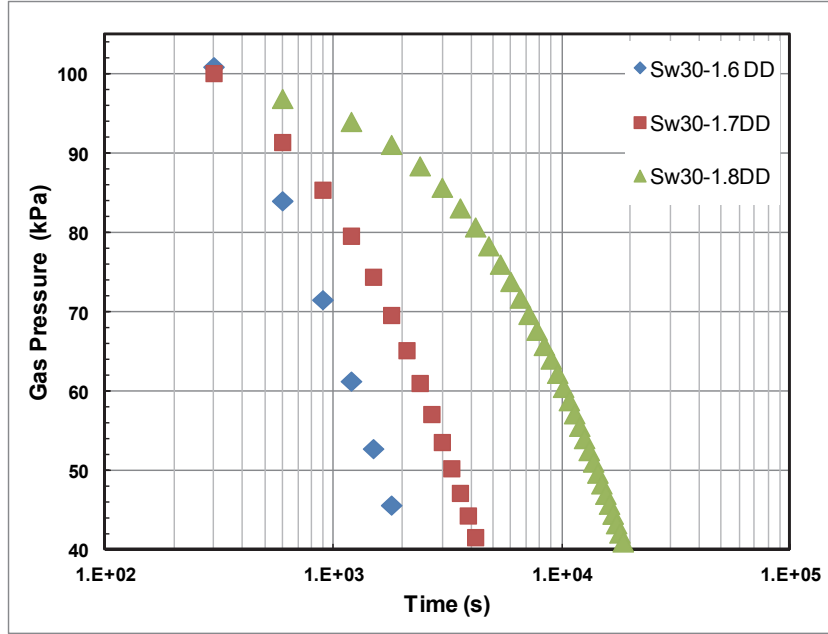
Figure 48: Gas Pressure vs. Time for Specimens Using Distilled Water at Dry Densities (DD) of 1.6, 1.7 and 1.8 Mg/m^3 and Degree of Saturation (Sw) of 30%
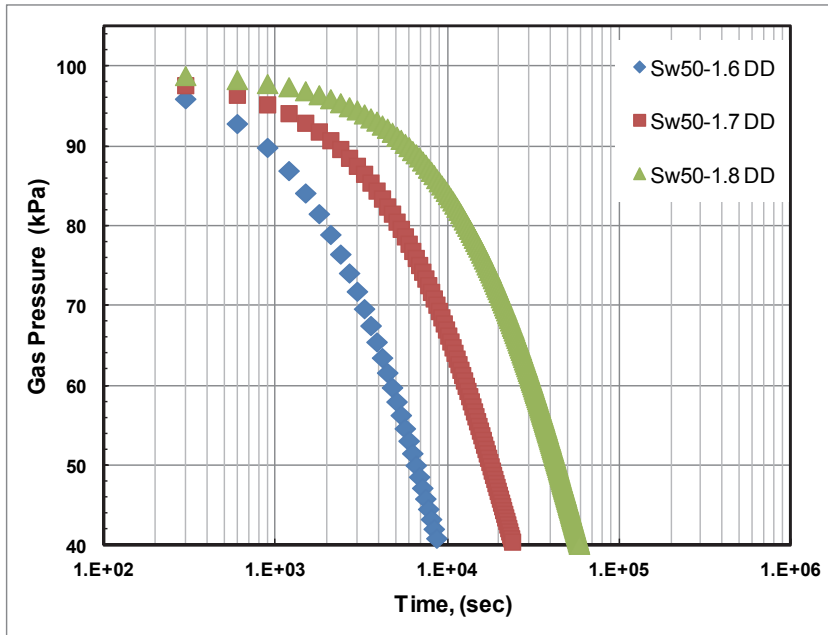
Figure 49: Gas Pressure vs. Time for Specimens Using Distilled Water at Dry Densities (DD) of 1.6, 1.7 and 1.8 Mg/m^3 and Degree of Saturation (Sw) of 50%
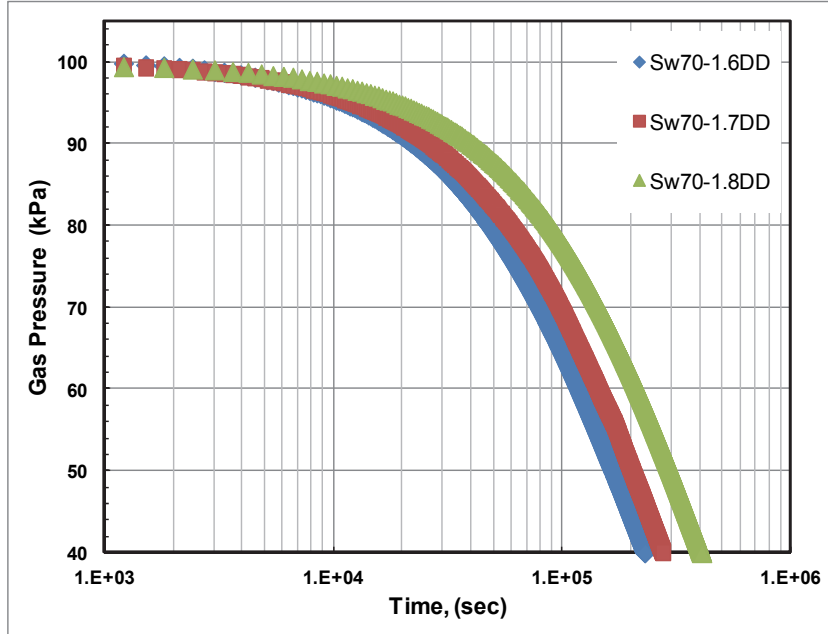
Figure 50: Gas Pressure vs. Time for Specimens Using Distilled Water at Dry Densities (DD) of 1.6, 1.7 and 1.8 Mg/m^3 and Degree of Saturation (Sw) of 70%
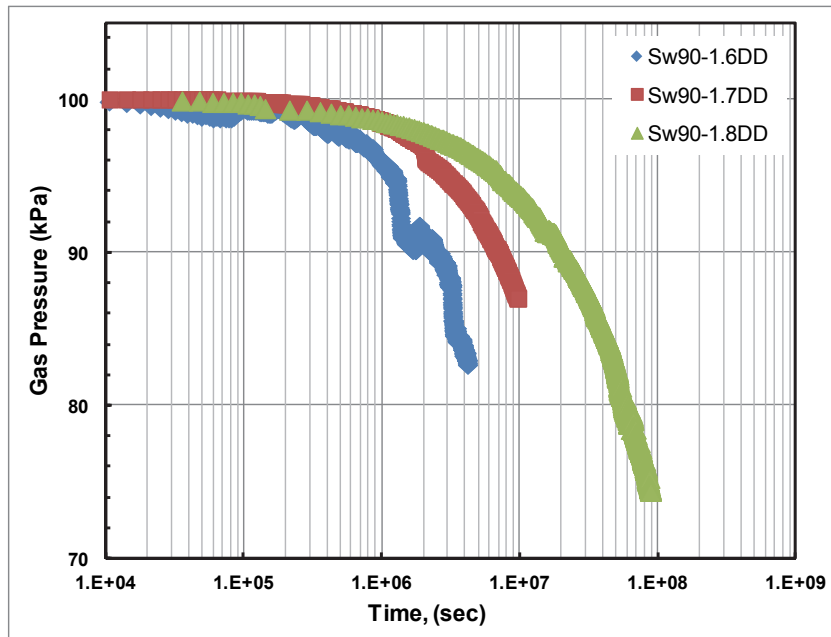
Figure 51: Gas Pressure vs. Time for Specimens Using Distilled Water at Dry Densities (DD) of 1.6, 1.7 and 1.8 Mg/m^3 and Degree of Saturation (Sw) of 90%
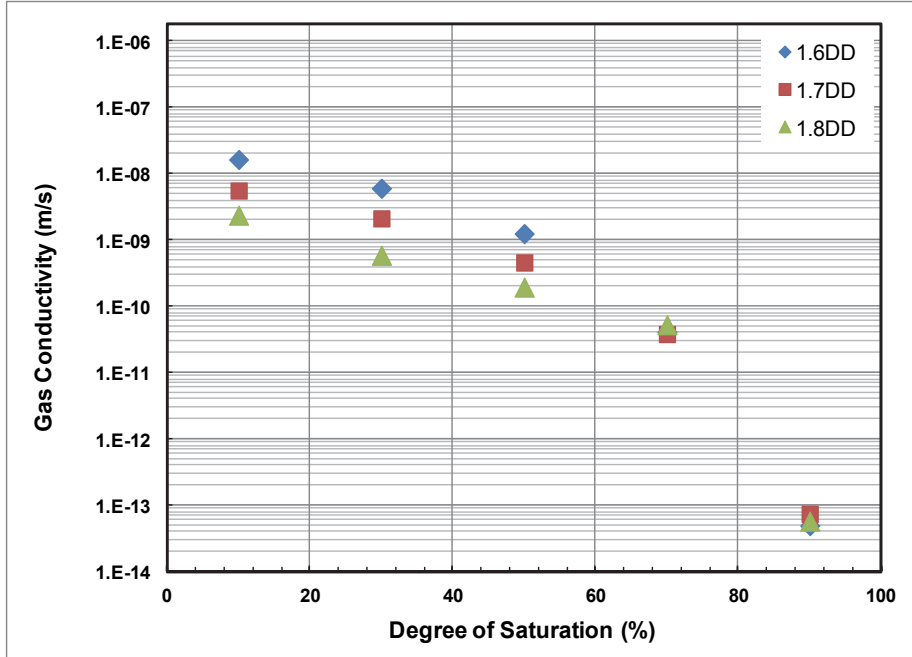
Figure 52: Gas Conductivity vs. Degree of Saturation for 70-30 BSM Specimens Prepared with Distilled Water at Various Dry Densities (DD) of 1.6, 1.7 and 1.8 Mg/m³
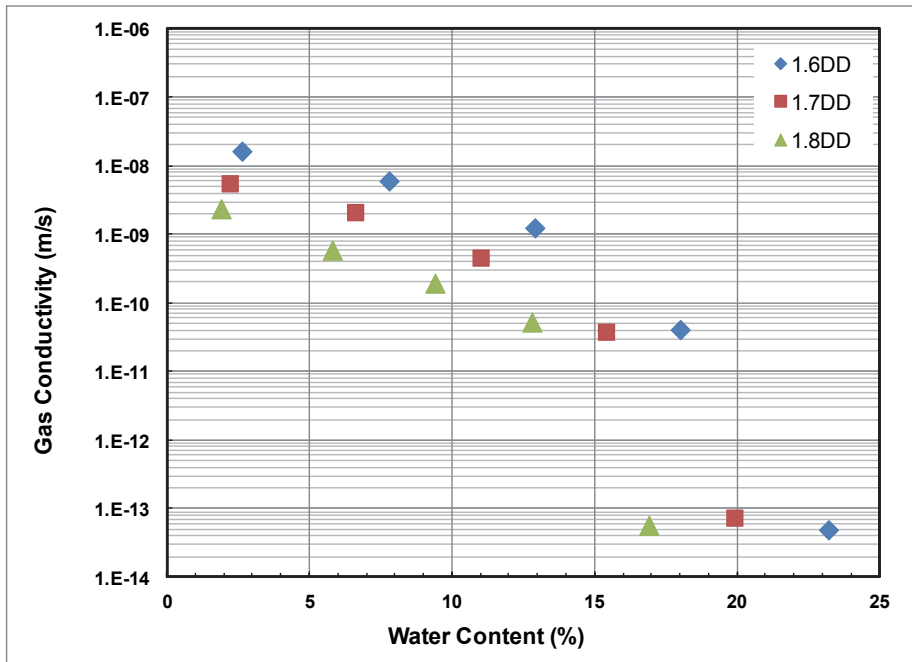
Figure 53: Gas Conductivity vs. Water Content for 70-30 BSM Specimens Prepared with Distilled Water at Various Dry Densities (DD) of 1.6, 1.7 and 1.8 Mg/m³
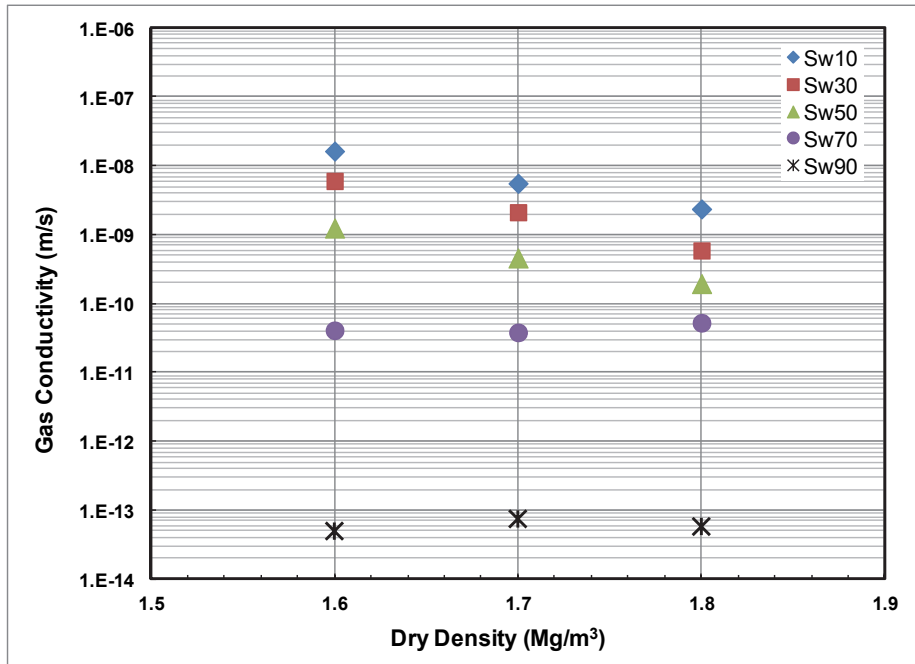
Figure 54: Gas Conductivity vs. Dry Density for 70-30 BSM Specimens Prepared with Distilled Water at Various Degree of Saturations (Sw)

3.6.1.4 Test Results for Saline Materials

The results of the gas pressure decay monitoring for tests conducted on specimens with dry density of 1.8 Mg/m^3 prepared using saline pore liquid (CR-10, SR-160, SR-270) are presented in Figures 55 through 57. These data show the same general pattern of behaviour as was observed for specimens prepared using distilled water, where an increase of degree of saturation results in slower decrease of gas pressure.

Figure 58 shows gas conductivity plotted against the degree of saturation for specimens at a given dry density of 1.8 Mg/m^3 using three saline solutions. Gas conductivity for those specimens decreases with increasing the degree of saturation. In general there is no discernible difference in gas conductivity for the specimens at the degree of saturation up to 50% and a slight difference is shown at 90% saturation. This indicates that there is little discernable effect of salinity on gas conductivity at degree of saturation less than approximately 50%.

At the degree of saturation of approximately 90%, some variance of gas conductivity can be observed in Figure 58. The gas conductivity of the specimens prepared with distilled water had lower gas conductivity than specimens prepared with saline solution. At higher saturation (e.g., Sw = 90%), it is likely that the swelling of the material may have more effect of the gas conductivity. Since the total volume of the specimens was constant, the swelling of the bentonite component may reduce the size of pore space that were available for gas transport and may result in lower gas conductivity. At a given dry density of 1.8 Mg/m^3 and degree of saturation (Sw) of 90%, it could be expected that an increase of salinity should result in higher gas conductivity. This trend was true for most specimens in Figure 58, except specimens CR10-1.8DD had gas conductivity

higher than specimens SR160-1.8DD. This may due to the variation of the actual properties of the specimens.

Gas conductivity for each saline solution is also plotted against water content for a given dry density of 1.8 Mg/m³ as shown in Figure 59. Similar to the results obtained from specimens using distilled water, gas conductivity decreases with increasing water content. Values of gas conductivity for CR10, SR160, and SR 270 solutions are very close at about 10% water content, however at water content over 10% gas conductivity for SR270 becomes higher than that for CR10 and SR160, perhaps reflecting differences in the pore size/shape of highly saline systems or differences in the mineral-water interaction.

Results of gas permeability tests for specimens prepared with distilled water at reference dry density are also shown in Figures 58 and 59. Except for the results at the highest degree of saturation, there is no discernable difference between the results of specimens prepared with distilled water and saline solution. At the highest degree of saturation/ water content, the gas permeability of specimens prepared with distilled water is relatively lower than the specimens prepared with saline solution.
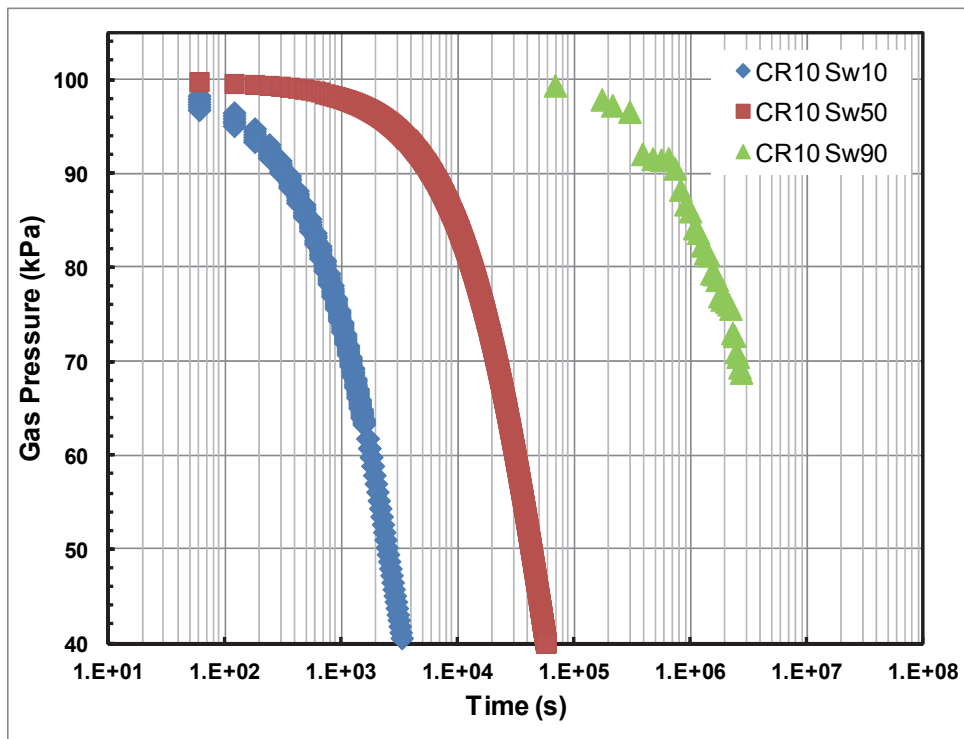
Figure 55: Gas Pressure vs. Time for 70-30 BSM Specimens at a Dry Density (DD) of 1.8 Mg/m³ Prepared Using CR10 for Sw = 10, 50 and 90%
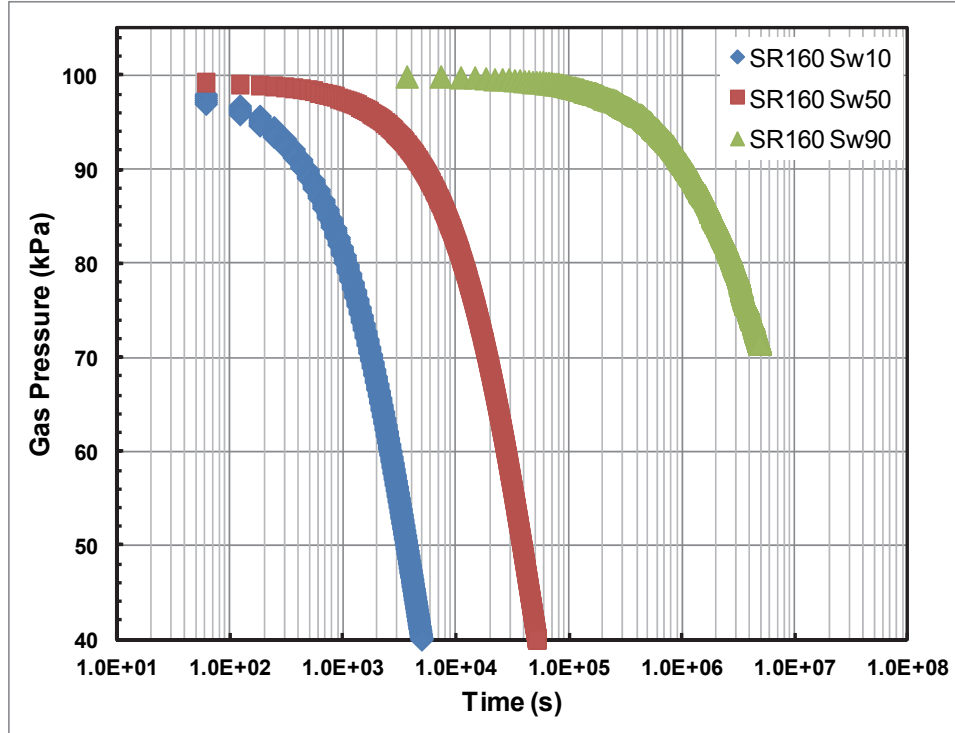
Figure 56: Gas Pressure vs. Time for 70-30 BSM Specimens at a Dry Density (DD) of 1.8 Mg/m³ Prepared Using SR160 for Sw = 10, 50 and 90%
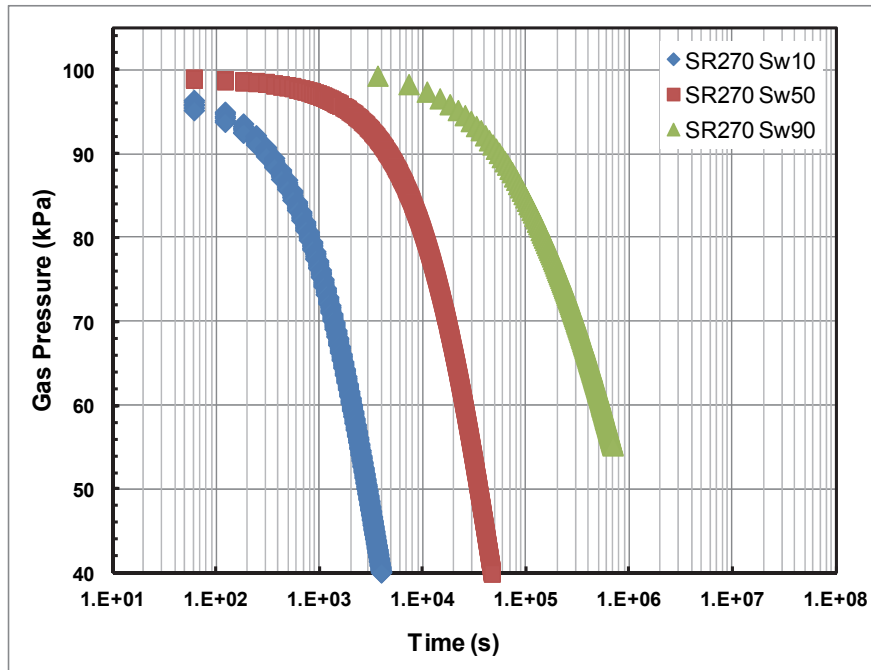
Figure 57: Gas Pressure vs. Time for 70-30 BSM Specimens at a Dry Density (DD) of 1.8 Mg/m³ Prepared Using SR270 for Sw = 10, 50 and 90%
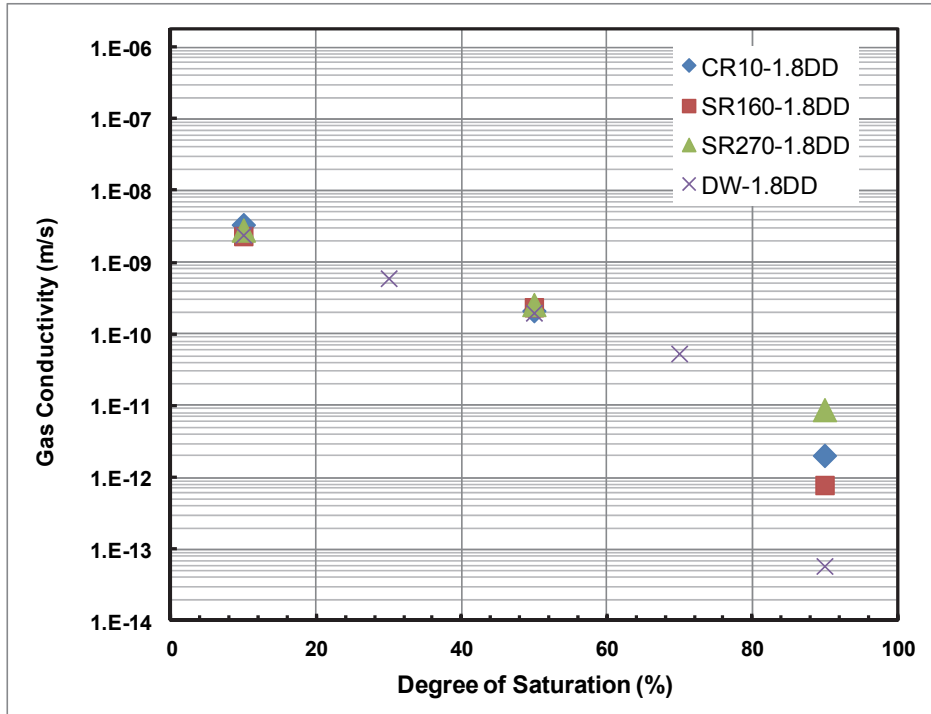
Figure 58: Gas Conductivity vs. Degree of Saturation for a Dry Density (DD) of 1.8 Mg/m³ Using Saline Solutions
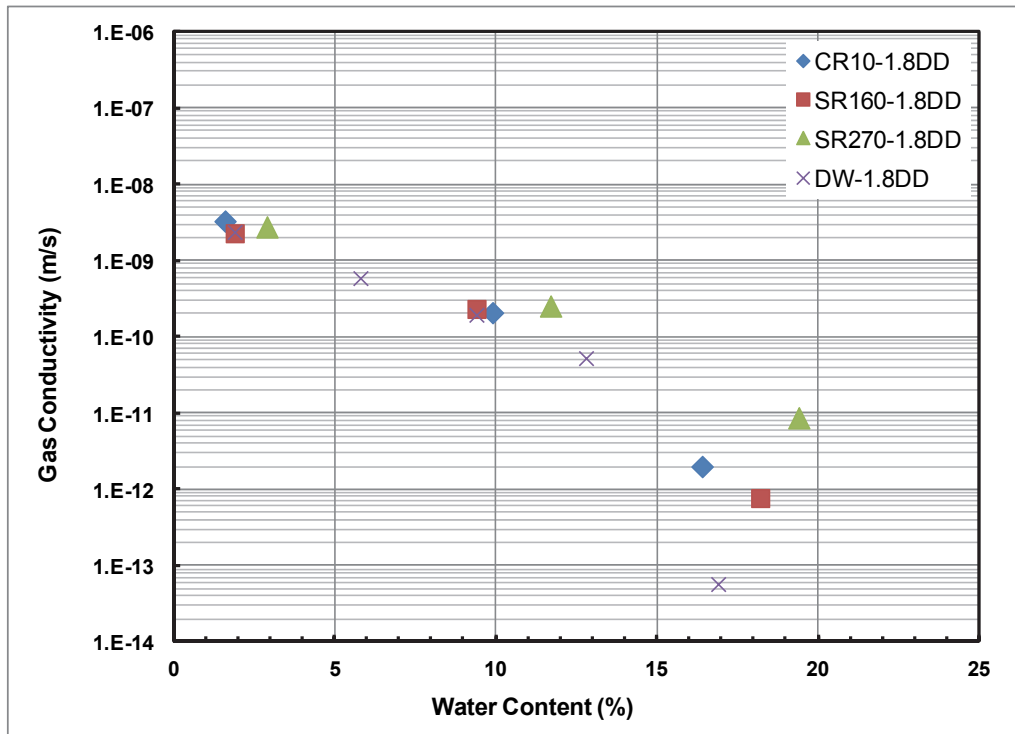
Figure 59: Gas Conductivity vs. Water Content for a Dry Density (DD) of 1.8 Mg/m³ Using Saline Solutions

3.6.1.4 Summary of Gas Permeability Tests

The gas permeability tests completed as part of this program of work, the properties of the 70-30 BSM specimens can be summarised as follows:

1. For a given dry density, gas permeability decreases with increasing degree of saturation.

2. For a given water content (degree of saturation), gas permeability decreases with dry density up to a degree of saturation of~50%, beyond which there is little effect of density change.

3. At a dry density of 1.8 Mg/m^3 and degree of saturation less than 50%, the salinity of the pore liquid shows little influence on gas permeability.

4. At a dry density of 1.8 Mg/m^3 and higher degree of saturation (e.g., 90%), the gas permeability of specimens prepared with distilled water is relatively lower than the specimens prepared with saline solution.

3.6.2 Measurement of the Soil-Water Characteristic Curve (SWCC)

3.6.2.1 Background

A series of suction-moisture tests were completed as part of this testing program. These tests were intended to provide the information necessary to develop a soil-water characteristic curve (SWCC) for the 70-30 BSM. The SWCC was determined using a vapour equilibrium technique (VET) (Blatz et al. 2008). A similar method has been successfully used to determine SWCC of a 50-50 BSM (e.g., Wan 1996; Blatz 2000; Anderson 2003). Environments of constant suction can be created in sealed containers using the osmotic potential of chemical solutions and these are used to instil a known suction in a BSM specimen. Twelve desiccators with 10 different values of target suctions in the range of 0.5 MPa to 160 MPa were utilized in these tests. Figure 60(b) shows 12 desiccators used for the tests. As temperature change could affect the test results, these desiccators were stored inside the environmental chamber during the test in order to keep the temperature constant at 25°C (see Figure 60(a)). The solutions used to provide the suctions were Potassium Chloride (KCl) solutions for lower suction (< 5 MPa) and Sulphuric Acid (H$_2$SO$_4$) solutions for higher suction (> 5 MPa). The concentration of the KCl and H$_2$SO$_4$ solutions corresponding to the preselected suction is provided in Table 15, which were determined using relationships outlined by Stokes and Robinson (1948) and Young (1967).

Table 15: Potassium Chloride (KCl) and Sulphuric Acid (H_2SO_4) Solution Corresponding to Selected Total Suctions

No.	Suction (MPa)	RH (%)	Type of solution	Concentration	
				TDS (g/L)	M (mol/L)
1	0.5	99.64	KCl	6.721	0.090
2	1	99.27	KCl	13.675	0.183
3	2	98.55	KCl	27.469	0.368
4	5	96.42	KCl	67.955	0.912
5	5	96.42	H_2SO_4	--	1.08
6	10	92.97	H_2SO_4	--	1.54
7	20	86.43	H_2SO_4	--	2.39
8	40	74.71	H_2SO_4	--	3.74
9A & 9B	80	55.82	H_2SO_4	--	5.46
10A & 10B	160	31.15	H_2SO_4	--	7.49

Note: These values are determined based on Young 1967, Stokes and Robinson 1949.

(a)   (b)
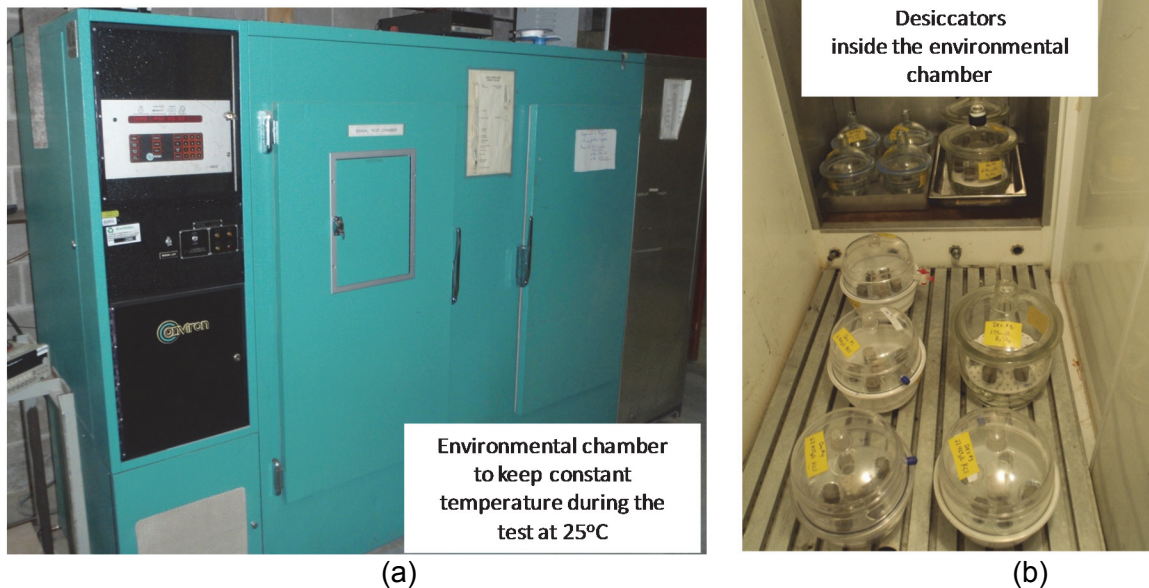
Figure 60: (a) Environmental Chamber and (b) Desiccators Utilized for SWCC Tests Using Vapour Equilibrium Techniques

The procedure used in the SWCC testing was as follows.
- The bentonite and sand materials were dried in the oven at temperature of 110±5°C for at least 24 hours.
- The pre-determined amount of bentonite, sand and liquid were mixed to achieve target water content. This 70-30 BSM mixture was then stored in a refrigerator inside a sealed container for at least 24 hours prior to specimen compaction to ensure the consistency of the moisture content of the mixture.

- For compacted specimens, the 70-30 BSM mixture was compacted in a compaction mould using a hydraulic press to obtained compacted specimens with target initial properties (i.e., dry density and water content). For loose specimens, the 70-30 BSM mixture was placed in the glass container.
- Prior to the test, the dimensions and weight of each specimen were measured using a calliper and digital scale, respectively. The water content of the left-over 70-30 BSM mixture was then measured based on the ASTM D2216-10. When a specimen was prepared using salt solution, the corrected water content was calculated using Equation (1). The initial dry density and water content of the specimen were calculated based on these measurements.
- Compacted specimens were placed in the desiccators after the sulphuric acid solutions had equilibrated with the vapour pressure in the headspace (3 days).
- The mass of the individual specimens was measured several times during the testing process and once their mass had stabilized the test was deemed to be complete.
- At the-end of testing, the concentration of KCl and H_2SO_4 solutions in the desiccators was measured to confirm that the suction was correct. The dimensions and weight of each specimen were measured using a calliper and digital scale, respectively. The water content of the left-over 70-30 BSM mixture was then measured based on the ASTM D2216-10. The initial dry density and water content of the specimen were calculated based on these measurements.

Figure 61 illustrates the changes of the water content of 6 specimens in a dessicator that had sulphuric acid solution corresponding to ~40 MPa suction. Specimens 18A-8, 18B-8, 18C-8, 16-8, and 14-8 had diameters of ~32 mm and thicknesses of ~32 mm. Specimen L-8 was a loose material. The gravimetric water content was calculated using two different methods: (1) based on initial measurements, and (2) based on the end of test (EOT) measurements. Only slight differences can be observed between the water content calculated based on initial and EOT measurements. Note that the final actual measurement of the water content was used for specimens prepared with distilled water.

As the equilibration time reported in previous tests of this type was 30 days for 50 mm diameter and 100 mm height specimen (Tang 1999) there was a change in the specimen size made to try and shorten the testing time. The SWCC tests done in this study used small specimens (32 mm diameter and 32 mm height) and loose materials to try to reduce the equilibration time and to determine the SWCC relationship of the 70-30 BSM. As can be seen in Figure 61, the time needed to achieve equilibrium was not discernibly reduced by specimen size reductions, however reduced specimen size allowed for a larger number of specimens to be tested at the same time in the available desiccators. The miniature compaction device used in the compaction tests (Figure 9) was used to prepare the specimens.

In total, 214 specimens were tested to generate the SWCC curve of the 70-30 BSM. The complete results of the SWCC measurements are provided in Appendix E. The effects of varying the initial dry density (loose material, 1.4 Mg/m^3, 1.6 Mg/m^3, and 1.8 Mg/m^3), initial water content of 18%, 24% and 32%, and different pore liquids (DW, CR10, SR160, and SR270 solutions) were evaluated in this study.

Dessicator no. 8 (H₂SO₄, S ~ 40 MPa)
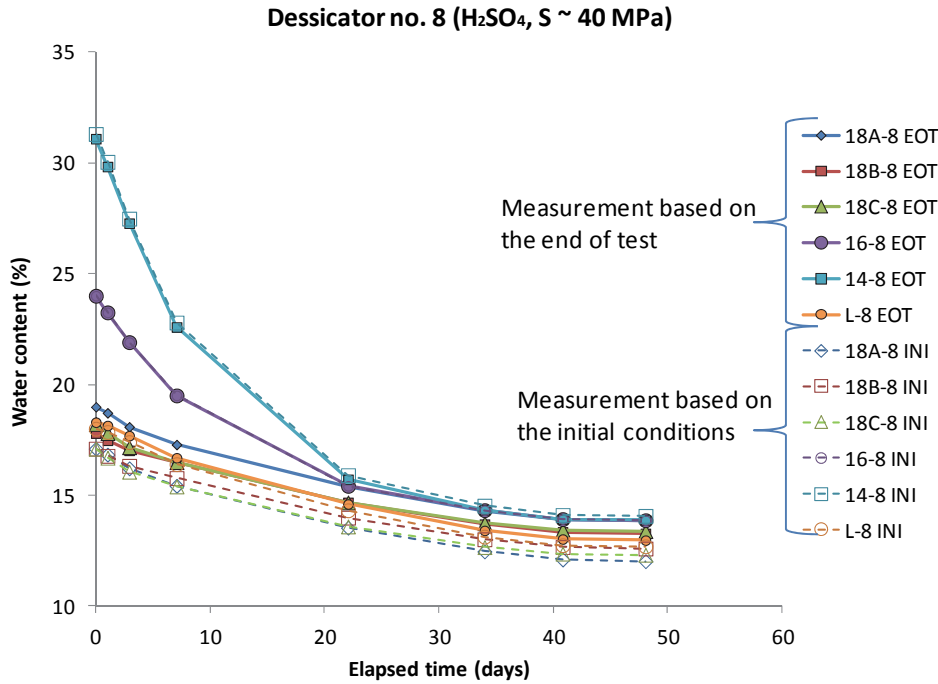
Figure 61: Water Content versus Time of BSM Specimens

3.6.2.2 Specimens Prepared Using Distilled Water

Figure 62 shows the water content versus suction of the specimens prepared with distilled water. The label in this figure has the following format:

> *"types of liquid used to prepare the specimens" – "target initial dry density in Mg/m³"- "target initial water content in %".*

For example, "DW-L-w18%" is specimens prepared with distilled water (DW), loose material (L) and had an initial target water content of 18%. "DW-1.4-w32%" is specimens prepared with distilled water (DW) having target initial dry density of 1.4 Mg/m³ and target initial water content of 32%. The water content and dry density plotted in this figure are from the end of test (EOT) measurements. These values are not equal to the initial target dry density and water content shown in the label. Complete SWCC data are provided in Appendix E.

Figure 62 shows the results for materials prepared using distilled water. For suction greater than 5 MPa, there is a clear pattern of decreasing suction with increasing water content for each specimen, but it is unclear for lower suctions (< 5 MPa). For suction greater than 5 MPa, a series of exponential trend lines for suction versus water content for specimens prepared with distilled water are shown in Figure 63. The equations with R^2 greater than 0.9 are also displayed in this figure showing a good correlation between the trend lines and data.
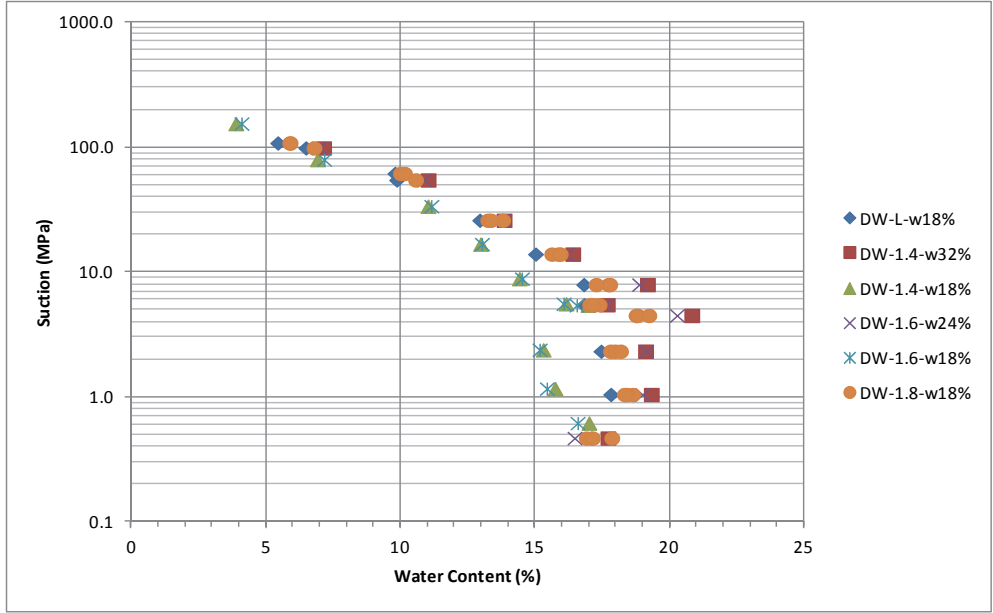
Figure 62: Water Content vs. Suction of Specimens Prepared with DW
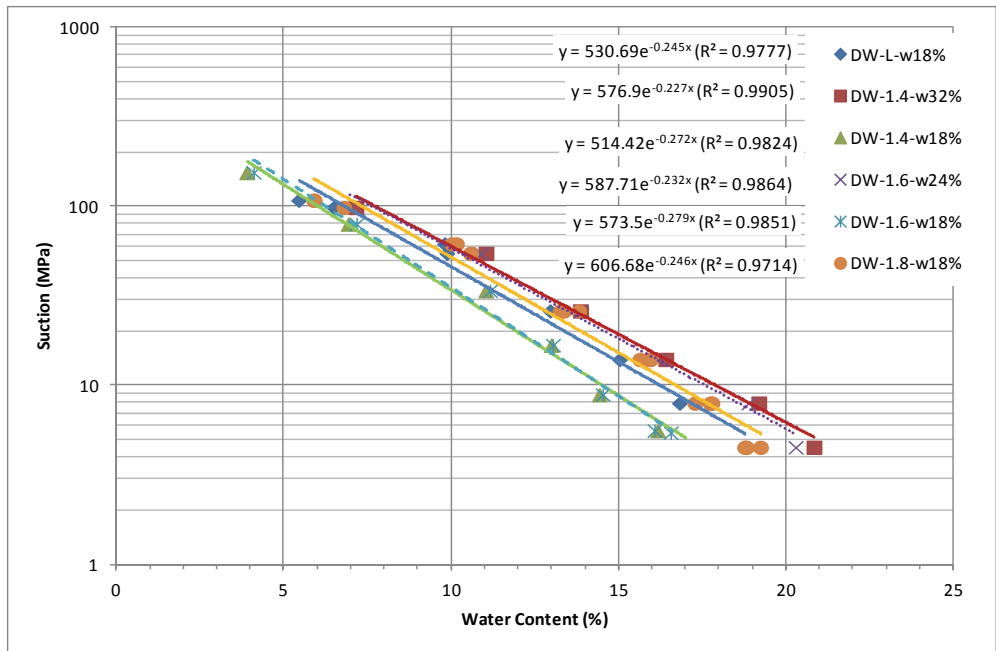
Figure 63: Exponential Trend Lines of Water Content vs Suction of Specimens Prepared with DW for Suction > 5 MPa

The effect of the initial water content on the suction behaviour of the 70-30 BSM is illustrated in Figure 64. For a given dry density, when the initial water content is higher, the suction tends to be greater for a given value of water content. This difference of the water content – suction trendlines seems to diminish in magnitude with increasing suction.
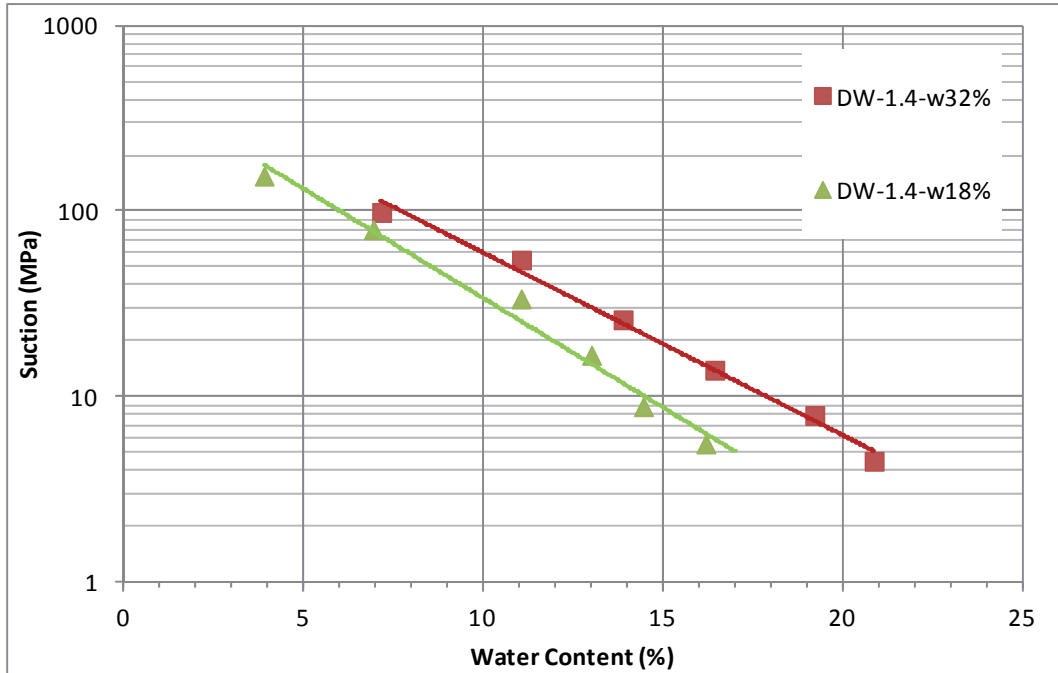
Figure 64: Effect of Initial Water Content on Specimens for a Given Dry Density

The bulk density and water content of the specimens were measured at the end of test and used to determine the degree of saturation of the specimens. Figure 65 shows the degree of saturations versus suctions for specimens prepared with distilled water.

Specimens DW-1.4-w18%, DW-1.6-w18% and DW-1.8-w18% were prepared from the same mixture having water content of 18%, but compacted to different dry densities of 1.4, 1.6, and 1.8 Mg/m³, respectively, that correspond to initial degree of saturations of approximately 50%, 68% and 90%, respectively. Specimens DW-1.4-w32% and DW-1.6-w24% were made from different mixtures having water contents of 32% and 24% and compacted at initial dry densities of 1.4 and 1.6 Mg/m³, respectively. These correspond to the initial degree of saturation of >90%.

The data in Figure 65 show an inconsistent pattern of suction versus saturation for most specimens. It seems that the maximum degree of saturation for each test cannot be greater than the initial degree of saturation. This is the result of the unconfined nature of the test, allowing the specimens to increase or decrease in volume as the result of water uptake/loss. The relationships of the degree of saturation versus suction may be dependent on the confinements of the tests. This may also be an indication that this particular method to determine the SWCC is more suitable for use when measuring the drying SWCC curve and development of a method that uses a confined, constant volume specimen might provide a more consistent pattern of suction versus degree of saturation. The data of specimens compacted at reference dry density of 1.8 Mg/m³ were used to estimate the SWCC relationships for backfill materials when the data was fit to a van Genuchten relationship (Section 3.6.3).
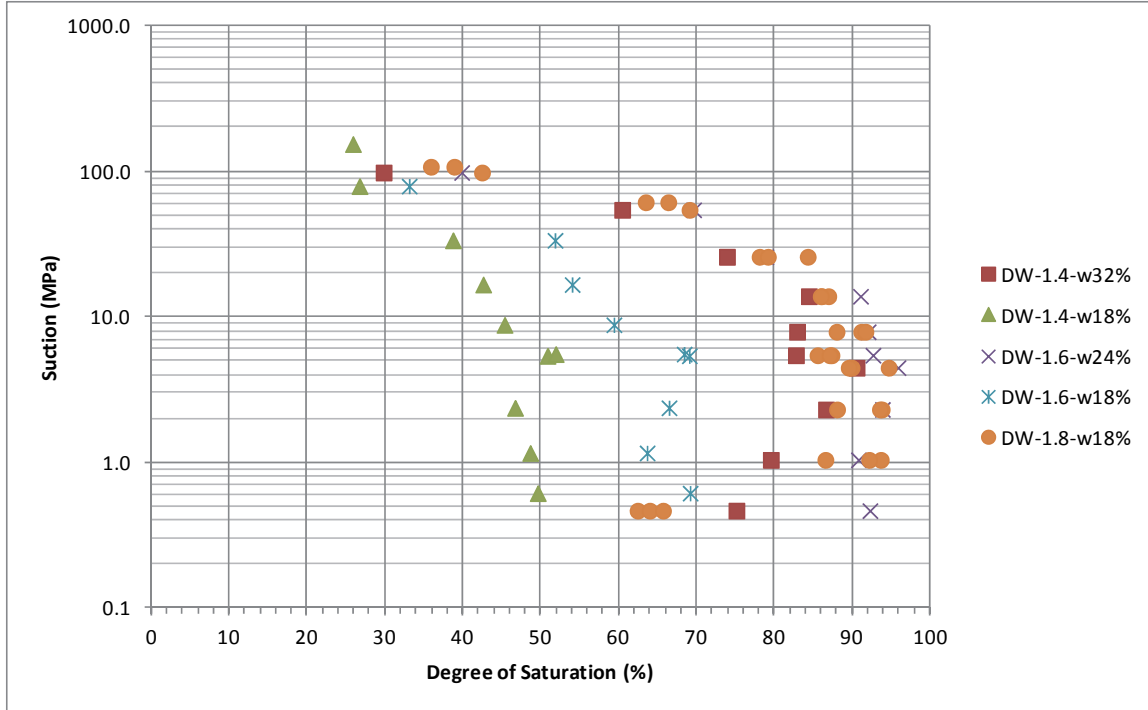
Figure 65: Degree of Saturation vs. Suction in Specimens Prepared with Distilled Water (DW)

3.6.2.3   Specimens Prepared Using Saline Pore liquid

The suction-water content behaviour and suction-degree of saturation behaviour for specimens prepared with CR10, SR160, and SR270 solutions are shown in Figures 66 to 71. The legend labels on these figures have the same format as previous figure (e.g., Figure 62), which is:

> "types of liquid used to prepare the specimens" – "target initial dry density in Mg/m³"- "target initial water content in %".

- "Types of liquid used to prepared the specimens" include: CR10, SR160, SR270;
- "Target initial dry density" include: L (loose material), 1.4, 1.6, 1.8 Mg/m³; and
- "Target initial water content" include: 18%, 24%, 32%.

The data displayed in these figures are the gravimetric water content ($\overline{w}$), degree of saturation (Sw), and dry density (ρ_{dry}) at the end of test, which are not the same as the values used in these labels. In some cases, the dry density of a specimen decreased from 1.8 Mg/m³ at installation to 0.8 Mg/m³ at the end of test.

At the beginning of the test, the total weight and volume after compaction were measured and used to calculate the bulk density of each specimen (ρ_{bulk}). The water content ($\overline{w}$) of the left over mixture was measured and correction due to remaining salt after oven-drying process was done according to ASTM D4542-07. The initial salinity of the solution was equal to the solution used to prepare the specimens. The dry density

(ρ_{dry}) of the specimen at the beginning of the test was determined from the bulk density and corrected water content (i.e., $\rho_{dry} = \rho_{bulk}/(1+ \bar{w})$). The masses of soil solids (M_s), salt (M_{salt}), and water (M_w) at the beginning of the test were then calculated based on these initial conditions.

During the test, total mass of each specimen (i.e., $M_{total} = M_s +M_w+M_{salt}$) was measured periodically, until it reached suction equilibrium, then the test was ended. Between installation and end of test, only mass of water (M_w) was changing, while the masses of soil solids (M_s) and salt (M_{salt}) were constant. The total mass measurement was then used to calculate the current solution content. At the end of test, the total mass and volume of each specimen were measured to calculate the bulk density. Oven-dried water content at the end of test was also measured.

The SWCC plots in Figures 66 to 71 show suctions as functions of the liquid content ($\bar{w}$) and degree of saturation at the end of test. The degree of saturation was calculated based on the water content and bulk density measurement at the beginning of test. Note that the salinity of the pore liquid was changed throughout the test as the water going into or leave the specimen.

For lower suction (s < 10 MPa), the degree of saturation and liquid contents are higher for specimens prepared with SR160 (Figures 68 and 69) and SR270 (Figures 70 and 71) in comparison to the CR10 (Figures 66 and 67). This may due to the following factors.

First, the specimens SR160 and SR270 were likely to follow the SWCC wetting curves, while the specimens CR10 were likely to follow the SWCC drying curves. Note that usually the wetting and drying curve of the SWCC do not follow the same paths. The final gravimetric water contents plotted on the SWCC for the SR160 and SR270 specimens higher than the initial gravimetric water contents, oppositely they are lower than initial gravimetric water content for CR10 specimens.

Secondly, the initial KCl and H_2SO_4 solution concentrations used in the desiccators corresponding to the lower suction (s < 10 MPa) were lower than the concentrations of the SR160 and SR270 solutions. Consequently, the specimens tend to absorb more water to reach concentration equilibrium. In contrast, the initial KCl and H_2SO_4 solution concentrations used in the desiccators corresponding to the lower suction (s < 10 MPa) were higher than the concentrations of the CR10 solution and the CR10 specimens tend to decrease the water content to reach concentration equilibrium.

Third, the specimens in the desiccators were unconfined and allowed to have volume change. Similar to the specimens prepared with distilled water, the specimens prepared with CR10 solution experienced larger swelling compared to SR160 and SR270. Consequently, the degree of saturation of specimens prepared with CR10 did not reach 100% saturation, as the large swelling occurred, an increase of liquid content were also followed by large increase of void ratio.

The suction-water content behaviours for specimens prepared with CR10, SR160, and SR270 solutions follow the trends observed for DW specimens. For suction greater than 5 MPa, there is a clear pattern of decreasing suction with increasing water content for each specimen. For lower suctions (< 5 MPa), the pattern is less clear. For suction greater than 5 MPa, a series of exponential trend lines for suction versus liquid content for specimens prepared with CR10, SR160, and SR270 are shown in Figures 72, 73,

and 74, respectively. The equations and the R² are also displayed in the figures showing a good correlation between the trend lines and data. The trend lines of degree of saturation versus suction are presented in Section 6.1.3.
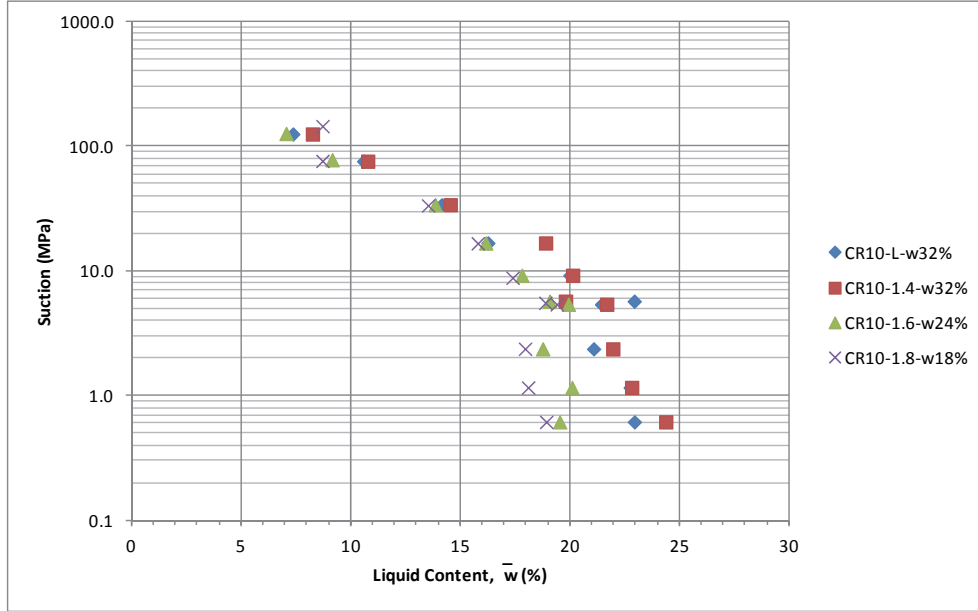
Figure 66: Suction vs. Liquid Content for Specimens Prepared with CR10 Solution
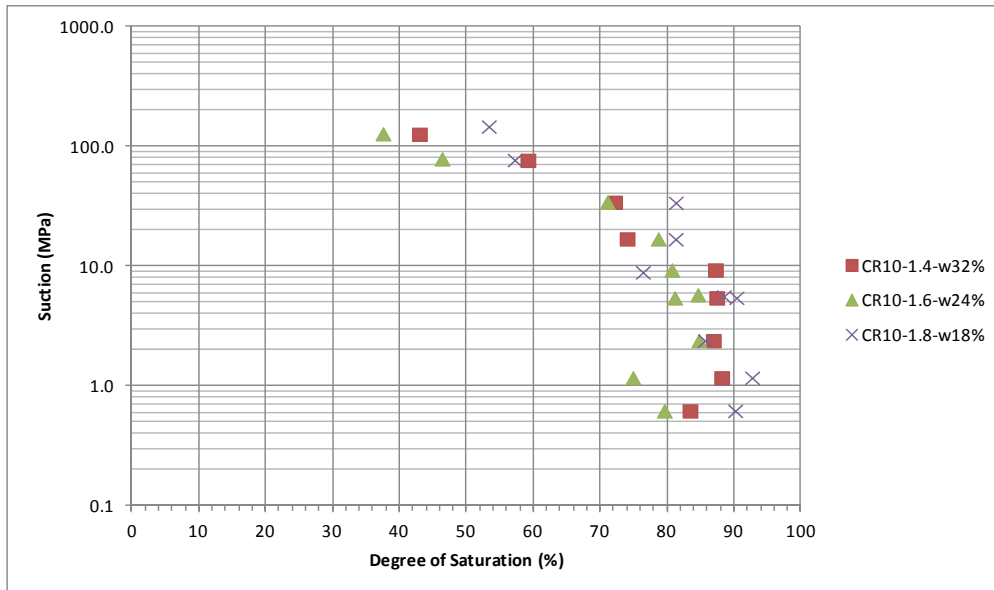
Figure 67: Suction vs. Degree of Saturation for Specimens Prepared with CR10 Solution
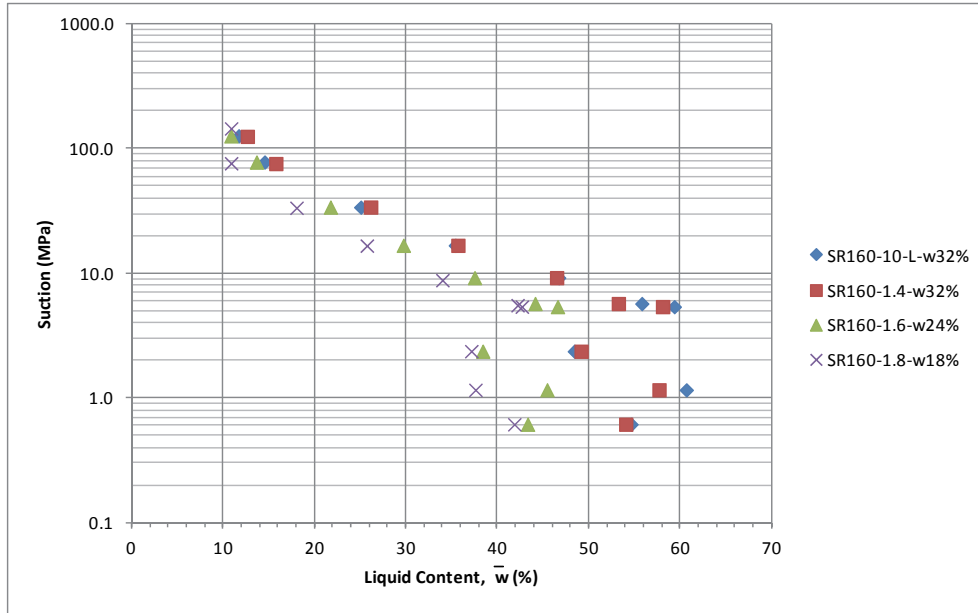
Figure 68: Suction vs. Liquid Content for Specimens Prepared with SR160 Solution
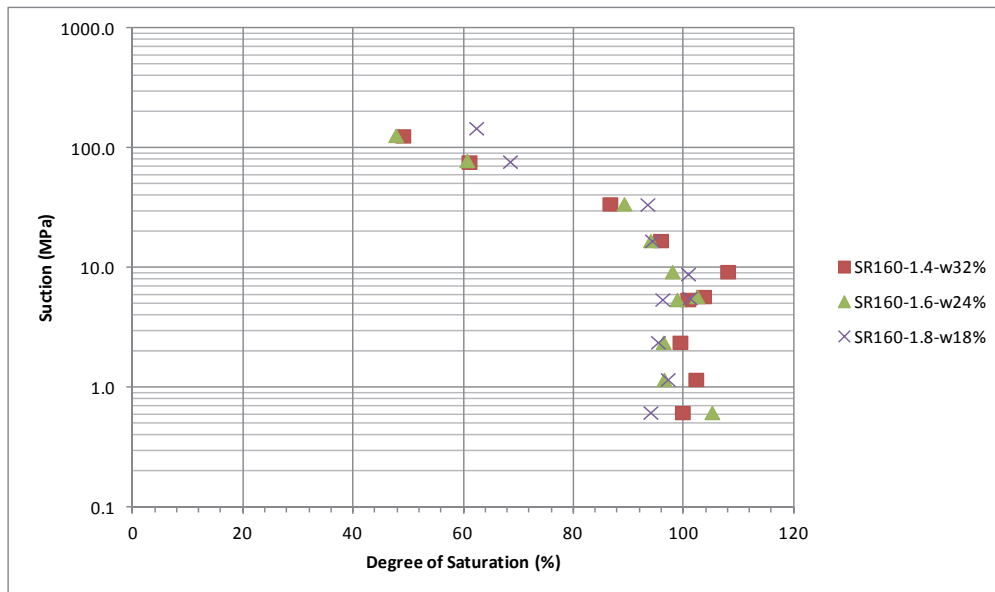
Figure 69: Suction vs. Degree of Saturation for Specimens Prepared with SR160 Solution
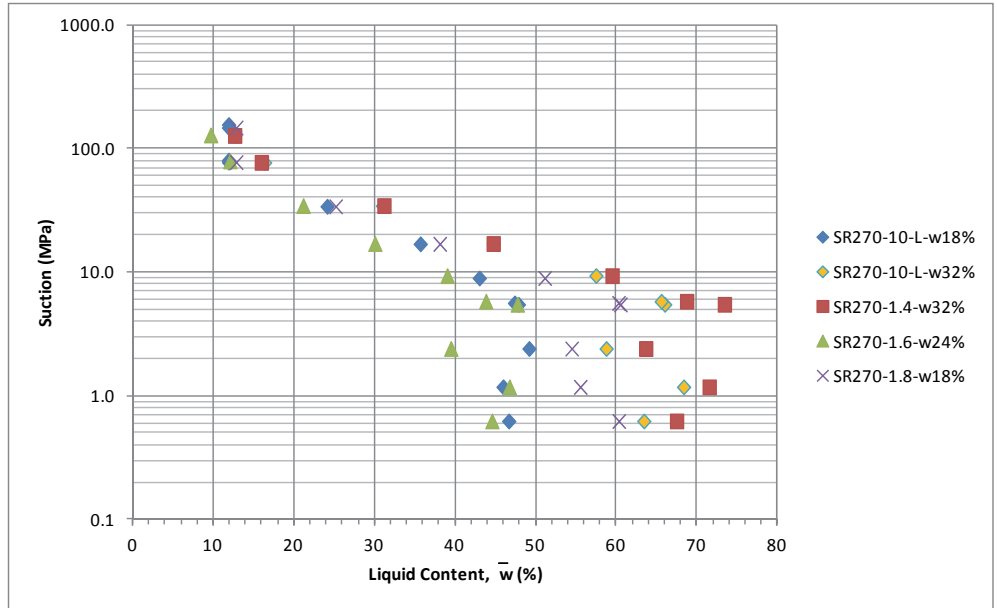
Figure 70: Suction vs. Liquid Contents for Specimens Prepared with SR270 Solution
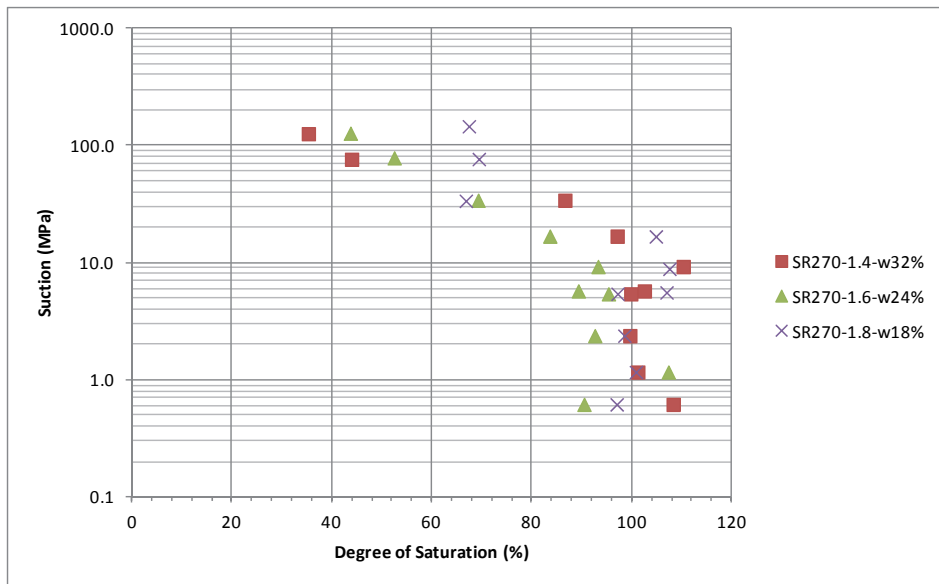
Figure 71: Suction vs. Degree of Saturation for Specimens Prepared with SR270 Solution
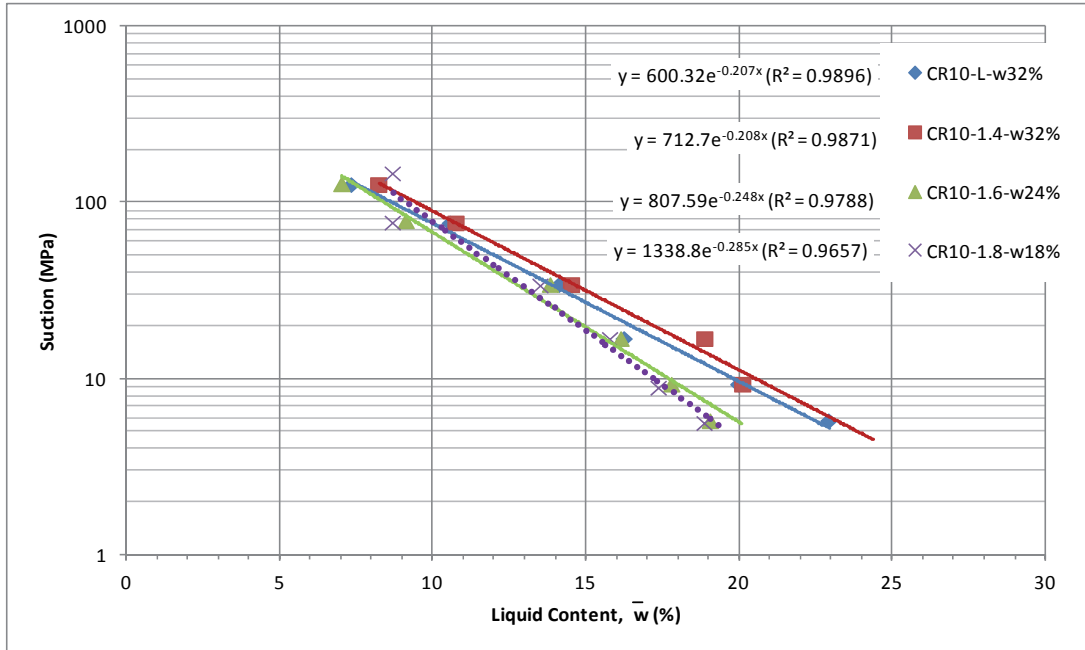
Figure 72: Exponential Trend Lines of Suction vs. Liquid Content for Specimens Prepared with CR10 Solution for Suction > 5 MPa
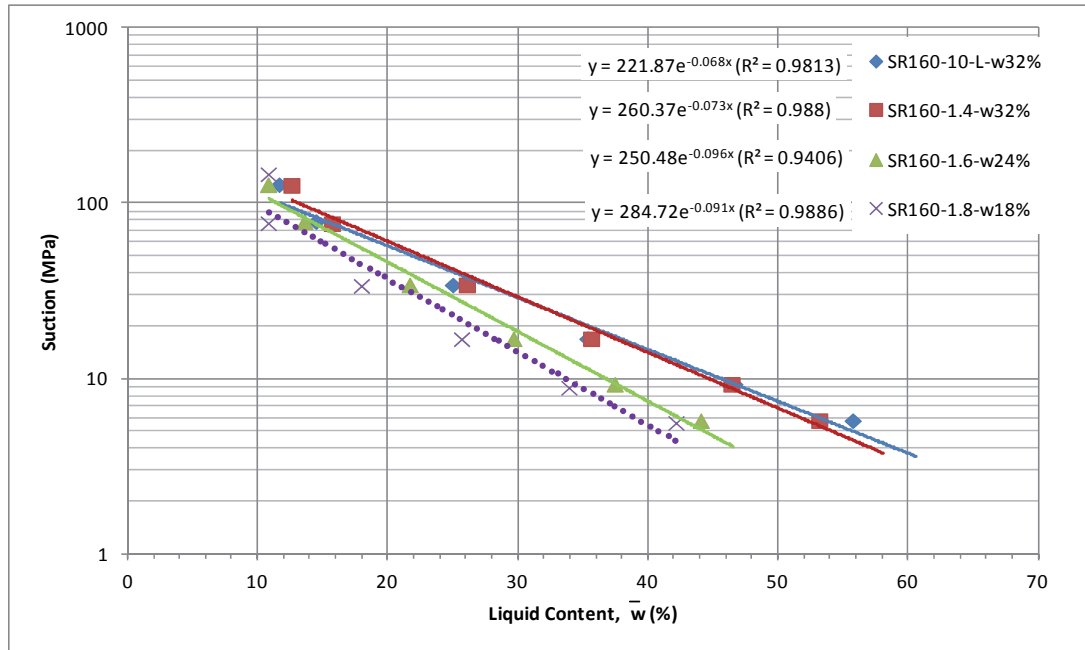
Figure 73: Exponential Trend Lines of Suction vs. Liquid Content for Specimens Prepared with SR160 Solution for Suction > 5 MPa
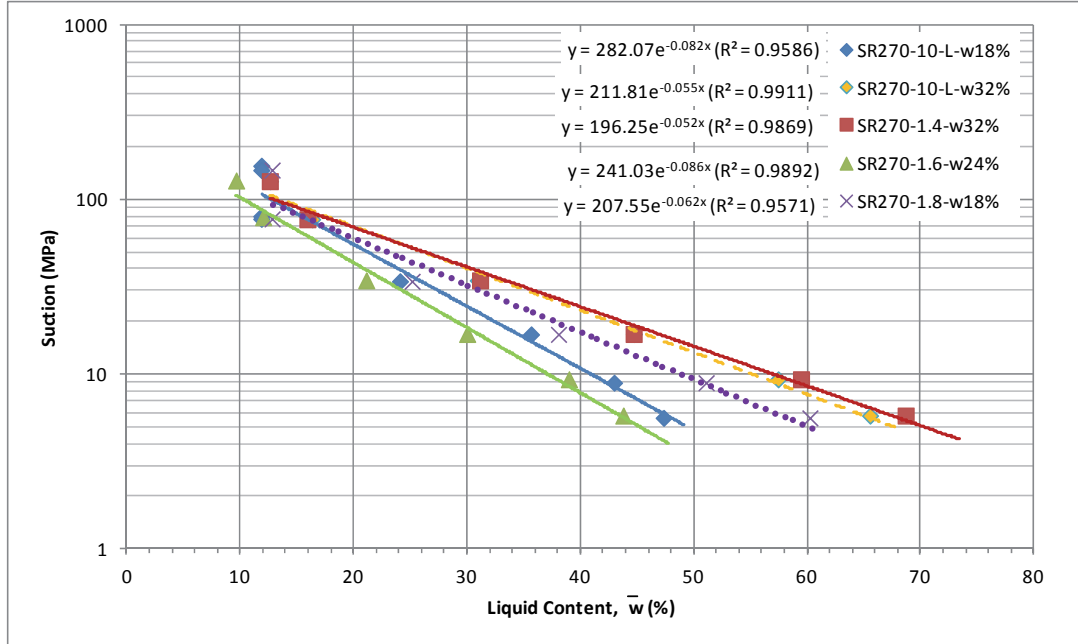
Figure 74: Exponential Trend Lines of Suction vs. Liquid Content for Specimens Prepared with SR270 Solution for Suction > 5 MPa

3.6.3 Determining the Parameters to Define Relationships between Gas Permeability and Suction

3.6.3.1 Background

Several models are available to describe the relationships of the gas permeability, degree of saturation, and suction. For the purpose of the study, the parameters of the van Genuchten capillary curve and the van Genuchten-Mualem-Luckner relative permeability curves were determined based on the results of the gas permeability and SWCC tests for 70-30 BSM. Using the available gas permeability and SWCC measurements, parameters of other models can be determined with curve-fitting method.

The van Genuchten capillary pressure equation is given by:

$$P_c = \frac{1}{\alpha} \left[S_{ec}^{-1/m_c} - 1 \right]^{1/n} \tag{11}$$

$$S_{ec} = \frac{S_l - S_{lr}}{1 - S_{lr}} \tag{12}$$

The van Genuchten-Mualem-Luckner relative permeability curves are given by:

$$k_{rg} = \left(1 - S_{e_k} \right)^{1/3} \left[1 - S_{e_k}^{1/m_k} \right]^{2m_k} \tag{13}$$

$$k_g = k_{rg} * k \tag{14}$$

$$S_{ek} = \frac{S_l - S_{lr}}{1 - S_{lr} - S_{gr}} \tag{15}$$

Where

   P_c is the capillary pressure, Pa;
   k_{rg} is the gas phase relative permeability (ratio);
   k   is the intrinsic permeability, m^2.
   S_{ec} is the effective degree of saturation for the capillary pressure relationship (volume ratio);
   S_{ek} is the effective degree of saturation for the relative permeability relationship (volume ratio);
   S_l is the liquid saturation (volume ratio);
   S_{lr} is the residual liquid saturation (volume ratio);
   S_{gr} is the residual gas saturation (volume ratio);
   m_c is a van Genuchten fitting parameter (unitless);
   m_k is a van Genuchten fitting parameter (unitless);
   n   is a van Genuchten fitting parameter (unitless); and
   α is a van Genuchten fitting parameter, Pa^{-1}.

For the purpose of fitting parameter in this study, some changes on the equations are made. First, parameters m_c and m_k for capillary curves and permeability are set to be independent. In addition, the value of intrinsic permeability (k) is replaced with a maximum gas conductivity corresponding to the lowest degree of saturation ($K_{g,max}$), which has a unit of m/s, so that Equation (14) becomes:

$$K_g = k_{rg} * K_{g,max} \tag{16}$$

3.6.3.2 Parameters to Define Gas Conductivity versus Degree of Saturation

Table 16 summarizes the fitting parameters that define the relationship of gas conductivity with the degree of saturation of specimens 70-30 BSM. Figures 75 and 76 show the comparison of the curves with the data points from the gas permeability tests. The curves in these figures were created by substituting parameters in Table 16 into Equations (13), (14), and (16).

Table 16: The van Genuchten-Mualem-Luckner Relative Permeability Parameters Estimated from the Gas Permeability Test Results

	Mixing Liquid	Dry density (Mg/m³)	S_{lr}	S_{gr}	m_k	$K_{g, max}$ (m/s)
DW-1.6DD	DW	1.6	0	0.07	1.5	3.28E-08
DW-1.7DD	DW	1.7	0	0.06	1.5	1.12E-08
DW-1.8DD	DW	1.8	0	0.05	1.5	4.74E-09
CR10-1.8DD	CR10	1.8	0	0	1.4	6.6E-09
SR160-1.8DD	SR160	1.8	0	0	1.5	4.58E-09
SR270-1.8DD	SR270	1.8	0	0	1.2	5.54E-09
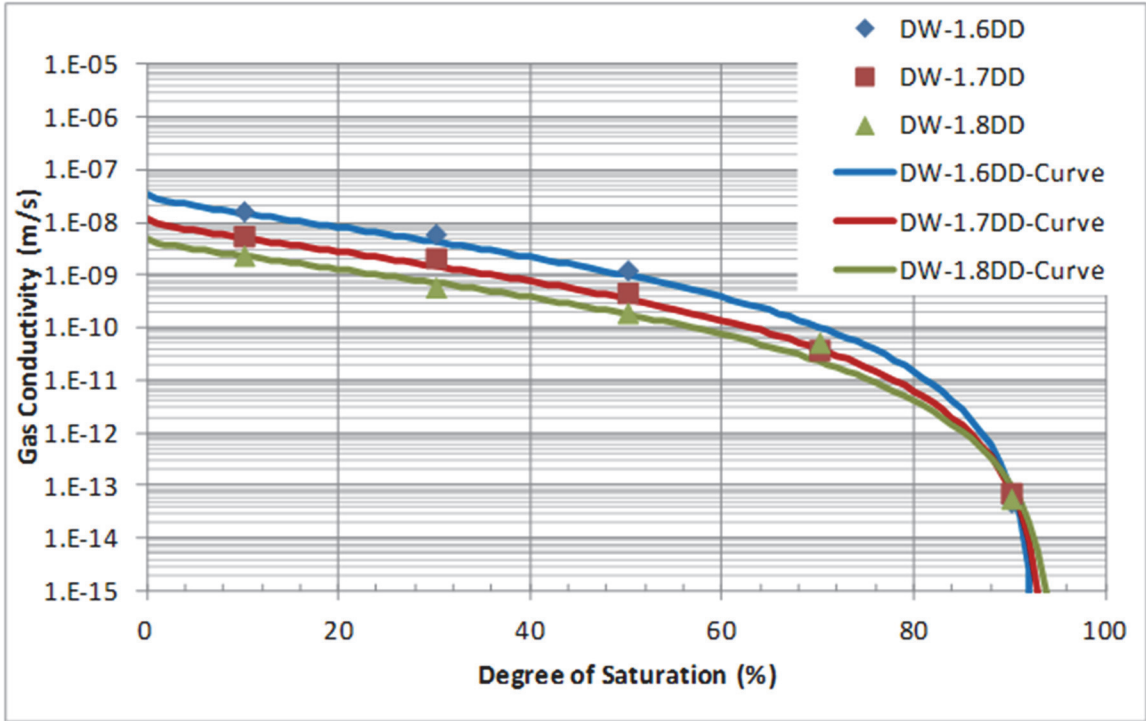
Figure 75: Gas Conductivity-Degree of Saturation Curves Compared to the Laboratory Test Data for Specimens Prepared with Distilled Water with Dry Densities Variation of 1.6, 1.7, and 1.8 Mg/m³
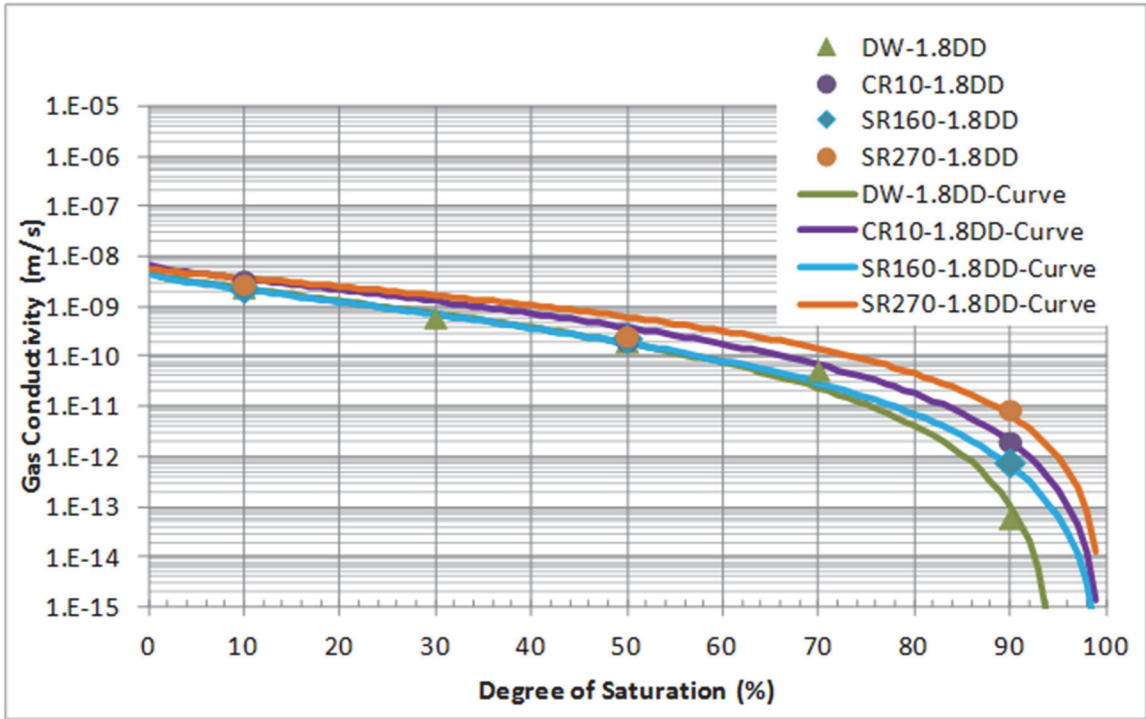
Figure 76: Gas Permeability-Degree of Saturation Curves Compared to the Laboratory Test Data for Specimens with Dry Density of 1.8 Mg/m³ Prepared with Various Groundwater

3.6.3.3 Parameters to Define Suction versus Degree of Saturation

The fitting parameters defining the relationship of degree of saturation and suction were estimated from the SWCC data results and summarized in Table 17. These parameters can be substituted in Equations (11) and (12) to generate the soil-water characteristic curve (SWCC).

Table 17: van Genuchten Parameters that Define Suction-Degree of Saturation for 70/30 Bentonite/Sand Materials Estimated from the SWCC Test Results

Liquid to prepare the specimen	S_{lr}	α [1/Pa]	m_c	n
DW	0	3.5×10^{-8}	0.40	1.68
CR10	0	6.7×10^{-8}	0.27	1.37
SR160	0	3.4×10^{-8}	0.28	1.39
SR270	0	2.8×10^{-8}	0.41	1.70

For material prepared with distilled water, these SWCC parameters were determined according the following process. The target dry density of the study is 1.8 Mg/m^3, so data from specimens DW-1.4-w32%, DW-1.6-w24% and DW-1.8-w18% were used in the analyses. Figure 77 shows the data used to determine the SWCC parameters for specimen prepared with distilled water. First, an exponential trend line was created from the data with suction greater than 10 MPa. The equation of this trend line is shown in Figure 77 and the R^2 = 0.86 indicating a good correlation with exponential trendline. More data variations can be observed at lower suction, so these data were not included in the curve-fitting process.

To simplify the analyses, parameter S_{lr} is assumed equal to 0, which means that 100% liquid saturation can be reach at some point, although it can be seen in the data that some of the specimens indicate that 100% saturation was not observed. As discussed previously, the SWCC data for lower suction need to be confirmed with different measurement methods, as there was no clear trend that can be seen from the results. Using solver function in MS-Excel, this exponential trend line was used to determine the remaining parameters (α, m_c, and n).

Similar methods were used to determine the fitting parameters of specimens prepared with CR10, SR160, and SR270 solutions. The data points used to generate the parameters combined with the exponential trend lines for data with s>10 MPa, their corresponding equation and R^2, van Genuchten curves are shown in Figures 78, 79 and 80. Figure 81 shows the SWCC curve for 70-30 BSM prepared with four different solutions. Note that the variations at lower suction are relatively large, especially for lower suction, which may be due to the limitation of the measurements methods used in this study. Further study using different methods are recommended to investigate this variation at lower suction.
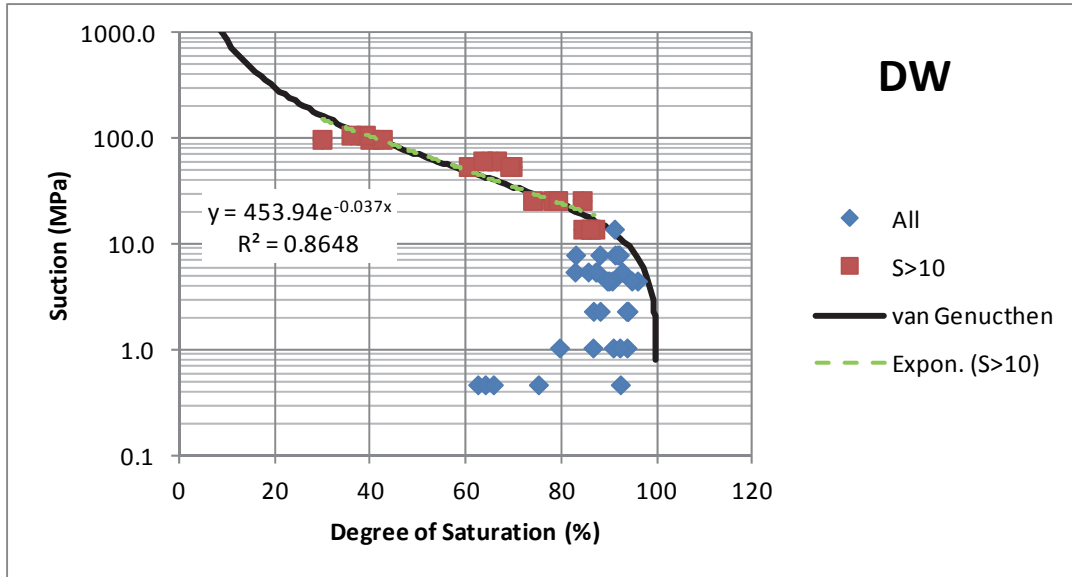
Figure 77: SWCC Data Points, Exponential Trend Line for Data with Suction (S>10 MPa, and van Genuchten Curve for Specimens Prepared with Distilled Water
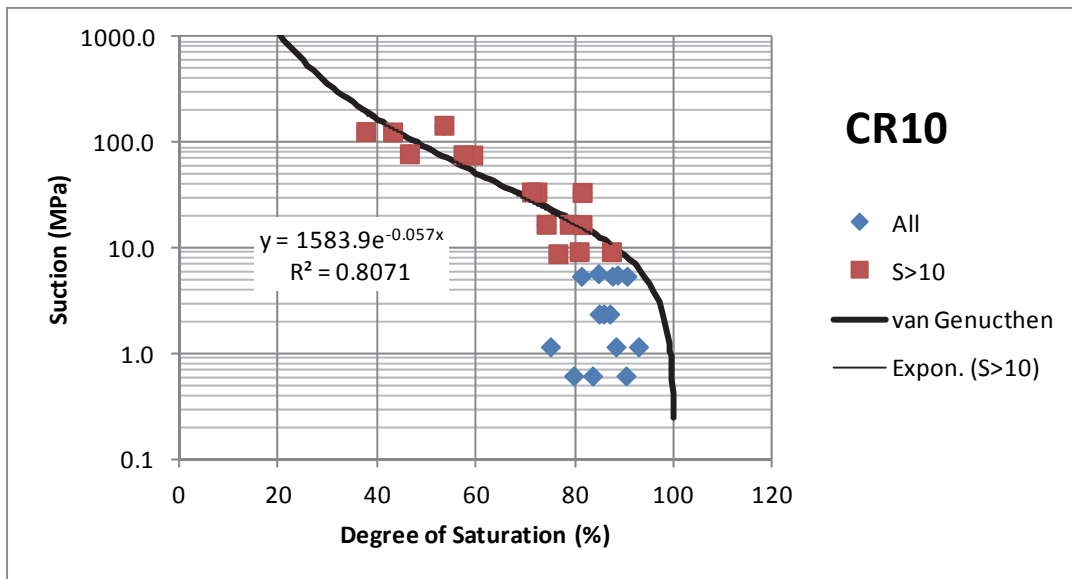
Figure 78: SWCC Data Points, Exponential Trend Line for Data with Suction (S>10 MPa, and van Genuchten Curve for Specimens Prepared with CR10 Solution
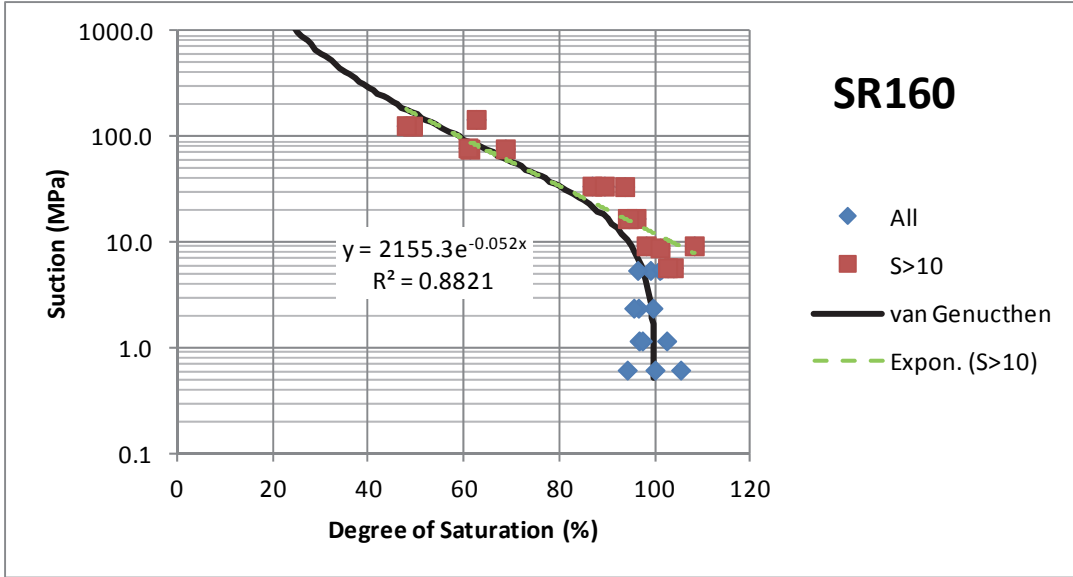
Figure 79: SWCC Data Points, Exponential Trend Line for Data with Suction (S>10 MPa, and van Genuchten Curve for Specimens Prepared with SR160 Solution
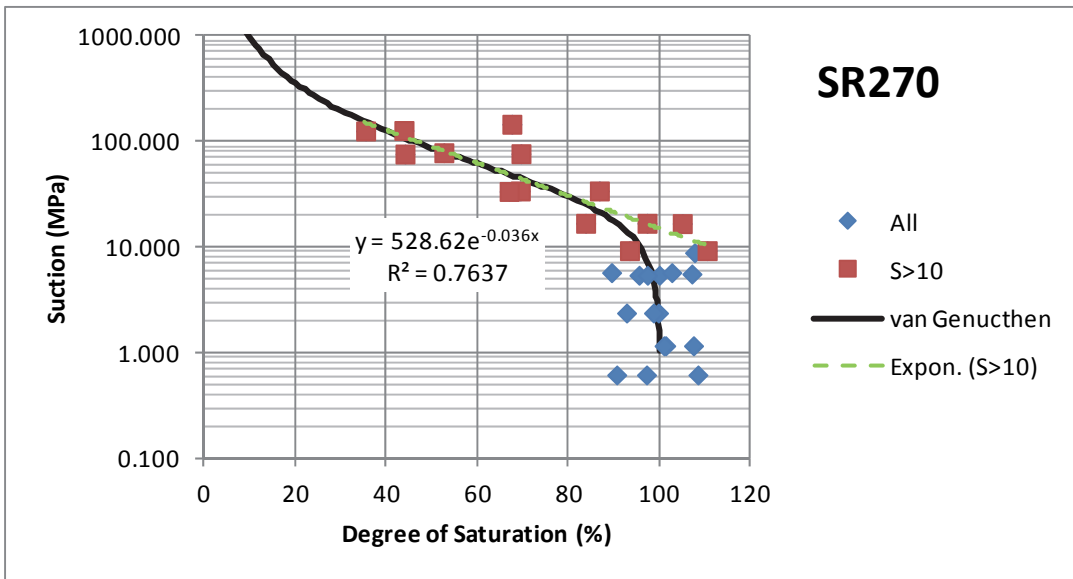
Figure 80: SWCC Data Points, Exponential Trend Line for Data with Suction (S>10 MPa, and van Genuchten Curve for Specimens Prepared with SR270 Solution
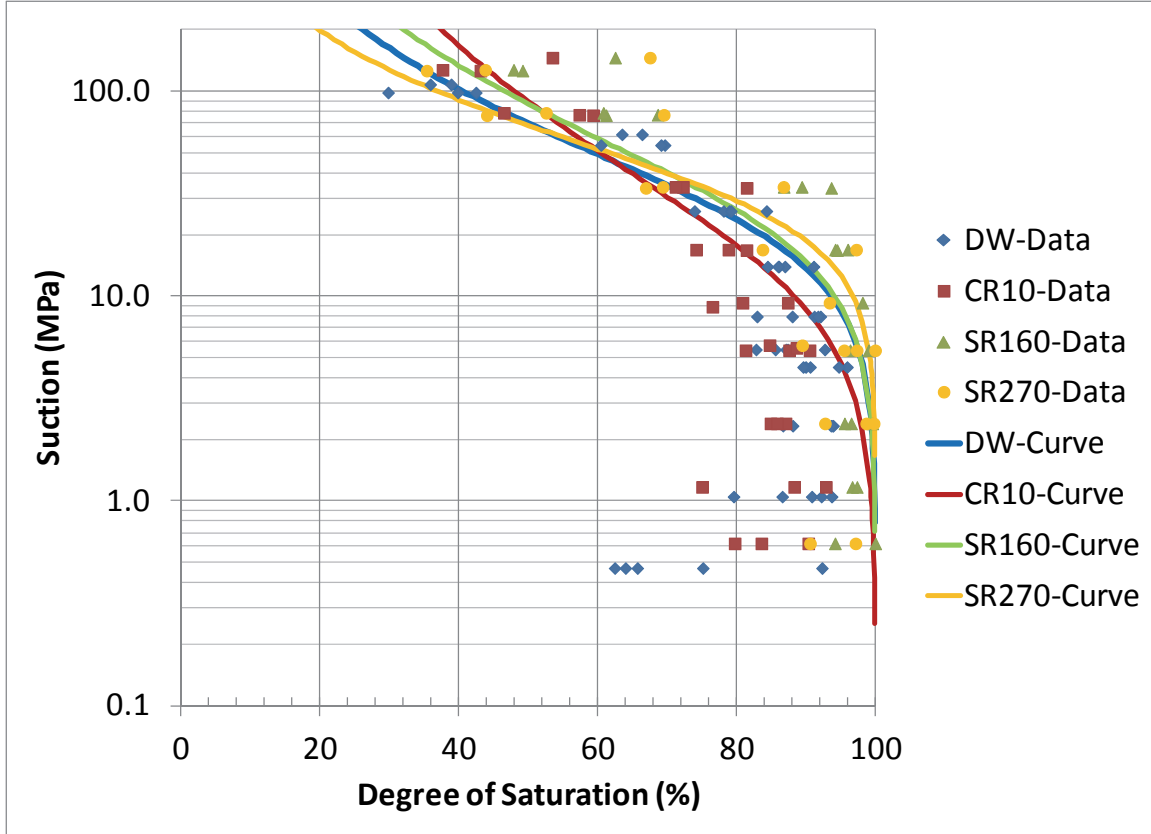
Figure 81: SWCC Data Points and van Genuchten Curve for Specimens Prepared with DW, CR10, SR160, and SR270 Solutions

4. SUMMARY

In this study, a series of tests has been completed to provide Hydro-Mechanical (H-M) and mineralogical characterization information on a 70-30 Bentonite-Sand Mixture (BSM) when it was tested using four different liquids. The liquids include distilled water (DW) and saline solutions (CR10, SR160, and SR270).

An important factor in evaluating the results of laboratory testing has been accounting for the salt component that remains in the specimens following completion of testing. The volume-mass properties presented in this study have been corrected due to the remaining salt after the oven-drying process according to ASTM D2216-10. The properties of the salt solution used for the correction are listed in Table 18.

Coefficients used to calculate dry density and EMDD of the 70-30 BSM are listed below:
- Specific gravity of all soil solids, G_s = 2.72
- Mass fraction of montmorillonite in clay fraction, f_m = 0.8
- Mass fraction of clay in dry solids, f_c = 0.7
- Specific gravity of aggregate solid, G_a = 2.65
- Specific gravity of non-montmorillonite component in clay, G_n = 2.645

When the 70-30 bentonite-sand material (BSM) is compacted to 1.8 Mg/m³, the hydraulic conductivity is less than 3 x 10⁻¹² m/s and swelling pressures are in excess of 900 kPa in

all of the groundwater environments examined. This indicates that the 70-30 BSM is a potentially suitable material for use in shaft backfilling as it provides both a low permeability and substantial swelling pressure.

Properties derived from each of the tests completed are summarized in Table 18 and Table 19 and are briefly described below.

Free Swell Tests
- Free Swell Index (FSI) of the BSM tested with DW was 9.0 mL/2g. The FSI tends to decrease with an increase of pore liquid salinity.

Consistency (Atterberg) Limits
- Liquid limit (LL), Plastic Limit (PL), and Plasticity Index (PI) of the BSM tested with water was 341, 31, and 309. The Atterberg limits tend to decrease with an increase of pore liquid salinity.

Compaction properties (Proctor)
- The results of compaction tests indicated that the maximum dry density was equal to approximately 1.83-1.86 Mg/m^3 at optimum gravimetric water content, corrected due to salt content of approximately 16%.
- Based on the results of the compaction tests, in order to achieve optimum compaction, 70-30 BSM should be placed at a reference dry density (ρ_{dry}) of approximately 1.8 Mg/m^3 and gravimetric water content (w) of 16%. These correspond to degree of saturation (S_w) of 85% and Effective Montmorillonite Dry Density (EMDD) of 1.44 Mg/m^3. Material properties at these reference points have been determined and shown in Table 18.

Hydraulic Conductivity and Swelling Pressure
- Saturated hydraulic conductivity (K_{w-sat}) tends to increase and swelling pressure (P_s) tends to decrease with an increase of pore liquid salinity. At reference dry density of 1.8 Mg/m^3, when the salinity increases from 0 to 270 g/L, K_{w-sat} increases from 8 x 10^{-14} m/s (DW) to 2x10^{-12} m/s (SR270) and P_s decreases from ~6.5 to ~0.9 MPa.

Gas Permeability Tests
- At a given dry density and degree of saturation, gas conductivity (K_g) tends to increase with an increase of pore liquid salinity. At a reference dry density of 1.8 Mg/m^3 and degree of saturation of 85%, K_g increases from 6 x 10^{-14} m/s to 8 x 10^{-12} m/s when the pore liquid salinity increases from 0 to 270 g/L.

- The van Genuchten-Mualem-Luckner Relative Permeability (Equations 11 to 14) was slightly modified and used to define S_w-K_g relationships. These parameters for BSM tested at reference dry density of 1.8 Mg/m^3 with different pore liquids are summarized in Table 18.

Table 18: Properties of 70-30 Bentonite-Sand Mixture (BSM)

Tests	Properties	Pore liquid Type			
		DW	CR10	SR160	SR270
Solution Properties	TDS (g/L)	0	10	160	270
	Density (Mg/m^3)	1	1.002	1.106	1.182
	Ratio of mass of salt to mass of saline solution, r	0	0.010	0.145	0.228
Free swell tests	Free Swell Index (FSI) (mL/2g)	9.0	7.3	4.3	3.5
Consistency (Atterberg) Limits	Liquid limit, LL (%)	341	124	51	30
	Plastic limit, PL (%)	31	30	26	24
	Plasticity Index, PI (%)	309	94	24	8
Compaction properties (Modified Proctor)	Maximum dry density (Mg/m^3)	1.83	1.83	1.86	1.86
	Optimum moisture content-corrected due to salt (OMC') (%)	16	16	16	16
Liquid Hydraulic Conductivity & Swelling Pressure	Saturated Hydraulic Conductivity, $k_{w\text{-}sat}$ (m/s) at 1.8 Mg/m^3 dry density	8×10^{-14}	7×10^{-14}	4×10^{-13}	3×10^{-12}
	Swelling Pressure, Ps (MPa) at 1.8 Mg/m^3 dry density	6.5	8	1.5	0.9
Gas Permeability	Gas conductivity, k_g (m/s), at 1.8 Mg/m^3 dry density and 85% S_w	6×10^{-14}	8×10^{-13}	2×10^{-12}	8×10^{-12}
	The van Genuchten-Mualem-Luckner Relative Permeability (Equations 11 to 14)				
	S_{lr}	0	0	0	0
	S_{gr}	0.05	0	0	0
	m_k	1.46	1.4	1.5	1.2
	$k_{g,\,max}$ (m/s)	4.7×10^{-9}	6.6×10^{-9}	4.6×10^{-9}	5.5×10^{-9}

Soil-water Characteristic Curve (SWCC) Tests
- From the SWCC data, two exponential trend lines have been determined to define:
  o relationships of suction and water content (for suction >5 MPa); and
  o relationships of suction and degree of saturation (for suction >10 MPa).
The equations, parameters and correlation coefficients of these trend lines are shown in Table 19. Note that these exponential relationships are only valid for a limited data range. Caution should be exercised when extrapolating these trend lines.

- In addition to these exponential trend lines, van Genuchten parameters for specimens prepared with various pore liquids were also done and the results were shown in Table 19.

- From these relationships the suctions at the reference water content (~16%) and degree of saturation (~85%) were determined. The suction of a specimen prepared with distilled water was approximately 12 to 19 MPa. For given properties, suction tends to increase with an increase of pore liquid salinity, except for CR10 solution.

- Note that the SWCC data from these tests was for the drying curve, the results presented in these tests would be lower than the wetting curve. There was uncertainty in the results of these SWCC data, especially at lower suction. Different methods and further literature study are recommended for future study to observe the behaviour of the specimens during wetting and at lower suctions.

Mechanical Properties
- As expected for clay material, the BSM has elasto-plastic behaviour. Parameters that define the void ratio (e)-log(vertical effective stress (σ_v')) and specific volume (V)-ln(mean effective stress (p')) relationships have been determined and shown in Table 19 from the results of 1D-consolidation tests and triaxial tests, including parameters swelling and compression indices (C_s and C_c) and parameters κ and λ. Parameters C_s and κ tend to decrease with an increase of pore liquid salinity, which is consistent with the results of swelling pressure tests showing a decrease of swelling pressure with an increase of pore liquid salinity. Parameters C_c and λ tend to decrease with an increase with pore liquid salinity.

- The 1D-modulus (M) and bulk density (K) have been determined from incremental data points. The values of M and K at a reference dry density of 1.8 Mg/m^3 was in the range of 8-80 MPa and 5-50 MPa. These analyses were done by assuming constant Poisson's ratio (ν) of 0.32 (within the range of typical value of the bentonite-sand material). These values would need to be reanalysed if ν was a measured value. The large range of M and K was due to the fact that the material was not linear elastic and stress-path dependent. These parameters were provided here as a reference and are limited to a very small range of stress-strain relationships. More complex models (e.g., elasto-plastic model) are more suitable for describing the behaviour of BSM.

- This study investigated the mechanical properties of BSM at 100% saturation. Evaluation of the material under unsaturated conditions is recommended for future study to investigate overall behaviour of the BSM. The results of both studies (i.e., saturated and unsaturated) should be integrated to determine the overall mechanical behaviour of the BSM under both saturated and unsaturated conditions.

Table 19: Properties of 70-30 Bentonite-Sand Mixture (BSM) Determined in this Study

Tests	Properties		Pore liquid Type			
			DW	CR10	SR160	SR270
Soil Water Characteristic Curve (SWCC)	Exponential Trend lines s-w Suction (s) = f ($\bar{w}$) for s> 10 MPa $s = A_w * e(B_w * \bar{w})$					
	A_w		606.68	1338.8	284.72	207.55
	B_w		-0.246	-0.285	-0.091	-0.062
	R_w^2		0.9714	0.9657	0.9406	0.9571
	Suction at 16% water content (MPa)		~12	~14	~66	~77
	Exponential Trend lines s-S_w Suction (s) = f (S_w) for suction > 10 MPa $s = A_s * e(B_s * \bar{S}_w)$, Sw has a unit [%]					
	A_s		453.94	1583.9	2155.3	528.67
	B_s		-0.037	-0.057	-0.052	-0.036
	R_s^2		0.8648	0.8071	0.8821	0.7637
	Suction at 85% Sw (MPa)		~19	~12	~26	~25
	SWCC parameters – van Genuchten (see Equations 11 & 12)					
	S_{lr}		0	0	0	0
	α [1/Pa]		3.5×10^{-8}	6.7×10^{-8}	3.4×10^{-8}	2.8×10^{-8}
	m_c		0.4	0.27	0.28	0.41
	N		1.68	1.37	1.39	1.70
Mechanical Properties	1D-modulus at reference dry density, M (MPa)		8-80			
	Bulk density at reference dry density, K (MPa)*		5-50			
	Elasto-plastic relationships					
	e-log (σ_v)	Cs	0.102	0.082	0.069	0.055
		Cc	0.292	0.258	0.173	0.210
	V-log (σ_v)	κ	0.054	0.056	0.030	0.020
		λ	0.127	0.093	0.075	0.105

*Calculated based on Poisson's ratio of 0.32

ACKNOWLEDGEMENTS

REFERENCES

Anderson, D.E.S. 2003. Evaluation and comparison of mechanical and hydraulic behaviour of two engineered clay sealing materials. M.Sc. Thesis, Department of Civil Engineering, University of Manitoba, Canada.

ASTM C136-06. Standard Test Method for Sieve Analyses of Fine and Coarse Aggregate

ASTM D1557-78. Standard Test Methods for Moisture-Density Relations of Soils and Soil-Aggregate Mixtures Using 10-lb (4.54-kg) Rammer and 18-in. (457-mm) Drop.

ASTM D2216-10. Standard Test Methods for Laboratory Determination of Water (Moisture) Content of Soil and Rock by Mass.

ASTM D2435-11 Standard Test Methods for One-Dimensional Consolidation Properties of Soils Using Incremental Loading.

ASTM D4318-10. Standard Test Methods for Liquid Limit, Plastic Limit, and Plasticity Index of Soils

ASTM D4542-07. Standard Test Method for Pore Water Extraction and Determination of the Soluble Salt Content of Soils by Refrectometer.

ASTM D5890 - 11 Standard Test Method for Swell Index of Clay Mineral Component of Geosynthetic Clay Liners.

Baumgartner, P., Snider G.R, 2002. Seal evaluation and assessment study (SEAS): Light backfill placement trials. Atomic Energy of Canada Limited Technical Record, TR-793.

Blatz, J.A. 2000. Elastic-plastic modelling of unsaturated high plastic lay using results form a new triaxial test with controlled suction. Ph.D. Thesis, Department of Civil Engineering, University of Manitoba, Canada.

Blatz, J.A., Y-J. Cui, and L. Oldecop. 2008. Vapour Equilibrium and Osmotic Technique for Suction Control. Geotech Geol. Eng. (2008) 26:661-673.

Davis, R.O. and Selvadurai, A.P.S. 1996. Elasticity and Geomechanics. Cambridge University Press.

Dixon, D.A. 1994. Sodium bentonites of Canada, the United States and Mexico: Sources, Reserves and Properties, in Engineering Materials for Waste Isolation, A.M.Crawford, H.S. Radhakrishna, M.Goutama and K.C.Lau eds. CSCE-Engineering Material Division, Special Publication, Aug. 1994.

Dixon, D.A. 1995. Towards an understanding of water structure and water movement through dense clays. Ph.D Thesis. University of Manitoba, Winnipeg, Canada. May 1995.

Dixon, D.A. and S.H. Miller. 1995. Comparison of the mineralogical composition, physical, swelling and hydraulic properties of bentonites from Canada, the United States and Japan. Atomic Energy of Canada Limited, Report AECL-11303, COG-95-156.

Dixon D. A, M. Gray and H. Thomas. 1985. A study of compaction properties of potential clay/sand buffer mixtures in nuclear fuel waste disposal. Engineering Geology, 21, pp. 247-255

Gautier M., Mullera F., Le Forestiera L., Benya J.-M. and Guegana R. 2010. NH4-smectite: Characterization, hydration properties and hydromechanical behaviour, Applied Clay Science (40).

Graham, J., K. Gelmich Halayko, H. Hume, T. Kirkham, M. Gray, and D. Oscarson. 2002. A capillarity-advective model for gas break-through in clays. Eng. Geol. Vol. 64, pp. 273-286.

JNC (Japan Nuclear Cycle Development Institute). 2000. H12: Project to Establish the Scientific and Technical Basis for HLW Disposal in Japan. Supporting Report 2: Repository Design and Engineering Technology.

Karnland, O. 2010. Chemical and mineralogical characterization of the bentonite buffer for the acceptance control procedure in a KBS-3 repository, Swedish Nuclear Fuel and Waste Management Company (SKB), Technical Record TR-10-60, Stockholm.

Lee, J-M and C.D. Shackelford. 2005. Solution Retention Capacity as an Alternative to the Swell Index Test for Sodium Bentonite. Geotechnical Testing Journal, Vol. 28, No. 1.

Martino, J.B., D.A. Dixon, B.E. Holowick and C-S. Kim. 2011. Enhanced Sealing Project (ESP): Seal Construction and Instrumentation Report. NWMO Technical Report APM-REP-01601-0003.

Priyanto, D.G., J.A. Blatz, G.A. Siemens, R. Offman, J.S. Boyle, and D.A. Dixon. 2008. The Effects of Initial Conditions and Liquid Composition on the One-Dimensional Consolidation Behaviour of Clay-Based Sealing Materials. Nuclear Waste Management Organization (NWMO) Technical Report No. NWMO TR-2008-06. Toronto, Canada.

Priyanto, D.G., J.A. Blatz, G.A. Siemens, R.B. Offman, J.S. Powell, and D.A. Dixon. 2008. The Effects of Fluid Composition on the One-Dimensional Consolidation Behaviour of Clay-Based Sealing Materials. Nuclear Waste Management Organization (NWMO) Technical Report No.NWMO TR-2008-20. Toronto, Canada.

Quigley, R.M. 1984. Quantitative mineralogy and preliminary pore-water chemistry of candidate buffer and backfill materials for a nuclear fuel waste disposal vault, Atomic Energy of Canada Limited, Technical Report, AECL 7827, Chalk River

Stokes, R.H., Robinson, R.A. 1949. Standard Solutions for Humidity Control at 25oC. Industrial and Engineering Chemistry Vol. 41, p. 2013.

Tang, G.X. 1999. Suction characteristics and elastic-plastic modelling of unsaturated sand-bentonite mixture. Ph.D. Thesis, Department of Civil Engineering, University of Manitoba, Canada.

Villar, M. 2002. Thermo-hydro-mechanical characterisation of a bentonite from Cabo de Gata: A study applied to the use of bentonite as sealing material in high level radioactive waste repositories, ENRESA Publicacion tecnica 04/2002, pp 88-90.

Wan, A.W.L. 1996. The use of thermocouple psychrometers to measure in-situ suctions and water contents in compacted clays. Ph.D. Thesis, Department of Civil and Geological Engineering, University of Manitoba, Canada.

Yoshimi, Y. and Osterberg, J.O. 1963. Compression of partially saturated cohesive soils. J. Soil Mechanics and Foundation Division. ASCE 89, SM 4:1-24.

Young, J. F. 1967. Humidity Control in the Laboratory using Salt Solutions – A Review.
    J. appl. Chem., 1967, Vol. 17, September.

APPENDICES

CONTENTS

APPENDIX A: PROCEDURES AND WORK INSTRUCTIONS

No.	Tests	References (ASTM/ Literature References/ AECL Work Instruction)
1.	Hydraulic Conductivity and Permeability Tests	Technique used is the <u>Fixed-Volume, Constant-Head Permeability Test as used by</u>: Pusch 1980. Swelling Pressures of highly compacted bentonite, SKB, TR-80-13. Pusch 1980. Permeability of highly compacted bentonite, SKB TR-80-16. Gray et al. 1986. Swelling pressures of compacted bentonite/sand mixtures, MRS Proc. 44, 523-530. Bucher et al. 1986. Wuell-, durchlassigkeits- und schrumpf- versuche an quartzsan-bentonit-emischen. NAGRA TB-86-13. Dixon et al. 1999. Hydraulic conductivity of clays in confined tests under low hydraulic gradients, CGJ 36(5) 53-68. Komine and Ogata 1999. Prediction for swelling characteristics of compacted bentonite, Can. Geotech. J., 33, (1) 11-22. AECL DE010.186, Procedure for conducting hydraulic conductivity and swelling pressure tests (W40.89)
2.	Particle Size Distribution	ASTM C136-06, Standard Test Method for Sieve Analysis of Fine and Coarse Aggregates.
3.	Moisture Content (gravimetric)	ASTM D2216 -10, Standard Test Methods for Laboratory Determination of Water (Moisture) content of soil and rock by mass. AECL DE010.181 – Determining Gravimetric Water Content (1999 June), based on ASTM D2216-10.
4.	Miniature Proctor Tests	A technique calibrated against the results of ASTM compaction tests completed using ASTM-D-1557-78. "Standard Test Method for Determining the Moisture-Density Relations of Soils" Dixon, D.A., M.N. Gray and A.W. Thomas. 1985. A study of compaction properties of potential clay/sand buffer mixtures in nuclear fuel waste disposal. Engineering Geology, 21, pp. 247-255. AECL-GSEB Work Instruction "Method to Determine Modified Compaction Density of Clay-Based Materials Using Miniature Compaction Device".

No.	Tests	References (ASTM/ Literature References/ AECL Work Instruction)
5.	Consistency Limits Tests (Atterberg Limits)	ASTM D4318-10, Standard Test Methods for Liquid Limit, Plastic Limit, and Plasticity Index of Soils.

AECL, Operating Procedure, Conducting Consistency Limit Tests, WT-507210-OP-001 |
6.	X-Ray Analysis for Mineralogical Composition	Powder Diffraction using Rietveld method
7.	Chemical composition of sand and clay materials	XRF analyses conducted in association with the XRD analyses.
8.	Calculation of volume-mass properties for soil specimen with salt content	ASTM D 4542 -07, Standard Test Method for Pore water extraction and determination of the soluble salt content of soils by refractometer
9.	Determination of gas permeability (k_{gas})	Technique as described by Villar 2002. Thermo-hydro-mechanical characterisation of a bentonite from Cabo de Gata: A study applied to the use of bentonite as sealing material in high level radioactive waste repositories, ENRESA Publicacion tecnica 04/2002, pp 88-90.
10.	Determination of Triaxial Consolidation parameter (K) to obtain *K'*	As per ASTM D4767-95. Standard test methods for consolidated undrained triaxial compression test for cohesive soils, pp 882-891.

APPENDIX B: X-RAY DIFFRACTION PATTERNS FOR BENTONITE AND SAND

Sample 2 – Aggregate <2 mm:
This material was crushed to a fine powder and a very small amount (<100mg) was mounted on a zero-background quartz plate. X-ray diffraction data was collected using a Bruker D8 micro-diffractometer. The sample is made up dominantly of quartz with minor albite, microcline and calcite. Dolomite does not appear to be present.
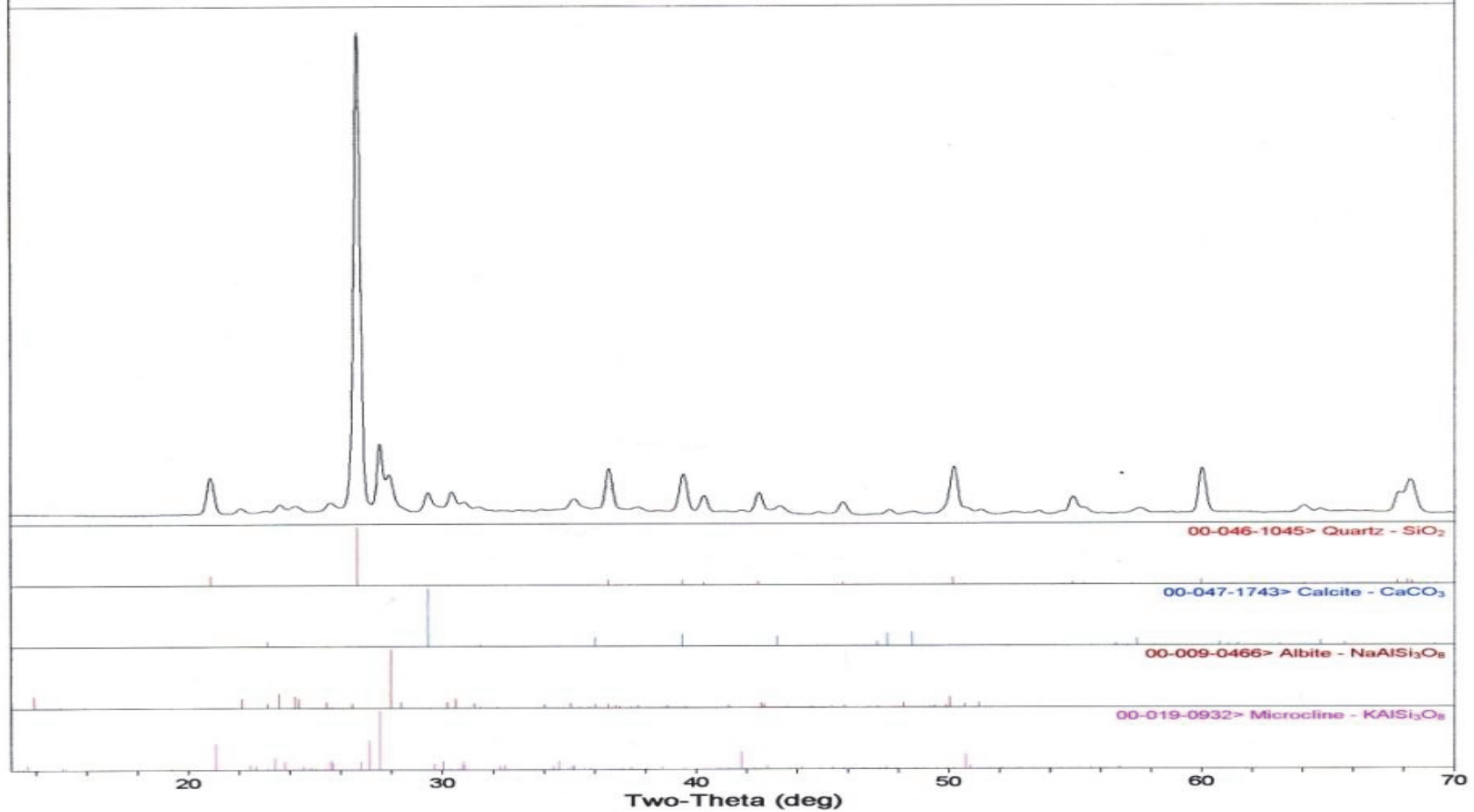
Figure B-1: X-ray diffraction pattern for fine portion of sand used in study (<2mm diameter)
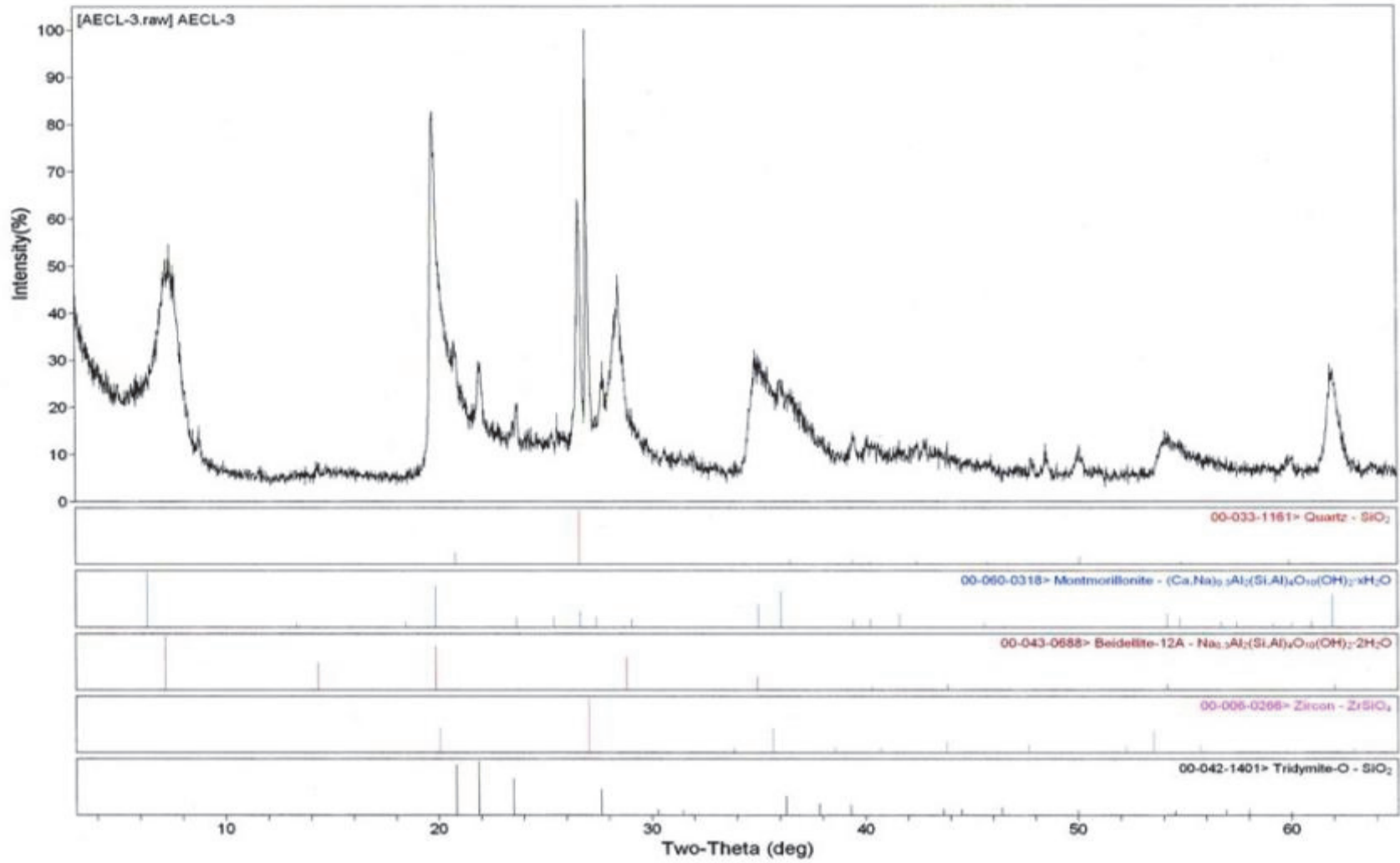
Figure B-2: X-Ray Diffraction pattern for National Standard Bentonite, University of Manitoba (Note: Beidelite is a swelling (smectite) clay), Cu-Kα radiation

APPENDIX C: DATA SHEET FOR NATIONAL STANDARD BENTONITE

BENTONITE *Performance Minerals LLC*

NATIONAL®
STANDARD Bentonite

Description	NATIONAL® STANDARD is a natural 200 mesh high purity Wyoming sodium bentonite. It is used as a binder and rheological modifier.
Applications/Functions	• Asphalt emulsion • Brick, ceramics • Cement • Industrial applications such as: detergent, paper • Foundry
Advantages	• Improves green and dry strength. • Increases water resistance. • General rheological modifier.

Screen Analysis		Typical	Specification
• Dry screen, percent minus 200 mesh	•		• 67.5 Min

Properties		Typical	Specification
• Moisture, percent	•		• 12 Max
• Swell Index	•		• 30.0 Min
• Specific Gravity	•	2.7	
• Bulk Density (lbs/ft^3 compacted)	•	73	
• Bulk Density (lbs/ft^3 uncompacted)	•	53	

Availability	NATIONAL® STANDARD can be purchased through any Bentonite Performance Minerals LLC assigned Reseller. To locate the BPM Reseller nearest you, contact the Customer Service Department in Houston or your area BPM Regional Sales Manager.

Bentonite Performance Minerals LLC
A Halliburton Company
3000 N. Sam Houston Pkwy E.
Houston, TX 77032
www.bentonite.com

Customer Service (281) 871-7900   **Fax** (281) 871-7940

APPENDIX D: RESULTS OF 1D-CONSOLIDATION TESTS
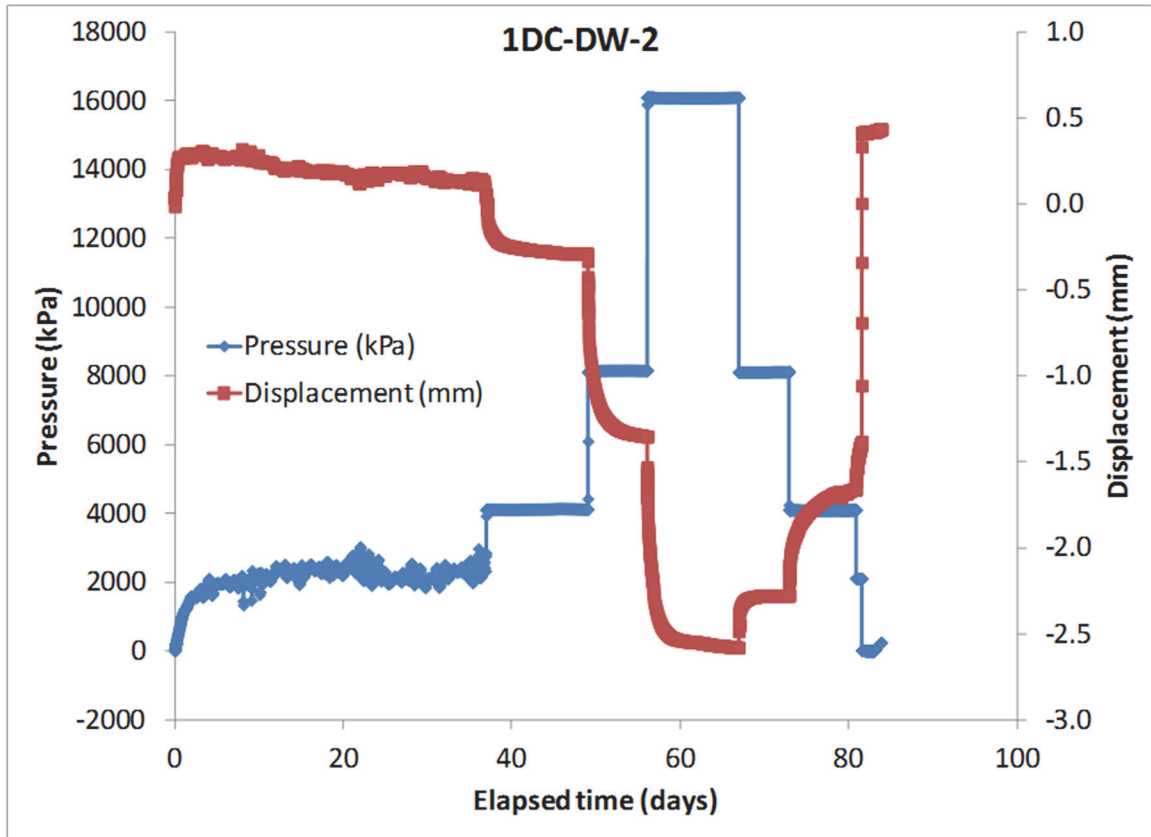
Figure D-1: Pressure and Displacement Measured During 1D-Consolidation Tests for Specimen 1DC-DW-2
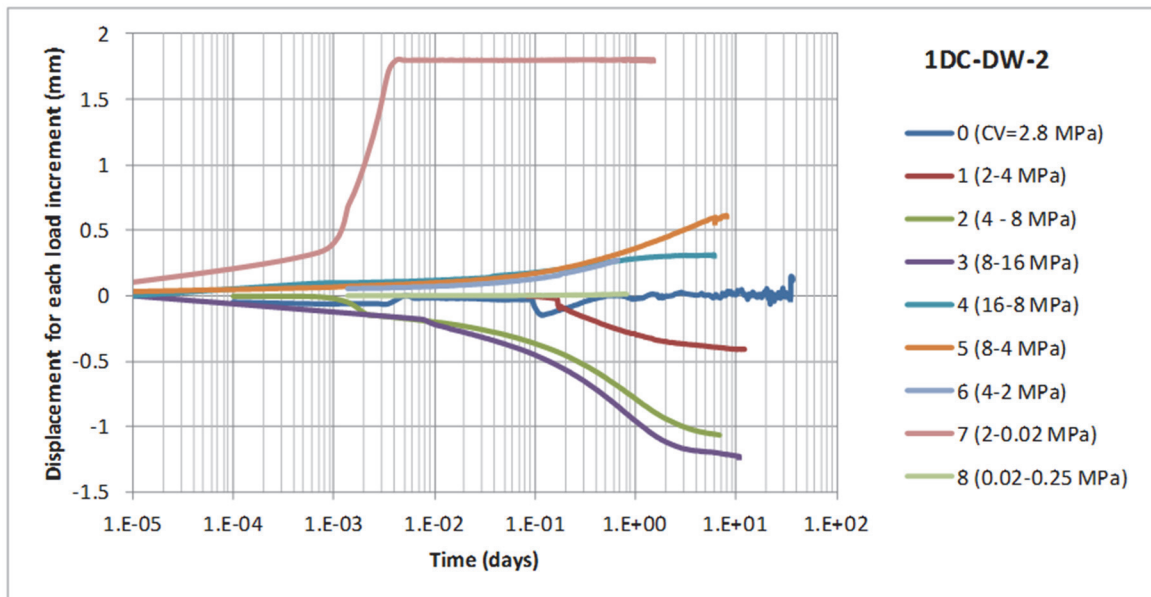
Figure D-2: Void Ratio versus Time for Each Load Increment for Specimen 1D-DW-2
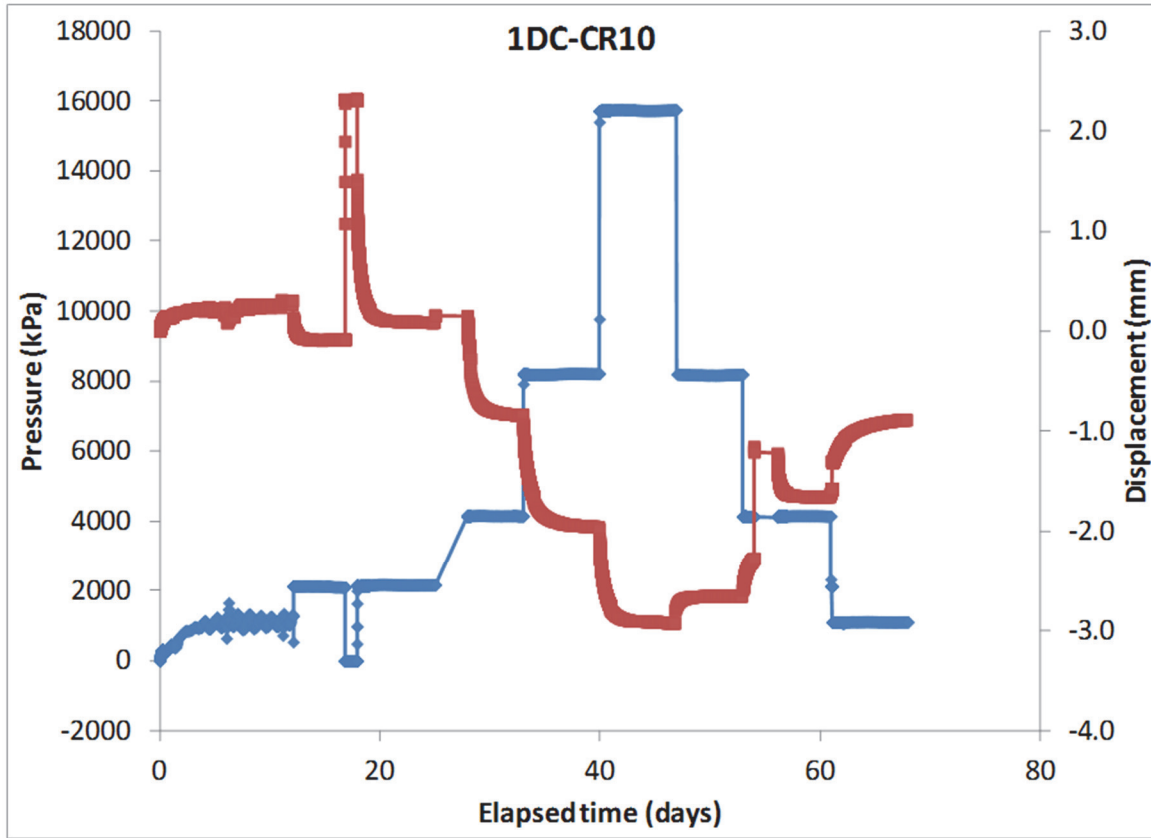
Figure D-3: Pressure and Displacement Measured During 1D-Consolidation Tests for Specimen 1DC-CR10
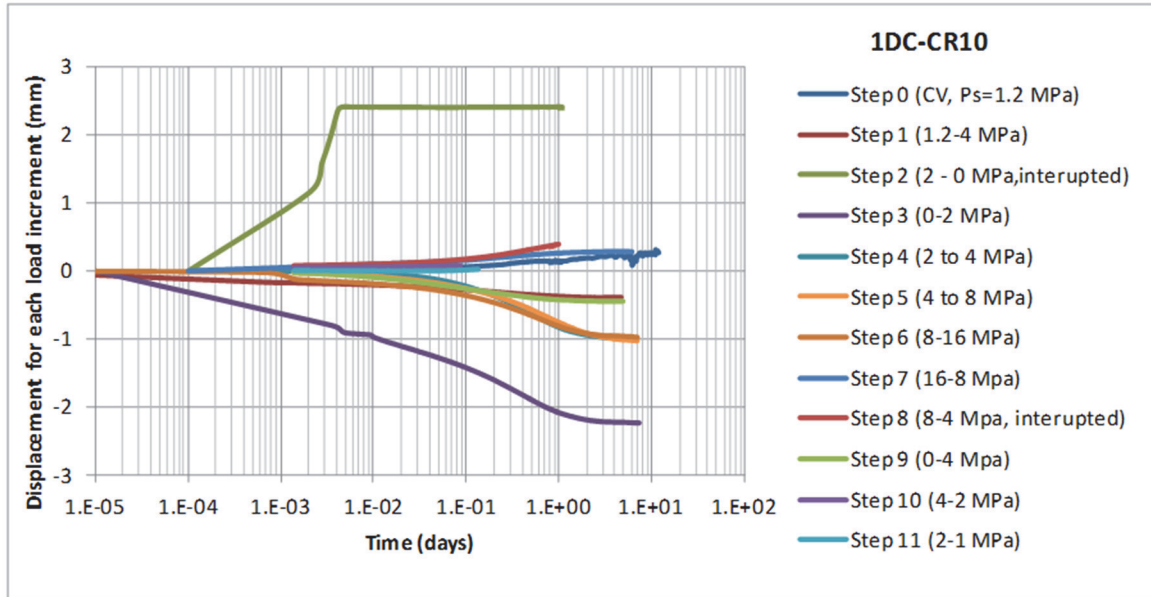
Figure D-4: Void Ratio versus Time for Each Load Increment for Specimen 1D-CR10
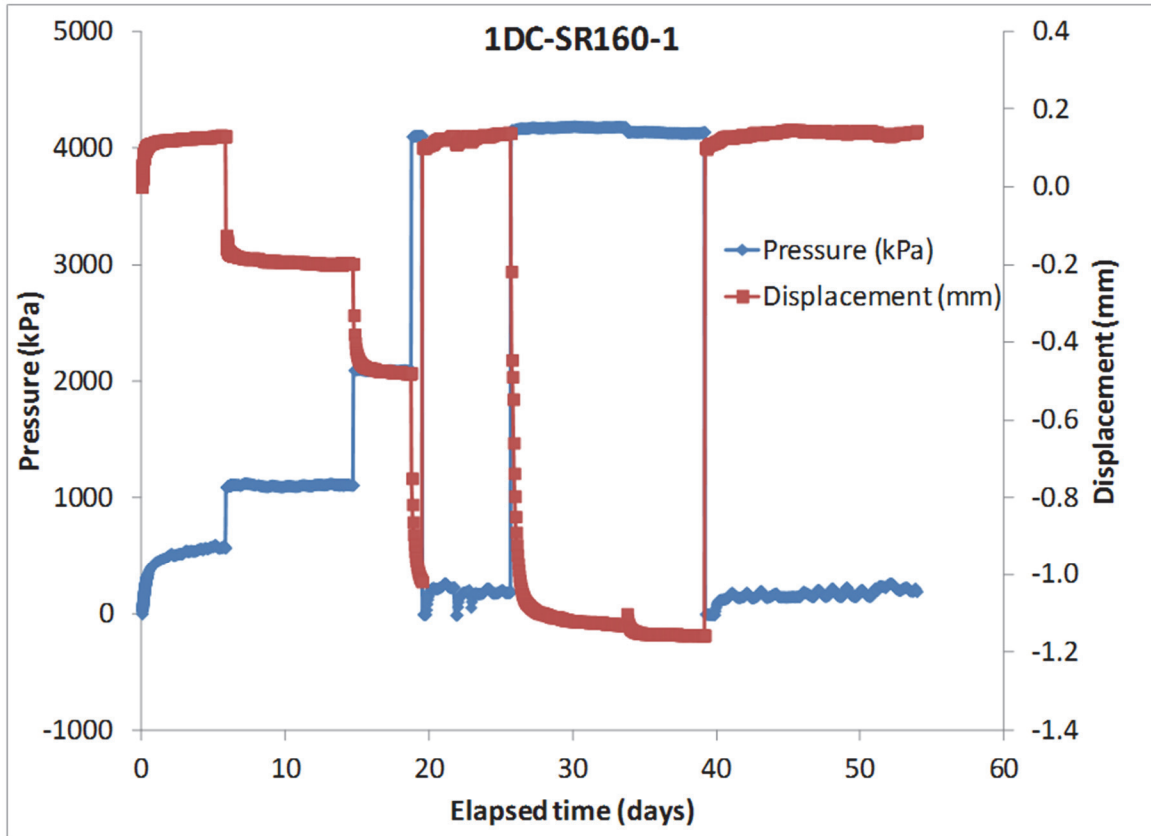
Figure D-5: Pressure and Displacement Measured During 1D-Consolidation Tests for Specimen 1DC-SR160-1
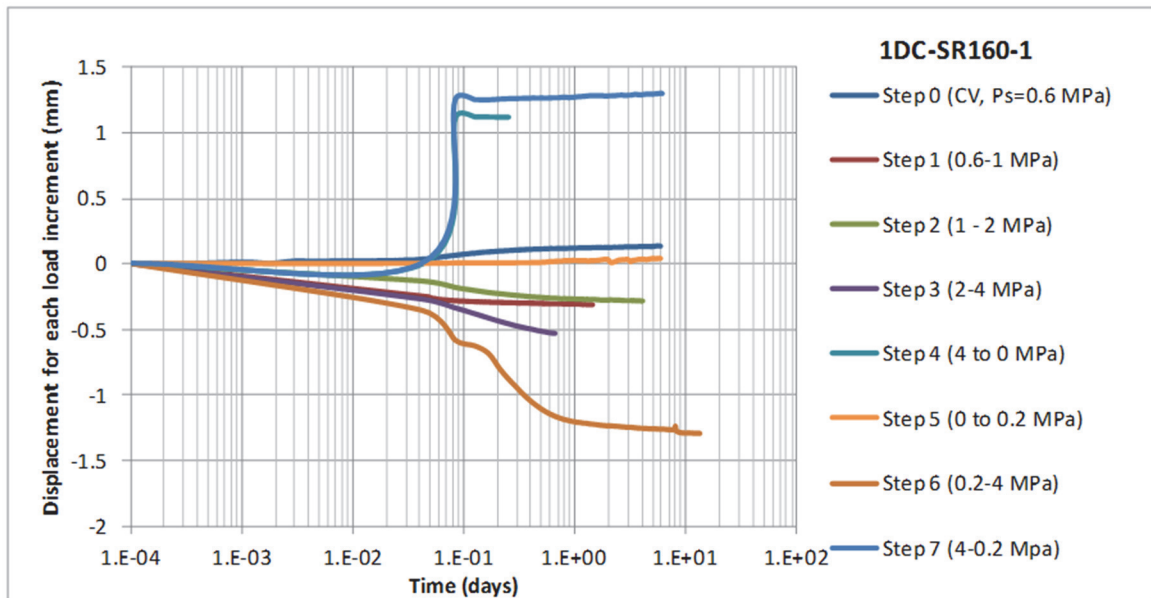
Figure D-6: Void Ratio versus Time for Each Load Increment for Specimen 1D-SR160-1
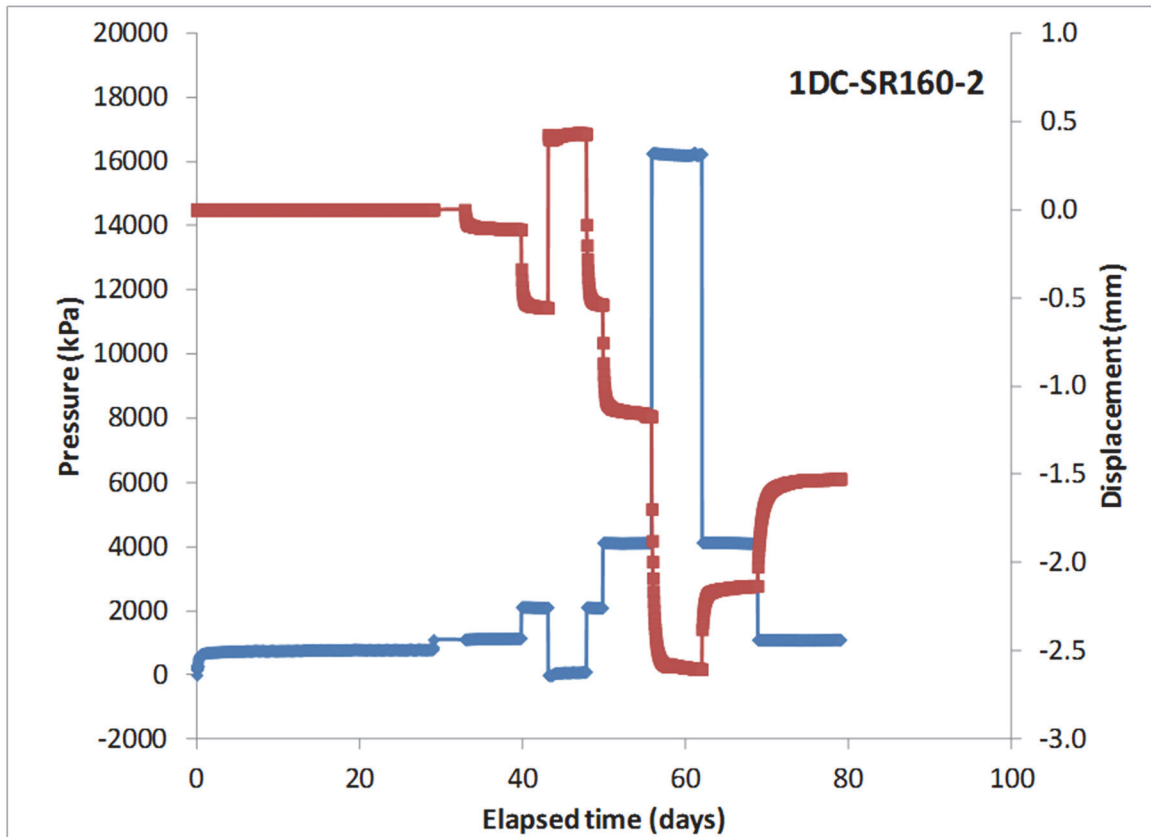
Figure D-7: Pressure and Displacement Measured During 1D-Consolidation Tests for Specimen 1DC-SR160-2
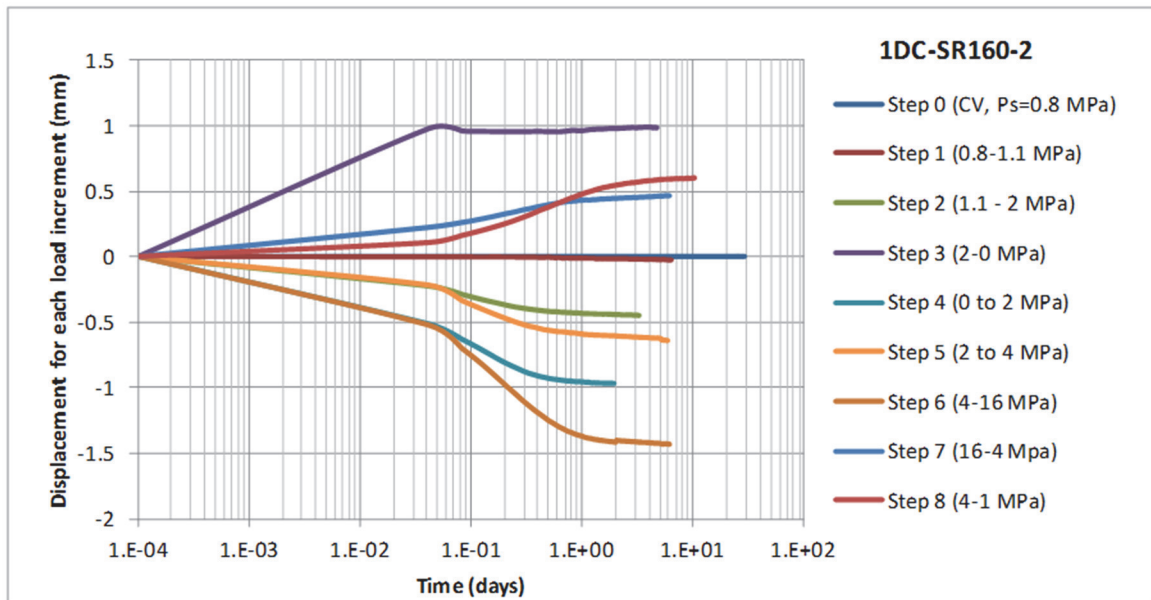
Figure D-8: Void Ratio versus Time for Each Load Increment for Specimen 1D-SR160-2
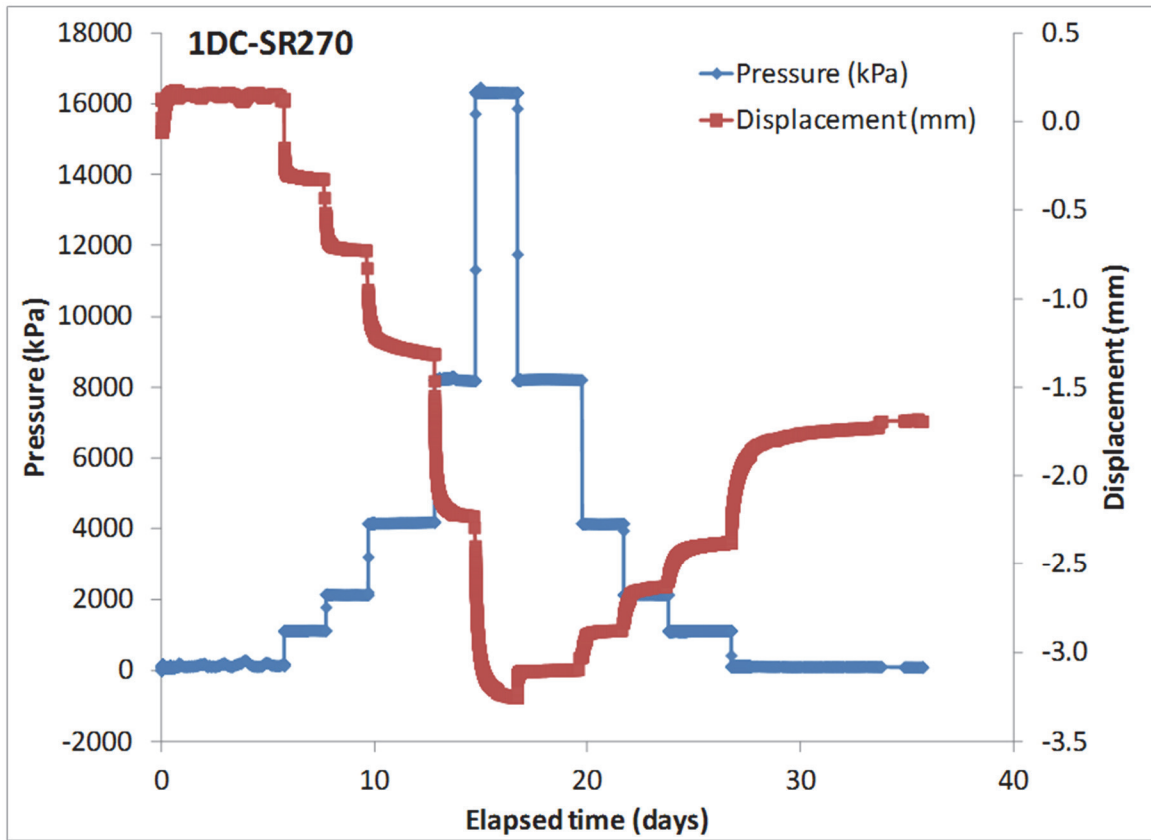
Figure D-9: Pressure and Displacement Measured During 1D-Consolidation Tests for Specimen 1DC-SR270
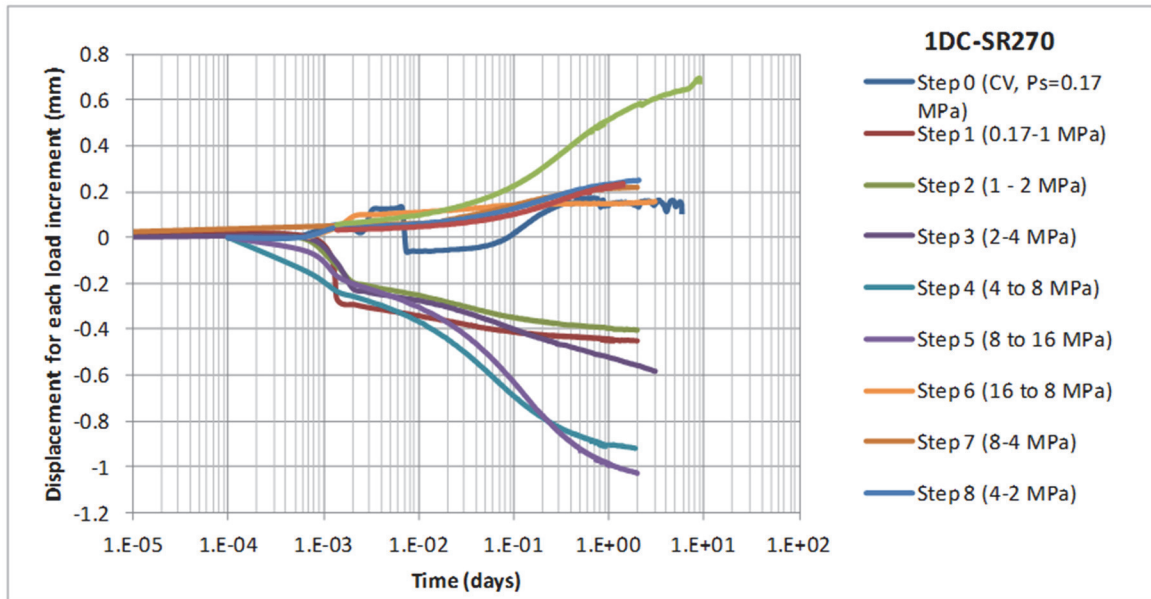
Figure D-10: Void Ratio versus Time for Each Load Increment for Specimen 1DC-SR270

Table D-1: 1D Consolidation Data for Specimen 1DC-DW-2

Vertical Press. (kPa)	Displacement (mm)	Thickness (mm)	Vol. (cm³)	Dry density (Mg/m³)	Void ratio, e	Spec. volume , V	Effective vertical stress (kPa)	Coeff. of consolidation, cv (m²/ s)	mv (1/Pa)	Hydraulic conductivity (m/s)	EMDD (Mg/m³)
100	0.000	20.70	40.57	1.744	0.558	1.558	90				1.375
2764	0.122	20.82	40.81	1.733	0.567	1.567	2755	5.0E-10	2.2E-09		1.363
4131	-0.288	20.41	40.01	1.768	0.536	1.536	4121	5.4E-10	1.4E-08	7.8E-15	1.402
8163	-1.351	19.35	37.93	1.865	0.456	1.456	8153	6.4E-10	1.3E-08	8.3E-15	1.514
16074	-2.580	18.12	35.52	1.992	0.364	1.364	16065	1.1E-09	8.0E-09	8.8E-15	1.667
8124	-2.276	18.42	36.11	1.959	0.386	1.386	8115	2.6E-10	2.1E-09	5.5E-16	1.626
4111	-1.658	19.04	37.32	1.895	0.433	1.433	4101	1.2E-09	8.4E-09	1.0E-14	1.549
2111	-1.386	19.31	37.86	1.869	0.453	1.453	2101	1.2E-07	7.2E-09		1.518
253	0.434	21.13	41.42	1.708	0.590	1.590	243	6.1E-10	5.1E-08		1.335

Table D-2: 1D Consolidation Data for Specimen 1DC-CR10

Vertical Press. (kPa)	Displaceme nt (mm)	Thickness (mm)	Vol. (cm^3)	Dry density (Mg/m^3)	Void ratio, e	Spec. volume , V	Effective vertical stress (kPa)	Coeff. of consolida tion, cv (m^2/ s)	mv (1/Pa)	Hydraulic conductiv ity (m/s)	EMDD (Mg/m^3)
100	0.000	20.35	39.34	1.807	0.503	1.503	90				1.446
1273	0.270	20.62	39.86	1.783	0.523	1.523	1263				1.419
2118	-0.029	20.32	39.28	1.810	0.501	1.501	2108	1.7E-09	1.7E-08	2.9E-14	1.449
2162	0.091	20.44	39.52	1.799	0.510	1.510	2152	1.8E-09	1.7E-08	3.1E-14	1.437
4143	-0.841	19.51	37.71	1.885	0.441	1.441	4133	6.6E-10	2.3E-08	1.5E-14	1.537
8214	-1.956	18.39	35.56	1.999	0.359	1.359	8205	6.6E-10	1.4E-08	9.3E-15	1.676
15754	-2.924	17.42	33.69	2.110	0.287	1.287	15744	6.5E-10	9.2E-09	6.0E-15	1.820
8197	-2.654	17.69	34.21	2.078	0.307	1.307	8187	2.6E-09	2.0E-09	5.3E-15	1.777
4131	-2.275	18.07	34.94	2.034	0.335	1.335	4121	8.8E-10	5.3E-09	4.7E-15	1.721
2118	-1.571	18.78	36.30	1.958	0.387	1.387	2108	1.4E-08	1.9E-08	2.8E-13	1.625
1101	-0.885	19.46	37.63	1.889	0.438	1.438	1091	1.4E-10	3.6E-08	5.2E-15	1.542

Table D-3: 1D Consolidation Data for Specimen 1DC-SR160-2

Vertical Press. (kPa)	Displaceme nt (mm)	Thickness (mm)	Vol. (cm^3)	Dry density (Mg/m^3)	Void ratio, e	Spec. volume , V	Effective vertical stress (kPa)	Coeff. of consolida tion, cv (m^2/ s)	mv (1/Pa)	Hydraulic conductiv ity (m/s)	EMDD (Mg/m^3)
100	0.000	19.96	38.86	1.810	0.500	1.500	90				1.450
805	0.000	19.96	38.86	1.810	0.500	1.500	795				1.450
1152	-0.114	19.85	38.64	1.821	0.492	1.492	1142	1.6E-10	1.6E-08	2.9E-15	1.462
2115	-0.558	19.40	37.78	1.862	0.458	1.458	2105	1.6E-10	2.3E-08	4.2E-15	1.510
2099	-0.538	19.42	37.82	1.860	0.460	1.460	2089	1.6E-10	2.3E-08	4.2E-15	1.508
4125	-1.173	18.79	36.58	1.923	0.412	1.412	4115	1.6E-10	1.6E-08	2.9E-15	1.583
16232	-2.604	17.36	33.79	2.082	0.305	1.305	16222	1.6E-10	6.3E-09	1.1E-15	1.782
4111	-2.132	17.83	34.71	2.027	0.340	1.340	4102	1.6E-10	2.2E-09	4.0E-16	1.711
1105	-1.525	18.43	35.89	1.960	0.386	1.386	1096	1.6E-10	1.1E-08	2.0E-15	1.628

Table D-4: 1D Consolidation Data for Specimen 1DC-SR270

Vertical Press. (kPa)	Displaceme nt (mm)	Thickness (mm)	Vol. (cm³)	Dry density (Mg/m³)	Void ratio, e	Spec. volume , V	Effective vertical stress (kPa)	Coeff. of consolida tion, cv (m²/ s)	mv (1/Pa)	Hydraulic conductiv ity (m/s)	EMDD (Mg/m³)
100	0.000	21.30	41.19	1.731	0.569	1.569	90				1.361
167	0.124	21.43	41.43	1.721	0.578	1.578	157				1.350
1120	-0.324	20.98	40.56	1.758	0.545	1.545	1111	1.2E-08	2.2E-08	3.1E-13	1.391
2122	-0.725	20.58	39.79	1.792	0.515	1.515	2112	7.1E-09	1.9E-08	1.6E-13	1.429
4203	-1.312	19.99	38.65	1.845	0.472	1.472	4193	2.2E-09	1.4E-08	3.6E-14	1.490
8190	-2.227	19.08	36.88	1.934	0.405	1.405	8180	4.6E-09	1.1E-08	6.3E-14	1.595
16321	-3.251	18.05	34.90	2.043	0.329	1.329	16312	2.3E-09	6.6E-09	1.8E-14	1.732
8217	-3.094	18.21	35.21	2.026	0.341	1.341	8207	8.6E-09	1.7E-06	1.7E-11	1.710
4157	-2.875	18.43	35.63	2.002	0.357	1.357	4148	3.1E-09	3.0E-09	1.1E-14	1.679
2126	-2.629	18.67	36.11	1.975	0.375	1.375	2117	1.4E-09	6.6E-09	1.1E-14	1.646
1116	-2.375	18.93	36.60	1.949	0.394	1.394	1106	9.8E-10	1.3E-08	1.6E-14	1.614
93	-1.691	19.61	37.92	1.881	0.444	1.444	83	7.7E-10	3.5E-08	3.2E-14	1.532

APPENDIX E: RESULTS OF SWCC MEASUREMENTS

Table E-1: SWCC Data, Part 1

			Dessicators					Properties		
Legend	Specimen No.	Batch	Dessicator No.	Solution	Suction-target (MPa)	Suction-EOT (MPa)	Duration (Days)	Mixing Liquid	wc-target (%)	Dry density-target (Mg/m³)
DW-L-w18%	L-1	1	1	KCl	0.5	0.47	48	DW	18	loose
	L-2	1	2	KCl	1	1.05	48	DW	18	loose
	L-3	1	3	KCl	2	2.33	48	DW	18	loose
	L-4	1	4	KCl	5	5.49	48	DW	18	loose
	L-5	1	5	H2SO4	5	4.51	48	DW	18	loose
	L-6	1	6	H2SO4	10	7.96	48	DW	18	loose
	L-7	1	7	H2SO4	20	13.96	48	DW	18	loose
	L-8	1	8	H2SO4	40	26.06	48	DW	18	loose
	L-9A	1	9A	H2SO4	80	61.72	48	DW	18	loose
	L-9B	1	9B	H2SO4	80	54.71	48	DW	18	loose
	L-10A	1	10A	H2SO4	160	108.24	48	DW	18	loose
	L-10B	1	10B	H2SO4	160	98.8	48	DW	18	loose
DW-1.4-w32%	14-1	1	1	KCl	0.5	0.47	48	DW	32	1.4
	14-2	1	2	KCl	1	1.05	48	DW	32	1.4
	14-3	1	3	KCl	2	2.33	48	DW	32	1.4
	14-4	1	4	KCl	5	5.49	48	DW	32	1.4
	14-5	1	5	H2SO4	5	4.51	48	DW	32	1.4
	14-6	1	6	H2SO4	10	7.96	48	DW	32	1.4
	14-7	1	7	H2SO4	20	13.96	48	DW	32	1.4
	14-8	1	8	H2SO4	40	26.06	48	DW	32	1.4
	14-9B	1	9B	H2SO4	80	54.71	48	DW	32	1.4

Legend	Specimen No.	Batch	Dessicators						Properties		
			Dessicator No.	Solution	Suction-target (MPa)	Suction-EOT (MPa)	Duration (Days)		Mixing Liquid	wc-target (%)	Dry density-target (Mg/m³)
	14-10B	1	10B	H2SO4	160	98.8	48		DW	32	1.4
DW-1.4-w18%	DW-14-1	2	1	KCl	0.5	2.39	152		DW	18	1.4
	DW-14-2	2	2	KCl	1	0.62	152		DW	18	1.4
	DW-14-3	2	3	KCl	2	1.17	152		DW	18	1.4
	DW-14-4	2	4	KCl	5	5.44	152		DW	18	1.4
	DW-14-5	2	5	H2SO4	5	5.59	152		DW	18	1.4
	DW-14-6	2	6	H2SO4	10	8.88	152		DW	18	1.4
	DW-14-7	2	7	H2SO4	20	16.79	152		DW	18	1.4
	DW-14-8	2	8	H2SO4	40	33.78	152		DW	18	1.4
	DW-14-9B	2	9B	H2SO4	80	79.7	152		DW	18	1.4
	DW-14-10B	2	10B	H2SO4	160	154.77	152		DW	18	1.4
DW-1.6-w24%	16-1	1	1	KCl	0.5	0.47	48		DW	24	1.6
	16-2	1	2	KCl	1	1.05	48		DW	24	1.6
	16-3	1	3	KCl	2	2.33	48		DW	24	1.6
	16-4	1	4	KCl	5	5.49	48		DW	24	1.6
	16-5	1	5	H2SO4	5	4.51	48		DW	24	1.6
	16-6	1	6	H2SO4	10	7.96	48		DW	24	1.6
	16-7	1	7	H2SO4	20	13.96	48		DW	24	1.6
	16-8	1	8	H2SO4	40	26.06	48		DW	24	1.6
	16-9B	1	9B	H2SO4	80	54.71	48		DW	24	1.6
	16-10B	1	10B	H2SO4	160	98.8	48		DW	24	1.6
DW-1.6-w18%	DW-16-1	2	1	KCl	0.5	2.39	152		DW	18	1.6
	DW-16-2	2	2	KCl	1	0.62	152		DW	18	1.6
	DW-16-3	2	3	KCl	2	1.17	152		DW	18	1.6

Legend	Specimen No.	Batch	Dessicators		Suction-target (MPa)	Suction-EOT (MPa)	Duration (Days)	Properties		
			Dessicator No.	Solution				Mixing Liquid	wc-target (%)	Dry density-target (Mg/m^3)
	DW-16-4	2	4	KCl	5	5.44	152	DW	18	1.6
	DW-16-5	2	5	H2SO4	5	5.59	152	DW	18	1.6
	DW-16-6	2	6	H2SO4	10	8.88	152	DW	18	1.6
	DW-16-7	2	7	H2SO4	20	16.79	152	DW	18	1.6
	DW-16-8	2	8	H2SO4	40	33.78	152	DW	18	1.6
	DW-16-9B	2	9B	H2SO4	80	79.7	152	DW	18	1.6
	DW-16-10B	2	10B	H2SO4	160	154.77	152	DW	18	1.6
DW-1.8-w18%	18A-1	1	1	KCl	0.5	0.47	48	DW	18	1.8
	18B-1	1	1	KCl	0.5	0.47	48	DW	18	1.8
	18C-1	1	1	KCl	0.5	0.47	48	DW	18	1.8
	18A-2	1	2	KCl	1	1.05	48	DW	18	1.8
	18B-2	1	2	KCl	1	1.05	48	DW	18	1.8
	18C-2	1	2	KCl	1	1.05	48	DW	18	1.8
	18A-3	1	3	KCl	2	2.33	48	DW	18	1.8
	18B-3	1	3	KCl	2	2.33	48	DW	18	1.8
	18C-3	1	3	KCl	2	2.33	48	DW	18	1.8
	18A-4	1	4	KCl	5	5.49	48	DW	18	1.8
	18B-4	1	4	KCl	5	5.49	48	DW	18	1.8
	18C-4	1	4	KCl	5	5.49	48	DW	18	1.8
	18A-5	1	5	H2SO4	5	4.51	48	DW	18	1.8
	18B-5	1	5	H2SO4	5	4.51	48	DW	18	1.8
	18C-5	1	5	H2SO4	5	4.51	48	DW	18	1.8
	18A-6	1	6	H2SO4	10	7.96	48	DW	18	1.8
	18B-6	1	6	H2SO4	10	7.96	48	DW	18	1.8

Legend	Specimen No.	Batch	Dessicators						Properties		
			Dessicator No.	Solution	Suction-target (MPa)	Suction-EOT (MPa)	Duration (Days)		Mixing Liquid	wc-target (%)	Dry density-target (Mg/m^3)
	18C-6	1	6	H2SO4	10	7.96	48		DW	18	1.8
	18A-7	1	7	H2SO4	20	13.96	48		DW	18	1.8
	18B-7	1	7	H2SO4	20	13.96	48		DW	18	1.8
	18C-7	1	7	H2SO4	20	13.96	48		DW	18	1.8
	18A-8	1	8	H2SO4	40	26.06	48		DW	18	1.8
	18B-8	1	8	H2SO4	40	26.06	48		DW	18	1.8
	18C-8	1	8	H2SO4	40	26.06	48		DW	18	1.8
	18A-9A	1	9A	H2SO4	80	61.72	48		DW	18	1.8
	18B-9A	1	9A	H2SO4	80	61.72	48		DW	18	1.8
	18C-9B	1	9B	H2SO4	80	54.71	48		DW	18	1.8
	18A-10A	1	10A	H2SO4	160	108.24	48		DW	18	1.8
	18B-10A	1	10A	H2SO4	160	108.24	48		DW	18	1.8
	18C-10B	1	10B	H2SO4	160	98.8	48		DW	18	1.8
CR10-L-w32%	CR10-L-1	3	1	KCl	2.39	2.390	134		CR10	32	Loose
	CR10-L-2	3	2	KCl	0.62	0.620	134		CR10	32	Loose
	CR10-L-3	3	3	KCl	1.17	1.170	134		CR10	32	Loose
	CR10-L-4	3	4	KCl	5.44	5.440	134		CR10	32	Loose
	CR10-L-5	3	5	H2SO4	5.59	5.760	134		CR10	32	Loose
	CR10-L-6	3	6	H2SO4	8.88	9.290	134		CR10	32	Loose
	CR10-L-7	3	7	H2SO4	16.79	16.880	134		CR10	32	Loose
	CR10-L-8	3	8	H2SO4	33.78	34.190	134		CR10	32	Loose
	CR10-L-9	3	9B	H2SO4	79.7	76.490	134		CR10	32	Loose
	CR10-L-10	3	10B	H2SO4	154.77	126.320	134		CR10	32	Loose
CR10-1.4-w32%	CR10-1.4-1	3	1	KCl	2.39	2.390	134		CR10	32	1.4

Legend	Specimen No.	Batch	Dessicator No.	Solution	Suction-target (MPa)	Suction-EOT (MPa)	Duration (Days)	Mixing Liquid	wc-target (%)	Dry density-target (Mg/m³)
			Dessicators					**Properties**		
	CR10-1.4-2	3	2	KCl	0.62	0.620	134	CR10	32	1.4
	CR10-1.4-3	3	3	KCl	1.17	1.170	134	CR10	32	1.4
	CR10-1.4-4	3	4	KCl	5.44	5.440	134	CR10	32	1.4
	CR10-1.4-5	3	5	H2SO4	5.59	5.760	134	CR10	32	1.4
	CR10-1.4-6	3	6	H2SO4	8.88	9.290	134	CR10	32	1.4
	CR10-1.4-7	3	7	H2SO4	16.79	16.880	134	CR10	32	1.4
	CR10-1.4-8	3	8	H2SO4	33.78	34.190	134	CR10	32	1.4
	CR10-1.4-9	3	9B	H2SO4	79.7	76.490	134	CR10	32	1.4
	CR10-1.4-10	3	10B	H2SO4	154.77	126.320	134	CR10	32	1.4
CR10-1.6-w24%	CR10-1.6-1	3	1	KCl	2.39	2.390	134	CR10	24	1.6
	CR10-1.6-2	3	2	KCl	0.62	0.620	134	CR10	24	1.6
	CR10-1.6-3	3	3	KCl	1.17	1.170	134	CR10	24	1.6
	CR10-1.6-4	3	4	KCl	5.44	5.440	134	CR10	24	1.6
	CR10-1.6-5	3	5	H2SO4	5.59	5.760	134	CR10	24	1.6
	CR10-1.6-6	3	6	H2SO4	8.88	9.290	134	CR10	24	1.6
	CR10-1.6-7	3	7	H2SO4	16.79	16.880	134	CR10	24	1.6
	CR10-1.6-8	3	8	H2SO4	33.78	34.190	134	CR10	24	1.6
	CR10-1.6-9	3	9A	H2SO4	76.89	78.610	134	CR10	24	1.6
	CR10-1.6-10	3	10A	H2SO4	146.25	127.480	134	CR10	24	1.6
CR10-1.8-w18%	CR10-18-1	2	1	KCl	0.5	2.39	152	CR10	18	1.8
	CR10-18-2	2	2	KCl	1	0.62	152	CR10	18	1.8
	CR10-18-3	2	3	KCl	2	1.17	152	CR10	18	1.8
	CR10-18-4	2	4	KCl	5	5.44	152	CR10	18	1.8

Legend	Specimen No.	Batch	Dessicators						Properties		
			Dessicator No.	Solution	Suction-target (MPa)	Suction-EOT (MPa)	Duration (Days)		Mixing Liquid	wc-target (%)	Dry density-target (Mg/m³)
	CR10-18-5	2	5	H2SO4	5	5.59	152		CR10	18	1.8
	CR10-18-6	2	6	H2SO4	10	8.88	152		CR10	18	1.8
	CR10-18-7	2	7	H2SO4	20	16.79	152		CR10	18	1.8
	CR10-18-8	2	8	H2SO4	40	33.78	152		CR10	18	1.8
	CR10-18-9A	2	9A	H2SO4	80	76.89	152		CR10	18	1.8
	CR10-18-10A	2	10A	H2SO4	160	146.25	152		CR10	18	1.8
SR160-10-L-w32%	SR160-L-1	3	1	KCl	2.39	2.390	134		SR160	32	Loose
	SR160-L-2	3	2	KCl	0.62	0.620	134		SR160	32	Loose
	SR160-L-3	3	3	KCl	1.17	1.170	134		SR160	32	Loose
	SR160-L-4	3	4	KCl	5.44	5.440	134		SR160	32	Loose
	SR160-L-5	3	5	H2SO4	5.59	5.760	134		SR160	32	Loose
	SR160-L-6	3	6	H2SO4	8.88	9.290	134		SR160	32	Loose
	SR160-L-7	3	7	H2SO4	16.79	16.880	134		SR160	32	Loose
	SR160-L-8	3	8	H2SO4	33.78	34.190	134		SR160	32	Loose
	SR160-L-9	3	9A	H2SO4	76.89	78.610	134		SR160	32	Loose
	SR160-L-10	3	10A	H2SO4	146.25	127.480	134		SR160	32	Loose
SR160-1.4-w32%	SR160-1.4-1	3	1	KCl	2.39	2.390	134		SR160	32	1.4
	SR160-1.4-2	3	2	KCl	0.62	0.620	134		SR160	32	1.4
	SR160-1.4-3	3	3	KCl	1.17	1.170	134		SR160	32	1.4
	SR160-1.4-4	3	4	KCl	5.44	5.440	134		SR160	32	1.4
	SR160-1.4-5	3	5	H2SO4	5.59	5.760	134		SR160	32	1.4
	SR160-1.4-6	3	6	H2SO4	8.88	9.290	134		SR160	32	1.4
	SR160-1.4-7	3	7	H2SO4	16.79	16.880	134		SR160	32	1.4

Legend	Specimen No.	Batch	Dessicators						Properties		
			Dessicator No.	Solution	Suction-target (MPa)	Suction-EOT (MPa)	Duration (Days)		Mixing Liquid	wc-target (%)	Dry density-target (Mg/m³)
	SR160-1.4-8	3	8	H2SO4	33.78	34.190	134		SR160	32	1.4
	SR160-1.4-9	3	9B	H2SO4	79.7	76.490	134		SR160	32	1.4
	SR160-1.4-10	3	10B	H2SO4	154.77	126.320	134		SR160	32	1.4
SR160-1.6-w24%	SR160-1.6-1	3	1	KCl	2.39	2.390	134		SR160	24	1.6
	SR160-1.6-2	3	2	KCl	0.62	0.620	134		SR160	24	1.6
	SR160-1.6-3	3	3	KCl	1.17	1.170	134		SR160	24	1.6
	SR160-1.6-4	3	4	KCl	5.44	5.440	134		SR160	24	1.6
	SR160-1.6-5	3	5	H2SO4	5.59	5.760	134		SR160	24	1.6
	SR160-1.6-6	3	6	H2SO4	8.88	9.290	134		SR160	24	1.6
	SR160-1.6-7	3	7	H2SO4	16.79	16.880	134		SR160	24	1.6
	SR160-1.6-8	3	8	H2SO4	33.78	34.190	134		SR160	24	1.6
	SR160-1.6-9	3	9A	H2SO4	76.89	78.610	134		SR160	24	1.6
	SR160-1.6-10	3	10A	H2SO4	146.25	127.480	134		SR160	24	1.6
SR160-1.8-w18%	SR160-18-1	2	1	KCl	0.5	2.39	152		SR160	18	1.8
	SR160-18-2	2	2	KCl	1	0.62	152		SR160	18	1.8
	SR160-18-3	2	3	KCl	2	1.17	152		SR160	18	1.8
	SR160-18-4	2	4	KCl	5	5.44	152		SR160	18	1.8
	SR160-18-5	2	5	H2SO4	5	5.59	152		SR160	18	1.8
	SR160-18-6	2	6	H2SO4	10	8.88	152		SR160	18	1.8
	SR160-18-7	2	7	H2SO4	20	16.79	152		SR160	18	1.8
	SR160-18-8	2	8	H2SO4	40	33.78	152		SR160	18	1.8
	SR160-18-9A	2	9A	H2SO4	80	76.89	152		SR160	18	1.8

Legend	Specimen No.	Batch	Dessicators					Properties		
			Dessicator No.	Solution	Suction-target (MPa)	Suction-EOT (MPa)	Duration (Days)	Mixing Liquid	wc-target (%)	Dry density-target (Mg/m^3)
	SR160-18-10A	2	10A	H2SO4	160	146.25	152	SR160	18	1.8
SR270-10-L-w18%	SR270-L-1	2	1	KCl	0.5	2.39	152	SR270	18	loose
	SR270-L-2	2	2	KCl	1	0.62	152	SR270	18	loose
	SR270-L-3	2	3	KCl	2	1.17	152	SR270	18	loose
	SR270-L-4	2	4	KCl	5	5.44	152	SR270	18	loose
	SR270-L-5	2	5	H2SO4	5	5.59	152	SR270	18	loose
	SR270-L-6	2	6	H2SO4	10	8.88	152	SR270	18	loose
	SR270-L-7	2	7	H2SO4	20	16.79	152	SR270	18	loose
	SR270-L-8	2	8	H2SO4	40	33.78	152	SR270	18	loose
	SR270-L-9B	2	9B	H2SO4	80	79.7	152	SR270	18	loose
	SR270-L-9A	2	9A	H2SO4	80	76.89	152	SR270	18	loose
	SR270-L-10B	2	10B	H2SO4	160	154.77	152	SR270	18	loose
	SR270-L-10A	2	10A	H2SO4	160	146.25	152	SR270	18	loose
SR270-10-L-w32%	SR270-L-1	3	1	KCl	2.39	2.390	134	SR270	32	Loose
	SR270-L-2	3	2	KCl	0.62	0.620	134	SR270	32	Loose
	SR270-L-3	3	3	KCl	1.17	1.170	134	SR270	32	Loose
	SR270-L-4	3	4	KCl	5.44	5.440	134	SR270	32	Loose
	SR270-L-5	3	5	H2SO4	5.59	5.760	134	SR270	32	Loose
	SR270-L-6	3	6	H2SO4	8.88	9.290	134	SR270	32	Loose
	SR270-L-7	3	7	H2SO4	16.79	16.880	134	SR270	32	Loose
	SR270-L-8	3	8	H2SO4	33.78	34.190	134	SR270	32	Loose
	SR270-L-9	3	9B	H2SO4	79.7	76.490	134	SR270	32	Loose

Legend	Specimen No.	Batch	Dessicators						Properties		
			Dessicator No.	Solution	Suction-target (MPa)	Suction-EOT (MPa)	Duration (Days)		Mixing Liquid	wc-target (%)	Dry density-target (Mg/m^3)
	SR270-L-10	3	10B	H2SO4	154.77	126.320	134		SR270	32	Loose
SR270-1.4-w32%	SR270-1.4-1	3	1	KCl	2.39	2.390	134		SR270	32	1.4
	SR270-1.4-2	3	2	KCl	0.62	0.620	134		SR270	32	1.4
	SR270-1.4-3	3	3	KCl	1.17	1.170	134		SR270	32	1.4
	SR270-1.4-4	3	4	KCl	5.44	5.440	134		SR270	32	1.4
	SR270-1.4-5	3	5	H2SO4	5.59	5.760	134		SR270	32	1.4
	SR270-1.4-6	3	6	H2SO4	8.88	9.290	134		SR270	32	1.4
	SR270-1.4-7	3	7	H2SO4	16.79	16.880	134		SR270	32	1.4
	SR270-1.4-8	3	8	H2SO4	33.78	34.190	134		SR270	32	1.4
	SR270-1.4-9	3	9B	H2SO4	79.7	76.490	134		SR270	32	1.4
	SR270-1.4-10	3	10B	H2SO4	154.77	126.320	134		SR270	32	1.4
SR270-1.6-w24%	SR270-1.6-1	3	1	KCl	2.39	2.390	134		SR270	24	1.6
	SR270-1.6-2	3	2	KCl	0.62	0.620	134		SR270	24	1.6
	SR270-1.6-3	3	3	KCl	1.17	1.170	134		SR270	24	1.6
	SR270-1.6-4	3	4	KCl	5.44	5.440	134		SR270	24	1.6
	SR270-1.6-5	3	5	H2SO4	5.59	5.760	134		SR270	24	1.6
	SR270-1.6-6	3	6	H2SO4	8.88	9.290	134		SR270	24	1.6
	SR270-1.6-7	3	7	H2SO4	16.79	16.880	134		SR270	24	1.6
	SR270-1.6-8	3	8	H2SO4	33.78	34.190	134		SR270	24	1.6
	SR270-1.6-9	3	9A	H2SO4	76.89	78.610	134		SR270	24	1.6
	SR270-1.6-10	3	10A	H2SO4	146.25	127.480	134		SR270	24	1.6

Legend	Specimen No.	Batch	Dessicators						Properties		
			Dessicator No.	Solution	Suction-target (MPa)	Suction-EOT (MPa)	Duration (Days)		Mixing Liquid	wc-target (%)	Dry density-target (Mg/m³)
SR270-1.8-w18%	SR270-18-1	2	1	KCl	0.5	2.39	152		SR270	18	1.8
	SR270-18-2	2	2	KCl	1	0.62	152		SR270	18	1.8
	SR270-18-3	2	3	KCl	2	1.17	152		SR270	18	1.8
	SR270-18-4	2	4	KCl	5	5.44	152		SR270	18	1.8
	SR270-18-5	2	5	H2SO4	5	5.59	152		SR270	18	1.8
	SR270-18-6	2	6	H2SO4	10	8.88	152		SR270	18	1.8
	SR270-18-7	2	7	H2SO4	20	16.79	152		SR270	18	1.8
	SR270-18-8	2	8	H2SO4	40	33.78	152		SR270	18	1.8
	SR270-18-9A	2	9A	H2SO4	80	76.89	152		SR270	18	1.8
	SR270-18-10A	2	10A	H2SO4	160	146.25	152		SR270	18	1.8

Table E-2: SWCC Data, Part 2

Legend	Specimen No.	Initial condition				
		Salinity, $r_{initial}$	wc (%)	wc-corrected (%)	Bulk density, initial (Mg/m³)	Dry density, initial (Mg/m³)
DW-L-w18%	L-1	0	18.0	18.0		
	L-2	0	18.0	18.0		
	L-3	0	18.0	18.0		
	L-4	0	18.0	18.0		
	L-5	0	18.0	18.0		
	L-6	0	18.0	18.0		
	L-7	0	18.0	18.0		
	L-8	0	18.0	18.0		
	L-9A	0	18.0	18.0		
	L-9B	0	18.0	18.0		
	L-10A	0	18.0	18.0		
	L-10B	0	18.0	18.0		
DW-1.4-w32%	14-1	0	31.3	31.3	1.83	1.40
	14-2	0	31.3	31.3	1.85	1.41
	14-3	0	31.3	31.3	1.88	1.43
	14-4	0	31.3	31.3	1.86	1.42
	14-5	0	31.3	31.3	1.87	1.43
	14-6	0	31.3	31.3	1.85	1.41
	14-7	0	31.3	31.3	1.86	1.42
	14-8	0	31.3	31.3	1.86	1.42
	14-9B	0	31.3	31.3	1.85	1.41
	14-10B	0	31.3	31.3	1.86	1.42

		Initial condition				
Legend	Specimen No.	Salinity, $r_{initial}$	wc (%)	wc-corrected (%)	Bulk density, initial (Mg/m^3)	Dry density, initial (Mg/m^3)
DW-1.4-w18%	DW-14-1	0	16.8	16.8	1.61	1.38
	DW-14-2	0	16.8	16.8	1.67	1.43
	DW-14-3	0	16.8	16.8	1.68	1.44
	DW-14-4	0	16.8	16.8	1.69	1.44
	DW-14-5	0	16.8	16.8	1.70	1.46
	DW-14-6	0	16.8	16.8	1.64	1.41
	DW-14-7	0	16.8	16.8	1.67	1.43
	DW-14-8	0	16.8	16.8	1.67	1.43
	DW-14-9B	0	16.8	16.8	1.70	1.45
	DW-14-10B	0	16.8	16.8	1.71	1.47
DW-1.6-w24%	16-1	0	24.0	24.0	2.03	1.63
	16-2	0	24.0	24.0	1.99	1.60
	16-3	0	24.0	24.0	1.99	1.60
	16-4	0	24.0	24.0	2.01	1.62
	16-5	0	24.0	24.0	1.98	1.60
	16-6	0	24.0	24.0	1.99	1.61
	16-7	0	24.0	24.0	1.98	1.60
	16-8	0	24.0	24.0	1.98	1.60
	16-9B	0	24.0	24.0	1.99	1.60
	16-10B	0	24.0	24.0	1.94	1.57
DW-1.6-w18%	DW-16-1	0	16.8	16.8	1.90	1.62
	DW-16-2	0	16.8	16.8	1.90	1.63
	DW-16-3	0	16.8	16.8	1.90	1.63
	DW-16-4	0	16.8	16.8	2.00	1.71

Legend	Specimen No.	Initial condition				
		Salinity, $r_{initial}$	wc (%)	wc-corrected (%)	Bulk density, initial (Mg/m^3)	Dry density, initial (Mg/m^3)
	DW-16-5	0	16.8	16.8	1.93	1.65
	DW-16-6	0	16.8	16.8	1.86	1.59
	DW-16-7	0	16.8	16.8	1.81	1.55
	DW-16-8	0	16.8	16.8	1.85	1.59
	DW-16-9B	0	16.8	16.8	1.86	1.59
	DW-16-10B	0	16.8	16.8	1.84	1.58
DW-1.8-w18%	18A-1	0	17.1	17.1	2.05	1.75
	18B-1	0	17.1	17.1	2.10	1.79
	18C-1	0	17.1	17.1	2.11	1.80
	18A-2	0	17.1	17.1	2.11	1.80
	18B-2	0	17.1	17.1	2.12	1.81
	18C-2	0	17.1	17.1	2.12	1.81
	18A-3	0	17.1	17.1	2.08	1.77
	18B-3	0	17.1	17.1	2.11	1.80
	18C-3	0	17.1	17.1	2.10	1.79
	18A-4	0	17.1	17.1	2.09	1.78
	18B-4	0	17.1	17.1	2.10	1.80
	18C-4	0	17.1	17.1	2.10	1.79
	18A-5	0	17.1	17.1	2.11	1.80
	18B-5	0	17.1	17.1	2.07	1.77
	18C-5	0	17.1	17.1	2.06	1.76
	18A-6	0	17.1	17.1	2.09	1.78
	18B-6	0	17.1	17.1	2.09	1.79
	18C-6	0	17.1	17.1	2.11	1.80

Legend	Specimen No.	Initial condition				
		Salinity, r $_{initial}$	wc (%)	wc-corrected (%)	Bulk density, initial (Mg/m^3)	Dry density, initial (Mg/m^3)
	18A-7	0	17.1	17.1	2.09	1.78
	18B-7	0	17.1	17.1	2.09	1.78
	18C-7	0	17.1	17.1	2.07	1.77
	18A-8	0	17.1	17.1	2.08	1.77
	18B-8	0	17.1	17.1	2.11	1.80
	18C-8	0	17.1	17.1	2.08	1.78
	18A-9A	0	17.1	17.1	2.10	1.80
	18B-9A	0	17.1	17.1	2.07	1.77
	18C-9B	0	17.1	17.1	2.10	1.79
	18A-10A	0	17.1	17.1	2.10	1.79
	18B-10A	0	17.1	17.1	2.09	1.78
	18C-10B	0	17.1	17.1	2.14	1.82
CR10-L-w32%	CR10-L-1	0.009975	32.6	33.0		
	CR10-L-2	0.009975	32.6	33.0		
	CR10-L-3	0.009975	32.6	33.0		
	CR10-L-4	0.009975	32.6	33.0		
	CR10-L-5	0.009975	32.6	33.0		
	CR10-L-6	0.009975	32.6	33.0		
	CR10-L-7	0.009975	32.6	33.0		
	CR10-L-8	0.009975	32.6	33.0		
	CR10-L-9	0.009975	32.6	33.0		
	CR10-L-10	0.009975	32.6	33.0		
CR10-1.4-w32%	CR10-1.4-1	0.009975	32.6	33.0	1.88	1.41
	CR10-1.4-2	0.009975	32.6	33.0	1.86	1.40

Legend	Specimen No.	Initial condition				
		Salinity, r initial	wc (%)	wc-corrected (%)	Bulk density, initial (Mg/m^3)	Dry density, initial (Mg/m^3)
	CR10-1.4-3	0.009975	32.6	33.0	1.89	1.42
	CR10-1.4-4	0.009975	32.6	33.0	1.86	1.40
	CR10-1.4-5	0.009975	32.6	33.0	1.80	1.36
	CR10-1.4-6	0.009975	32.6	33.0	1.86	1.40
	CR10-1.4-7	0.009975	32.6	33.0	1.80	1.35
	CR10-1.4-8	0.009975	32.6	33.0	1.84	1.39
	CR10-1.4-9	0.009975	32.6	33.0	1.86	1.40
	CR10-1.4-10	0.009975	32.6	33.0	1.87	1.41
CR10-1.6-w24%	CR10-1.6-1	0.009975	23.7	24.0	1.98	1.60
	CR10-1.6-2	0.009975	23.7	24.0	1.97	1.59
	CR10-1.6-3	0.009975	23.7	24.0	1.93	1.56
	CR10-1.6-4	0.009975	23.7	24.0	1.93	1.56
	CR10-1.6-5	0.009975	23.7	24.0	1.96	1.58
	CR10-1.6-6	0.009975	23.7	24.0	1.95	1.57
	CR10-1.6-7	0.009975	23.7	24.0	1.96	1.58
	CR10-1.6-8	0.009975	23.7	24.0	1.98	1.60
	CR10-1.6-9	0.009975	23.7	24.0	1.93	1.56
	CR10-1.6-10	0.009975	23.7	24.0	1.98	1.60
CR10-1.8-w18%	CR10-18-1	0.009975	17.5	17.7	2.09	1.78
	CR10-18-2	0.009975	17.5	17.7	2.12	1.80
	CR10-18-3	0.009975	17.5	17.7	2.13	1.81
	CR10-18-4	0.009975	17.5	17.7	2.13	1.81
	CR10-18-5	0.009975	17.5	17.7	2.09	1.77

		Initial condition				
Legend	Specimen No.	Salinity, $r_{initial}$	wc (%)	wc-corrected (%)	Bulk density, initial (Mg/m^3)	Dry density, initial (Mg/m^3)
	CR10-18-6	0.009975	17.5	17.7	2.11	1.80
	CR10-18-7	0.009975	17.5	17.7	2.06	1.75
	CR10-18-8	0.009975	17.5	17.7	2.11	1.79
	CR10-18-9A	0.009975	17.5	17.7	2.10	1.78
	CR10-18-10A	0.009975	17.5	17.7	2.12	1.80
SR160-10-L-w32%	SR160-L-1	0.144724	27.9	34.3		
	SR160-L-2	0.144724	27.9	34.3		
	SR160-L-3	0.144724	27.9	34.3		
	SR160-L-4	0.144724	27.9	34.3		
	SR160-L-5	0.144724	27.9	34.3		
	SR160-L-6	0.144724	27.9	34.3		
	SR160-L-7	0.144724	27.9	34.3		
	SR160-L-8	0.144724	27.9	34.3		
	SR160-L-9	0.144724	27.9	34.3		
	SR160-L-10	0.144724	27.9	34.3		
SR160-1.4-w32%	SR160-1.4-1	0.144724	27.9	34.3	1.82	1.35
	SR160-1.4-2	0.144724	27.9	34.3	1.86	1.38
	SR160-1.4-3	0.144724	27.9	34.3	1.82	1.36
	SR160-1.4-4	0.144724	27.9	34.3	1.82	1.36
	SR160-1.4-5	0.144724	27.9	34.3	1.84	1.37
	SR160-1.4-6	0.144724	27.9	34.3	1.86	1.39
	SR160-1.4-7	0.144724	27.9	34.3	1.85	1.38
	SR160-1.4-8	0.144724	27.9	34.3	1.84	1.37

		Initial condition				
Legend	Specimen No.	Salinity, $r_{initial}$	wc (%)	wc-corrected (%)	Bulk density, initial (Mg/m^3)	Dry density, initial (Mg/m^3)
	SR160-1.4-9	0.144724	27.9	34.3	1.86	1.39
	SR160-1.4-10	0.144724	27.9	34.3	1.83	1.37
SR160-1.6-w24%	SR160-1.6-1	0.144724	20.8	25.2	1.94	1.55
	SR160-1.6-2	0.144724	20.8	25.2	1.97	1.57
	SR160-1.6-3	0.144724	20.8	25.2	1.94	1.55
	SR160-1.6-4	0.144724	20.8	25.2	2.01	1.60
	SR160-1.6-5	0.144724	20.8	25.2	1.96	1.57
	SR160-1.6-6	0.144724	20.8	25.2	1.95	1.56
	SR160-1.6-7	0.144724	20.8	25.2	1.97	1.57
	SR160-1.6-8	0.144724	20.8	25.2	1.91	1.53
	SR160-1.6-9	0.144724	20.8	25.2	1.95	1.56
	SR160-1.6-10	0.144724	20.8	25.2	1.95	1.56
SR160-1.8-w18%	SR160-18-1	0.144724	14.5	17.4	2.15	1.83
	SR160-18-2	0.144724	14.5	17.4	2.13	1.82
	SR160-18-3	0.144724	14.5	17.4	2.16	1.84
	SR160-18-4	0.144724	14.5	17.4	2.14	1.82
	SR160-18-5	0.144724	14.5	17.4	2.14	1.83
	SR160-18-6	0.144724	14.5	17.4	2.14	1.82
	SR160-18-7	0.144724	14.5	17.4	2.13	1.81
	SR160-18-8	0.144724	14.5	17.4	2.10	1.79
	SR160-18-9A	0.144724	14.5	17.4	2.15	1.84
	SR160-18-10A	0.144724	14.5	17.4	2.14	1.82

		Initial condition				
Legend	Specimen No.	Salinity, $r_{initial}$	wc (%)	wc-corrected (%)	Bulk density, initial (Mg/m^3)	Dry density, initial (Mg/m^3)
SR270-10-L-w18%	SR270-L-1	0.228339	14.6	19.8		
	SR270-L-2	0.228339	14.6	19.8		
	SR270-L-3	0.228339	14.6	19.8		
	SR270-L-4	0.228339	14.6	19.8		
	SR270-L-5	0.228339	14.6	19.8		
	SR270-L-6	0.228339	14.6	19.8		
	SR270-L-7	0.228339	14.6	19.8		
	SR270-L-8	0.228339	14.6	19.8		
	SR270-L-9B	0.228339	14.6	19.8		
	SR270-L-9A	0.228339	14.6	19.8		
	SR270-L-10B	0.228339	14.6	19.8		
	SR270-L-10A	0.228339	14.6	19.8		
SR270-10-L-w32%	SR270-L-1	0.228339	23.5	32.8		
	SR270-L-2	0.228339	23.5	32.8		
	SR270-L-3	0.228339	23.5	32.8		
	SR270-L-4	0.228339	23.5	32.8		
	SR270-L-5	0.228339	23.5	32.8		
	SR270-L-6	0.228339	23.5	32.8		
	SR270-L-7	0.228339	23.5	32.8		
	SR270-L-8	0.228339	23.5	32.8		
	SR270-L-9	0.228339	23.5	32.8		
	SR270-L-10	0.228339	23.5	32.8		

Legend	Specimen No.	Initial condition				
		Salinity, $r_{initial}$	wc (%)	wc-corrected (%)	Bulk density, initial (Mg/m^3)	Dry density, initial (Mg/m^3)
SR270-1.4-w32%	SR270-1.4-1	0.228339	23.5	32.8	1.82	1.37
	SR270-1.4-2	0.228339	23.5	32.8	1.85	1.40
	SR270-1.4-3	0.228339	23.5	32.8	1.83	1.38
	SR270-1.4-4	0.228339	23.5	32.8	1.90	1.43
	SR270-1.4-5	0.228339	23.5	32.8	1.85	1.39
	SR270-1.4-6	0.228339	23.5	32.8	1.82	1.37
	SR270-1.4-7	0.228339	23.5	32.8	1.85	1.39
	SR270-1.4-8	0.228339	23.5	32.8	1.83	1.38
	SR270-1.4-9	0.228339	23.5	32.8	1.84	1.39
	SR270-1.4-10	0.228339	23.5	32.8	1.86	1.40
SR270-1.6-w24%	SR270-1.6-1	0.228339	12.7	17.1	1.94	1.66
	SR270-1.6-2	0.228339	12.7	17.1	1.91	1.63
	SR270-1.6-3	0.228339	12.7	17.1	1.95	1.67
	SR270-1.6-4	0.228339	12.7	17.1	1.97	1.68
	SR270-1.6-5	0.228339	12.7	17.1	1.92	1.64
	SR270-1.6-6	0.228339	12.7	17.1	1.93	1.65
	SR270-1.6-7	0.228339	12.7	17.1	1.96	1.67
	SR270-1.6-8	0.228339	12.7	17.1	1.88	1.61
	SR270-1.6-9	0.228339	12.7	17.1	1.93	1.65
	SR270-1.6-10	0.228339	12.7	17.1	1.93	1.65
SR270-1.8-w18%	SR270-18-1	0.228339	14.8	20.1	2.14	1.78
	SR270-18-2	0.228339	14.8	20.1	2.11	1.76

Legend	Specimen No.	Initial condition				
		Salinity, r $_{initial}$	wc (%)	wc-corrected (%)	Bulk density, initial (Mg/m^3)	Dry density, initial (Mg/m^3)
	SR270-18-3	0.228339	14.8	20.1	2.14	1.78
	SR270-18-4	0.228339	14.8	20.1	2.13	1.78
	SR270-18-5	0.228339	14.8	20.1	2.12	1.77
	SR270-18-6	0.228339	14.8	20.1	2.16	1.80
	SR270-18-7	0.228339	14.8	20.1	2.10	1.75
	SR270-18-8	0.228339	14.8	20.1	2.10	1.75
	SR270-18-9A	0.228339	14.8	20.1	2.20	1.83
	SR270-18-10A	0.228339	14.8	20.1	2.12	1.77

Table E-3: SWCC Data, Part 3

Legend	Specimen No.	End of Test Bulk density, EOT (g/cc)	wc', used the initial data as reference (%)	wc measured at EOT (%)	wc'(%)	Dry density (Mg/m^3)	Void ratio, e	Sw (%)	Final wc (%)	Sw (%)	Suction (MPa)
DW-L-w18%	L-1		17.792	17.121	17.792				17.12		0.470
	L-2		17.521	17.840	17.521				17.84		1.050
	L-3		17.769	17.479	17.769				17.48		2.330
	L-4		16.431	16.849	16.431				16.85		5.490
	L-5		18.278	18.786	18.278				18.79		4.510
	L-6		17.292	16.837	17.292				16.84		7.960
	L-7		15.071	15.046	15.071				15.05		13.960
	L-8		12.692	12.972	12.692				12.97		26.060
	L-9A		9.136	9.822	9.136				9.82		61.720
	L-9B		11.052	9.887	11.052				9.89		54.710
	L-10A		6.582	5.464	6.582				5.46		108.240
	L-10B		6.889	6.509	6.889				6.51		98.800
DW-1.4-w32%	14-1	1.957	17.382	17.735	17.382	1.668	0.629	75.083	17.74	75.08	0.470
	14-2	1.936	20.009	19.348	20.009	1.613	0.684	79.510	19.35	79.51	1.050
	14-3	1.997	20.277	19.135	20.277	1.660	0.636	86.594	19.13	86.59	2.330
	14-4	2.001	18.569	17.711	18.569	1.687	0.610	82.733	17.71	82.73	5.490
	14-5	2.010	21.291	20.853	21.291	1.657	0.639	90.513	20.85	90.51	4.510
	14-6	1.998	18.749	19.205	18.749	1.682	0.614	82.874	19.20	82.87	7.960
	14-7	2.062	16.678	16.429	16.678	1.767	0.537	84.388	16.43	84.39	13.960
	14-8	2.042	14.067	13.881	14.067	1.790	0.517	73.872	13.88	73.87	26.060
	14-9B	2.024	10.830	11.055	10.830	1.827	0.487	60.409	11.06	60.41	54.710

Legend	Specimen No.	End of Test							Final		
		Bulk density, EOT (g/cc)	wc', used the initial data as reference (%)	wc measured at EOT (%)	wc'(%)	Dry density (Mg/m³)	Void ratio, e	Sw (%)	wc (%)	Sw (%)	Suction (MPa)
	14-10B	1.846	6.159	7.171	6.159	1.739	0.562	29.787	7.17	29.79	98.800
DW-1.4-w18%	DW-14-1	1.62	16.289	15.330	16.289	1.394	0.948	46.659	15.33	46.66	2.390
	DW-14-2	1.63	17.487	17.031	17.487	1.387	0.958	49.580	17.03	49.58	0.620
	DW-14-3	1.64	16.560	15.771	16.560	1.411	0.925	48.609	15.77	48.61	1.170
	DW-14-4	1.63	18.031	16.998	18.031	1.383	0.963	50.830	17.00	50.83	5.440
	DW-14-5	1.66	17.591	16.180	17.591	1.414	0.921	51.879	16.18	51.88	5.590
	DW-14-6	1.61	15.987	14.445	15.987	1.387	0.958	45.312	14.45	45.31	8.880
	DW-14-7	1.63	14.123	13.004	14.123	1.429	0.901	42.570	13.00	42.57	16.790
	DW-14-8	1.65	11.947	11.051	11.947	1.477	0.839	38.689	11.05	38.69	33.780
	DW-14-9B	1.68	7.265	6.944	7.265	1.562	0.739	26.696	6.94	26.70	79.700
	DW-14-10B	1.65	7.265	3.908	7.265	1.540	0.763	25.847	3.91	25.85	154.770
DW-1.6-w24%	16-1	2.088	18.285	16.499	18.285	1.765	0.538	92.232	16.50	92.23	0.470
	16-2	2.038	20.042	19.020	20.042	1.698	0.600	90.756	19.02	90.76	1.050
	16-3	2.063	20.047	19.144	20.047	1.719	0.580	93.828	19.14	93.83	2.330
	16-4	2.090	18.322	17.656	18.322	1.767	0.537	92.618	17.66	92.62	5.490
	16-5	2.070	20.489	20.305	20.489	1.718	0.581	95.831	20.30	95.83	4.510
	16-6	2.064	19.317	18.899	19.317	1.730	0.570	92.002	18.90	92.00	7.960
	16-7	2.112	16.824	16.196	16.824	1.808	0.502	91.017	16.20	91.02	13.960
	16-8	2.093	13.869	13.869	13.869	1.838	0.478	78.874	13.87	78.87	26.060
	16-9B	2.119	10.752	10.908	10.752	1.913	0.420	69.590	10.91	69.59	54.710
	16-10B	1.945	7.301	6.990	7.301	1.813	0.498	39.806	6.99	39.81	98.800
DW-1.6-w18%	DW-16-1	1.90	16.124	15.199	16.124	1.637	0.659	66.434	15.20	66.43	2.390

Legend	Specimen No.	End of Test							Final		
		Bulk density, EOT (g/cc)	wc', used the initial data as reference (%)	wc measured at EOT (%)	wc'(%)	Dry density (Mg/m³)	Void ratio, e	Sw (%)	wc (%)	Sw (%)	Suction (MPa)
	DW-16-2	1.90	17.039	16.611	17.039	1.627	0.669	69.140	16.61	69.14	0.620
	DW-16-3	1.86	16.399	15.467	16.399	1.597	0.700	63.613	15.47	63.61	1.170
	DW-16-4	1.89	17.524	16.575	17.524	1.608	0.689	69.037	16.58	69.04	5.440
	DW-16-5	1.88	17.553	16.090	17.553	1.600	0.697	68.369	16.09	68.37	5.590
	DW-16-6	1.81	16.252	14.541	16.252	1.558	0.744	59.360	14.54	59.36	8.880
	DW-16-7	1.80	14.395	13.055	14.395	1.575	0.724	53.992	13.05	53.99	16.790
	DW-16-8	1.86	12.184	11.175	12.184	1.657	0.639	51.792	11.17	51.79	33.780
	DW-16-9B	1.82	7.351	7.193	7.351	1.694	0.604	33.068	7.19	33.07	79.700
	DW-16-10B	1.70	7.351	4.118	7.351	1.583	0.716	27.878	4.12	27.88	154.770
DW-1.8-w18%	18A-1	1.838	16.629	16.937	16.629	1.576	0.724	62.394	16.94	62.39	0.470
	18B-1	1.847	16.939	17.879	16.939	1.580	0.719	63.945	17.88	63.94	0.470
	18C-1	1.880	16.508	17.161	16.508	1.614	0.683	65.653	17.16	65.65	0.470
	18A-2	2.048	17.987	18.655	17.987	1.736	0.565	86.505	18.65	86.50	1.050
	18B-2	2.108	17.882	18.439	17.882	1.788	0.519	93.615	18.44	93.62	1.050
	18C-2	2.096	17.898	18.351	17.898	1.778	0.528	92.125	18.35	92.12	1.050
	18A-3	2.077	17.290	17.831	17.290	1.771	0.534	88.008	17.83	88.01	2.330
	18B-3	2.119	17.426	18.000	17.426	1.805	0.505	93.746	18.00	93.75	2.330
	18C-3	2.126	17.044	18.205	17.044	1.817	0.495	93.511	18.20	93.51	2.330
	18A-4	2.095	15.773	17.410	15.773	1.809	0.501	85.503	17.41	85.50	5.490
	18B-4	2.112	15.669	17.060	15.669	1.826	0.488	87.292	17.06	87.29	5.490
	18C-4	2.101	16.031	17.181	16.031	1.810	0.500	87.052	17.18	87.05	5.490
	18A-5	2.114	17.963	18.785	17.963	1.792	0.516	94.631	18.78	94.63	4.510
	18B-5	2.082	17.744	18.834	17.744	1.768	0.536	89.873	18.83	89.87	4.510

Legend	Specimen No.	End of Test							Final		
		Bulk density, EOT (g/cc)	wc', used the initial data as reference (%)	wc measured at EOT (%)	wc'(%)	Dry density (Mg/m³)	Void ratio, e	Sw (%)	wc (%)	Sw (%)	Suction (MPa)
	18C-5	2.080	17.700	19.257	17.700	1.767	0.537	89.509	19.26	89.51	4.510
	18A-6	2.080	17.143	17.753	17.143	1.776	0.529	87.940	17.75	87.94	7.960
	18B-6	2.109	17.018	17.805	17.018	1.802	0.507	91.110	17.81	91.11	7.960
	18C-6	2.113	16.990	17.296	16.990	1.806	0.504	91.639	17.30	91.64	7.960
	18A-7	2.128	14.668	15.888	14.668	1.856	0.463	86.009	15.89	86.01	13.960
	18B-7	2.128	14.928	15.647	14.928	1.852	0.467	86.886	15.65	86.89	13.960
	18C-7	2.134	14.438	15.967	14.438	1.865	0.456	85.912	15.97	85.91	13.960
	18A-8	2.145	12.020	13.825	12.020	1.915	0.418	78.057	13.83	78.06	26.060
	18B-8	2.175	12.594	13.273	12.594	1.932	0.406	84.238	13.27	84.24	26.060
	18C-8	2.144	12.312	13.381	12.312	1.909	0.423	79.124	13.38	79.12	26.060
	18A-9A	2.165	8.952	10.027	8.952	1.987	0.367	66.330	10.03	66.33	61.720
	18B-9A	2.147	8.788	10.174	8.788	1.974	0.376	63.439	10.17	63.44	61.720
	18C-9B	2.155	9.741	10.591	9.741	1.964	0.383	69.066	10.59	69.07	54.710
	18A-10A	2.068	5.520	5.924	5.520	1.960	0.386	38.857	5.92	38.86	108.240
	18B-10A	2.056	5.135	5.912	5.135	1.955	0.389	35.854	5.91	35.85	108.240
	18C-10B	2.070	6.129	6.811	6.129	1.951	0.392	42.419	6.81	42.42	98.800
CR10-L-w32%	CR10-L-1		21.077	17.225	21.077				21.08		2.390
	CR10-L-2		22.938	17.126	22.938				22.94		0.620
	CR10-L-3		22.749	17.945	22.749				22.75		1.170
	CR10-L-4		21.443	20.657	21.443				21.44		5.440
	CR10-L-5		22.931	16.893	22.931				22.93		5.760
	CR10-L-6		19.995	17.673	19.995				19.99		9.290
	CR10-L-7		16.254	16.311	16.254				16.25		16.880

Legend	Specimen No.	End of Test							Final		
		Bulk density, EOT (g/cc)	wc', used the initial data as reference (%)	wc measured at EOT (%)	wc'(%)	Dry density (Mg/m³)	Void ratio, e	Sw (%)	wc (%)	Sw (%)	Suction (MPa)
	CR10-L-8		14.139	13.636	14.139				14.14		34.190
	CR10-L-9		10.582	9.040	10.582				10.58		76.490
	CR10-L-10		7.354	5.961	7.354				7.35		126.320
CR10-1.4-w32%	CR10-1.4-1	1.97	21.954	18.172	21.954	1.611	0.685	86.993	21.95	86.99	2.390
	CR10-1.4-2	1.88	24.372	18.080	24.372	1.515	0.793	83.506	24.37	83.51	0.620
	CR10-1.4-3	1.96	22.814	19.436	22.814	1.596	0.702	88.236	22.81	88.24	1.170
	CR10-1.4-4	1.98	21.672	20.135	21.672	1.624	0.673	87.503	21.67	87.50	5.440
	CR10-1.4-5	1.59	19.795	19.234	19.795	1.323	1.052	51.095	19.79		5.760
	CR10-1.4-6	2.01	20.121	18.002	20.121	1.670	0.626	87.312	20.12	87.31	9.290
	CR10-1.4-7	1.91	18.886	15.538	18.886	1.605	0.692	74.108	18.89	74.11	16.880
	CR10-1.4-8	2.01	14.536	13.707	14.536	1.756	0.547	72.235	14.54	72.24	34.190
	CR10-1.4-9	2.01	10.765	9.545	10.765	1.819	0.493	59.284	10.76	59.28	76.490
	CR10-1.4-10	1.93	8.244	6.092	8.244	1.787	0.520	43.075	8.24	43.08	126.320
CR10-1.6-w24%	CR10-1.6-1	2.02	18.754	16.249	18.754	1.697	0.600	84.829	18.75	84.83	2.390
	CR10-1.6-2	1.95	19.531	17.794	19.531	1.630	0.666	79.676	19.53	79.68	0.620
	CR10-1.6-3	1.89	20.090	19.199	20.090	1.572	0.728	74.979	20.09	74.98	1.170
	CR10-1.6-4	1.95	19.924	18.456	19.924	1.630	0.666	81.233	19.92	81.23	5.440
	CR10-1.6-5	2.01	19.068	18.072	19.068	1.685	0.612	84.687	19.07	84.69	5.760
	CR10-1.6-6	2.00	17.806	17.231	17.806	1.699	0.599	80.803	17.81	80.80	9.290
	CR10-1.6-7	2.03	16.154	15.681	16.154	1.744	0.557	78.771	16.15	78.77	16.880
	CR10-1.6-8	2.02	13.849	13.385	13.849	1.777	0.529	71.156	13.85	71.16	34.190
	CR10-1.6-9	1.93	9.142	8.652	9.142	1.770	0.534	46.458	9.14	46.46	78.610

		End of Test							Final		
Legend	Specimen No.	Bulk density, EOT (g/cc)	wc', used the initial data as reference (%)	wc measured at EOT (%)	wc'(%)	Dry density (Mg/m³)	Void ratio, e	Sw (%)	wc (%)	Sw (%)	Suction (MPa)
	CR10-1.6-10	1.93	7.041	5.748	7.041	1.801	0.508	37.616	7.04	37.62	127.480
CR10-1.8-w18%	CR10-18-1	2.04	17.947	16.371	17.947	1.732	0.568	85.741	17.95	85.74	2.390
	CR10-18-2	2.06	18.916	16.847	18.916	1.731	0.569	90.262	18.92	90.26	0.620
	CR10-18-3	2.10	18.088	16.699	18.088	1.776	0.529	92.793	18.09	92.79	1.170
	CR10-18-4	2.05	19.402	17.882	19.402	1.716	0.583	90.453	19.40	90.45	5.440
	CR10-18-5	2.04	18.876	17.019	18.876	1.720	0.579	88.559	18.88	88.56	5.590
	CR10-18-6	1.97	17.380	15.352	17.380	1.679	0.617	76.471	17.38	76.47	8.880
	CR10-18-7	2.06	15.795	13.407	15.795	1.778	0.527	81.362	15.79	81.36	16.790
	CR10-18-8	2.12	13.523	11.525	13.523	1.871	0.451	81.388	13.52	81.39	33.780
	CR10-18-9A	2.09	8.704	8.560	8.704	1.923	0.413	57.302	8.70	57.30	76.890
	CR10-18-10A	2.05	8.704	4.682	8.704	1.883	0.442	53.438	8.70	53.44	146.250
SR160-10-L-w32%	SR160-L-1		48.406	41.005	48.406				48.41		2.390
	SR160-L-2		54.622	45.244	54.622				54.62		0.620
	SR160-L-3		60.660	54.022	60.660				60.66		1.170
	SR160-L-4		59.343	53.665	59.343				59.34		5.440
	SR160-L-5		55.792	48.413	55.792				55.79		5.760
	SR160-L-6		46.700	40.712	46.700				46.70		9.290
	SR160-L-7		35.397	28.869	35.397				35.40		16.880
	SR160-L-8		25.048	20.465	25.048				25.05		34.190
	SR160-L-9		14.527	9.187	14.527				14.53		78.610
	SR160-L-10		11.687	6.725	11.687				11.69		127.480

Legend	Specimen No.	End of Test							Final		
		Bulk density, EOT (g/cc)	wc', used the initial data as reference (%)	wc measured at EOT (%)	wc'(%)	Dry density (Mg/m³)	Void ratio, e	Sw (%)	wc (%)	Sw (%)	Suction (MPa)
SR160-1.4-w32%	SR160-1.4-1	1.73	49.148	40.406	49.148	1.160	1.342	99.476	49.15	99.48	2.390
	SR160-1.4-2	1.69	54.034	45.462	54.034	1.100	1.469	99.906	54.03	99.91	0.620
	SR160-1.4-3	1.69	57.671	50.468	57.671	1.073	1.530	102.343	57.67	102.34	1.170
	SR160-1.4-4	1.67	58.070	49.170	58.070	1.060	1.563	100.891	58.07	100.89	5.440
	SR160-1.4-5	1.74	53.225	44.607	53.225	1.135	1.393	103.745	53.22	103.74	5.760
	SR160-1.4-6	1.84	46.477	39.501	46.477	1.253	1.168	108.115	46.48	108.12	9.290
	SR160-1.4-7	1.83	35.683	28.028	35.683	1.351	1.010	95.935	35.68	95.94	16.880
	SR160-1.4-8	1.88	26.128	19.187	26.128	1.494	0.818	86.728	26.13	86.73	34.190
	SR160-1.4-9	1.85	15.756	9.761	15.756	1.598	0.700	61.151	15.76	61.15	76.490
	SR160-1.4-10	1.80	12.640	7.025	12.640	1.599	0.699	49.137	12.64	49.14	126.320
SR160-1.6-w24%	SR160-1.6-1	1.81	38.389	29.744	38.389	1.305	1.081	96.427	38.39	96.43	2.390
	SR160-1.6-2	1.84	43.304	36.268	43.304	1.283	1.117	105.271	43.30	105.27	0.620
	SR160-1.6-3	1.73	45.425	37.833	45.425	1.193	1.277	96.574	45.42	96.57	1.170
	SR160-1.6-4	1.75	46.575	41.358	46.575	1.192	1.279	98.932	46.57	98.93	5.440
	SR160-1.6-5	1.81	44.115	37.424	44.115	1.253	1.168	102.546	44.11	102.55	5.760
	SR160-1.6-6	1.83	37.495	31.539	37.495	1.332	1.039	98.053	37.50	98.05	9.290
	SR160-1.6-7	1.90	29.708	24.393	29.708	1.462	0.857	94.118	29.71	94.12	16.880
	SR160-1.6-8	1.99	21.731	16.789	21.731	1.635	0.661	89.317	21.73	89.32	34.190
	SR160-1.6-9	1.92	13.646	9.045	13.646	1.687	0.610	60.768	13.65	60.77	78.610

Legend	Specimen No.	End of Test							Final		
		Bulk density, EOT (g/cc)	wc', used the initial data as reference (%)	wc measured at EOT (%)	wc'(%)	Dry density (Mg/m³)	Void ratio, e	Sw (%)	wc (%)	Sw (%)	Suction (MPa)
	SR160-1.6-10	1.86	10.848	6.293	10.848	1.681	0.616	47.836	10.85	47.84	127.480
SR160-1.8-w18%	SR160-18-1	1.81	37.143	34.327	37.143	1.321	1.057	95.465	37.14	95.47	2.390
	SR160-18-2	1.74	41.851	38.598	41.851	1.230	1.208	94.095	41.85	94.10	0.620
	SR160-18-3	1.82	37.593	32.003	37.593	1.325	1.050	97.255	37.59	97.25	1.170
	SR160-18-4	1.76	42.675	35.782	42.675	1.232	1.204	96.271	42.68	96.27	5.440
	SR160-18-5	1.81	42.206	31.548	42.206	1.274	1.132	101.240	42.21	101.24	5.590
	SR160-18-6	1.90	33.977	26.363	33.977	1.419	0.914	100.942	33.98	100.94	8.880
	SR160-18-7	1.96	25.720	19.630	25.720	1.561	0.740	94.400	25.72	94.40	16.790
	SR160-18-8	2.10	18.020	14.194	18.020	1.783	0.523	93.555	18.02	93.56	33.780
	SR160-18-9A	2.11	10.868	8.638	10.868	1.899	0.430	68.586	10.87	68.59	76.890
	SR160-18-10A	2.04	10.868	5.250	10.868	1.844	0.473	62.465	10.87	62.46	146.250
SR270-10-L-w18%	SR270-L-1		49.175	42.667	49.175				49.17		2.390
	SR270-L-2		46.659	43.749	46.659				46.66		0.620
	SR270-L-3		45.957	42.007	45.957				45.96		1.170
	SR270-L-4		47.862	43.721	47.862				47.86		5.440
	SR270-L-5		47.378	41.037	47.378				47.38		5.590
	SR270-L-6		43.008	34.124	43.008				43.01		8.880
	SR270-L-7		35.685	25.877	35.685				35.69		16.790
	SR270-L-8		24.124	15.308	24.124				24.12		33.780

Legend	Specimen No.	End of Test							Final		
		Bulk density, EOT (g/cc)	wc', used the initial data as reference (%)	wc measured at EOT (%)	wc'(%)	Dry density (Mg/m^3)	Void ratio, e	Sw (%)	wc (%)	Sw (%)	Suction (MPa)
	SR270-L-9B		11.898	6.182	11.898				11.90		79.700
	SR270-L-9A		11.898	6.594	11.898				11.90		76.890
	SR270-L-10B		11.898	3.871	11.898				11.90		154.770
	SR270-L-10A		11.898	3.996	11.898				11.90		146.250
SR270-10-L-w32%	SR270-L-1		58.747	48.587	58.747				58.75		2.390
	SR270-L-2		63.422	53.759	63.422				63.42		0.620
	SR270-L-3		68.360	57.783	68.360				68.36		1.170
	SR270-L-4		66.014	57.259	66.014				66.01		5.440
	SR270-L-5		65.583	54.382	65.583				65.58		5.760
	SR270-L-6		57.477	49.388	57.477				57.48		9.290
	SR270-L-7		44.758	35.484	44.758				44.76		16.880
	SR270-L-8		30.991	21.837	30.991				30.99		34.190
	SR270-L-9		16.380	8.547	16.380				16.38		76.490
	SR270-L-10		12.670	6.167	12.670				12.67		126.320
SR270-1.4-w32%	SR270-1.4-1	1.63	63.654	52.679	63.654	0.993	1.734	99.674	63.65	99.67	2.390
	SR270-1.4-2	1.69	67.492	57.041	67.492	1.009	1.692	108.346	67.49	108.35	0.620
	SR270-1.4-3	1.60	71.529	60.070	71.529	0.931	1.919	101.258	71.53	101.26	1.170
	SR270-1.4-4	1.57	73.421	61.210	73.421	0.906	1.997	99.874	73.42	99.87	5.440
	SR270-1.4-5	1.63	68.732	56.209	68.732	0.963	1.820	102.596	68.73	102.60	5.760
	SR270-1.4-6	1.76	59.491	48.595	59.491	1.102	1.464	110.360	59.49	110.36	9.290

Legend	Specimen No.	End of Test							Final		
		Bulk density, EOT (g/cc)	wc', used the initial data as reference (%)	wc measured at EOT (%)	wc'(%)	Dry density (Mg/m^3)	Void ratio, e	Sw (%)	wc (%)	Sw (%)	Suction (MPa)
	SR270-1.4-7	1.75	44.735	34.650	44.735	1.207	1.251	97.153	44.74	97.15	16.880
	SR270-1.4-8	1.80	31.184	21.913	31.184	1.374	0.977	86.682	31.18	86.68	34.190
	SR270-1.4-9	1.59	15.964	8.635	15.964	1.368	0.985	43.997	15.96	44.00	76.490
	SR270-1.4-10	1.55	12.652	6.121	12.652	1.377	0.972	35.345	12.65	35.34	126.320
SR270-1.6-w24%	SR270-1.6-1	1.76	39.477	34.262	39.477	1.259	1.157	92.661	39.48	92.66	2.390
	SR270-1.6-2	1.68	44.581	39.604	44.581	1.162	1.338	90.503	44.58	90.50	0.620
	SR270-1.6-3	1.83	46.737	41.563	46.737	1.245	1.182	107.371	46.74	107.37	1.170
	SR270-1.6-4	1.70	47.728	42.544	47.728	1.151	1.359	95.394	47.73	95.39	5.440
	SR270-1.6-5	1.68	43.821	38.347	43.821	1.165	1.332	89.374	43.82	89.37	5.760
	SR270-1.6-6	1.77	39.027	34.682	39.027	1.272	1.136	93.309	39.03	93.31	9.290
	SR270-1.6-7	1.79	30.050	25.738	30.050	1.375	0.976	83.664	30.05	83.66	16.880
	SR270-1.6-8	1.80	21.153	16.849	21.153	1.485	0.829	69.317	21.15	69.32	34.190
	SR270-1.6-9	1.87	12.061	7.802	12.061	1.673	0.624	52.524	12.06	52.52	78.610
	SR270-1.6-10	1.86	9.676	5.682	9.676	1.697	0.600	43.763	9.68	43.76	127.480
SR270-1.8-w18%	SR270-18-1	1.68	54.473	46.825	54.473	1.086	1.501	98.585	54.47	98.58	2.390
	SR270-18-2	1.62	60.318	51.671	60.318	1.010	1.688	97.049	60.32	97.05	0.620
	SR270-18-3	1.69	55.532	47.189	55.532	1.089	1.495	100.904	55.53	100.90	1.170
	SR270-18-4	1.62	60.520	49.767	60.520	1.009	1.691	97.226	60.52	97.23	5.440
	SR270-18-5	1.72	60.279	43.337	60.279	1.074	1.530	107.016	60.28	107.02	5.590
	SR270-18-6	1.79	51.127	34.928	51.127	1.186	1.291	107.598	51.13	107.60	8.880
	SR270-18-7	1.89	38.105	26.071	38.105	1.367	0.987	104.887	38.11	104.89	16.790

Legend	Specimen No.	End of Test							Final		
		Bulk density, EOT (g/cc)	wc', used the initial data as reference (%)	wc measured at EOT (%)	wc'(%)	Dry density (Mg/m^3)	Void ratio, e	Sw (%)	wc (%)	Sw (%)	Suction (MPa)
	SR270-18-8	1.68	25.191	15.355	25.191	1.342	1.023	66.870	25.19	66.87	33.780
	SR270-18-9A	2.04	12.847	7.606	12.847	1.808	0.502	69.464	12.85	69.46	76.890
	SR270-18-10A	2.02	12.847	4.739	12.847	1.790	0.517	67.473	12.85	67.47	146.250